VOLUME 3 SEPTEMBER, 1930 NUMBER 3

NATIONAL
RESEARCH COUNCIL
of CANADA

CANADIAN JOURNAL OF RESEARCH

CANADA

Published under the authority
of the
Chairman of the Subcommittee of the
Privy Council on Scientific and Industrial Research

OTTAWA • CANADA

CONTENTS

	PAGE
The Effect of Radiant Energy on Growth and Sporulation in *Colletotrichum Phomoides*—*A. H. Hutchinson and M. R. Ashton*	187
Feed Flavor or Stable Odor in Milk caused by an Atypical Strain of *Aërobacter Oxytocum*—*Wilfrid Sadler and M. Lenora Irwin*	200
Specific Heats and Latent Heat of Fusion of Ice—*W. H. Barnes and O. Maass*	205
The Influence of Hydrogen Ion on the Fenton Reaction—*W. H. Hatcher and M. G. Sturrock*	214
The Heating of Electrolytes in High Frequency Fields—*J. C. McLennan and A. C. Burton*	224
Action of High Speed Electrons on Methane, Oxygen and Carbon Monoxide—*J. C. McLennan and J. V. S. Glass*	241
The Physical Characters of Penumbral Shadows and their Significance in Roentgenography—*Paul M. Andrus*	252
Distribution of Stress in Parallel Welding Fillets—*H. M. MacKay and A. M. Bain*	260
The Design of Corners in Fluid Channels—*G. J. Klein, K. F. Tupper and J. J. Green*	272

* * *

Publication and Subscriptions

The Canadian Journal of Research is published monthly by the National Research Council of Canada, Ottawa, to which address all correspondence should be directed.

The subscription rate is $3.00 per year to any part of the world. Single copies are thirty-five cents each.

Canadian Journal *of* Research

Issued by The National Research Council of Canada

VOLUME 3 SEPTEMBER, 1930 NUMBER 3

THE EFFECT OF RADIANT ENERGY ON GROWTH AND SPORULATION IN *COLLETOTRICHUM PHOMOIDES*[1]

By A. H. Hutchinson[2] and M. R. Ashton[3]

Abstract

Experiments were performed on *Colletotrichum phomoides*, a fungus which is a common cause of ripe-rot on tomatoes.

The lines of the mercury arc spectrum may be grouped into three classes on the basis of their effect on the growth of *Colletotrichum:* those which cause constant retardation, those which cause constant stimulation and those which cause primary retardation followed by stimulation.

On the basis of the effect on the production of spores, there are two classes of lines in the mercury arc spectrum, *i.e.*, those which hasten spore development and those which have no apparent effect. Spore production is generally hastened by monochromatic light causing retardation or extreme stimulation of growth, and is apparently not affected by light which moderately stimulates growth; moreover, an optimum duration is shown for the illumination causing the accelerated development of spores.

Evidence is given that the effect of monochromatic light is upon the protoplasm and not the culture, since cultures grown on non-irradiated media from irradiated spores show the same effects as those obtained by irradiating three-day cultures. In many cases, in *Colletotrichum*, the effect of irradiation is evident in the culture 10 days after the spores have been illuminated.

There is a marked similarity in the effect upon the growth of *Colletotrichum*, *Yeast* and *Paramoecium*.

Introduction

Most of the previous investigations on the effects of ultra-violet radiation upon fungi have been concerned with the effect on sporulation and the determination of the fungicidal action of these rays.

Stevens (9, 10) found that radiation "almost instantly initiates the development of reproductive structures in great numbers where they would not have occurred without radiation, but in no cases were structures initiated that were not known to be occasionally produced by these fungi in the natural course of events". He points out that these results may be due to the sudden inhibition

[1] *Manuscript received June 23, 1930.*

Contribution from the laboratories of the University of British Columbia, Vancouver, Canada, with financial assistance from the National Research Council of Canada.

[2] *Professor of Botany, University of British Columbia.*

[3] *Research Assistant.*

of growth caused by these rays, but on the other hand it is known that many other causes of inhibition do not call forth this decided development of reproductive structures.

Ramsay and Bailey (7) irradiated species of *Macrosporium* and *Fusarium* and state that there is a definite stimulation of sporulation caused by ultra-violet light, which seems to be the direct result of stimulation rather than the indirect result of inhibition. Greatest sporulation is obtained from λ 2800-2535 Å. Stimulation of spore production occurs below λ 2535 Å, but there is also some lethal effect and retardation of mycelial development. It was also found that long exposures to direct sunlight through filters transmitting no lower than λ 3132 Å induce abundant sporulation in both *Macrosporium* and *Fusarium*.

Bovie (1) working on the fungicidal action of ultra-violet light found that spores of certain fungi were killed by exposures of 10 min. to wave-lengths shorter than λ 2925 Å, and that exposure to longer wave-lengths for 120 min. was not lethal. He also states that the Schumann rays (2) were lethal to colorless spores and not to dark spores.

Fulton and Coblentz (3) irradiated the spores of 27 species of fungi with ultra-violet light for various periods of time, and found that the lethal effect resulted after comparatively short exposures, although the time required to kill varied with the type of fungus. They found that the lethal effect varied and was inversely proportional to the wave-length. The mycelium was also found to be more easily killed than the ungerminated spores.

Methods

The present experiments deal with the effect of radiant energy on the sporulation and the growth of *Colletotrichum phomoides*, a fungus which is a common cause of ripe-rot on tomatoes. In these experiments a Cooper-Hewitt quartz mercury lamp was used on an alternating current of 110 volts with a resistance of 12 ohms in series. In some cases direct exposures were made at a distance of 12 cm. from the source of light, and in other experiments monochromatic light as projected through a Hilger monochromatic illuminator was used.

Bacto potato dextrose agar was used as the nutrient medium, 40 gm. in 1,000 cc. of distilled water, and 20 cc. of this preparation was poured into each petrie dish. Plantings of the fungus were made on this agar and were allowed to grow for three days before irradiation or the taking of measurements.

It was found that when this nutrient medium was used a single spore culture developed and completely occupied a petrie dish in about 11-12 days, growing about 0.7 cm. per day, and developing acervuli no earlier than the eighth day.

The experiments can be divided into groups: (1) the determination of the normal growth curve; (2) the irradiation of the growing cultures with the full light from the quartz mercury lamp for varying periods of time and the determination of the effect on growth and formation of acervuli; (3) irradiation of a

suspension of the spores in sterile water with (a) the full light from the quartz mercury lamp, and (b) various monochromatic lines of the spectrum from a monochromatic illuminator, the spores being afterwards plated.

Experiment 1

Determination of the Normal Growth Curve

Control cultures were kept for each set of experiments described, and altogether, readings were taken from 20 plates, grown at room conditions of light, temperature, etc. The averages of the readings for each day were taken as criteria for the normal growth curve (Tables II-III). Fig. 1-8 show graphically the nature of the growth curve during the first 11 days from the time of inoculation. Three phases of growth are evident, (1) a lag period which continues during the first four days, with an average growth of 0.6 cm. per day, (2) a period of rapid growth extending from the fourth to the sixth day, with an average daily growth of 0.85 cm. and (3) a secondary lag period from the sixth to the eleventh day averaging a daily growth of 0.74 cm. *Colletotrichum* evidently follows the usual type of normal growth curve (6, 8).

Experiment 2

Direct Irradiation of Growing Cultures

Single spores of *Colletotrichum* were isolated and single spore cultures developed on the agar plates. These cultures were allowed to grow for a period of three days and were then irradiated at a distance of 12 cm. by means of a Lab-arc, for varying periods of time. In some cases a half circle of black cardboard was placed over half of the culture so that only one side of the plate obtained the rays from the Lab-arc. In this way it was possible to have the control experiment (one-half of the culture) growing under identically the same conditions as the irradiated culture. The line of separation between the irradiated and the control half was quite distinct, although a portion of the culture was exposed to reflected rays instead of direct rays. In all cases growth was retarded and sporulation accelerated in the area irradiated with the full mercury arc spectrum. (See Plate I.)

Effect of Direct Irradiation on the Rate of Growth

Three-day cultures were irradiated for varying periods of time, and beginning the next day careful measurements of the amount of the growth were made. In order to ensure accuracy, two diameters of the growth at right angles to each other were measured and the average of these two readings taken as the measure of the size of the culture.

It was found that irradiation for three minutes caused stunting, and the culture did not afterwards regain the normal growth rate. Irradiation of one and two minutes caused stunting in direct relation to the time of exposure, but from which the culture returned to normal. Thirty seconds exposure and less caused a slight initial stunting from which the culture ultimately recovered and even exceeded the control in growth rate.

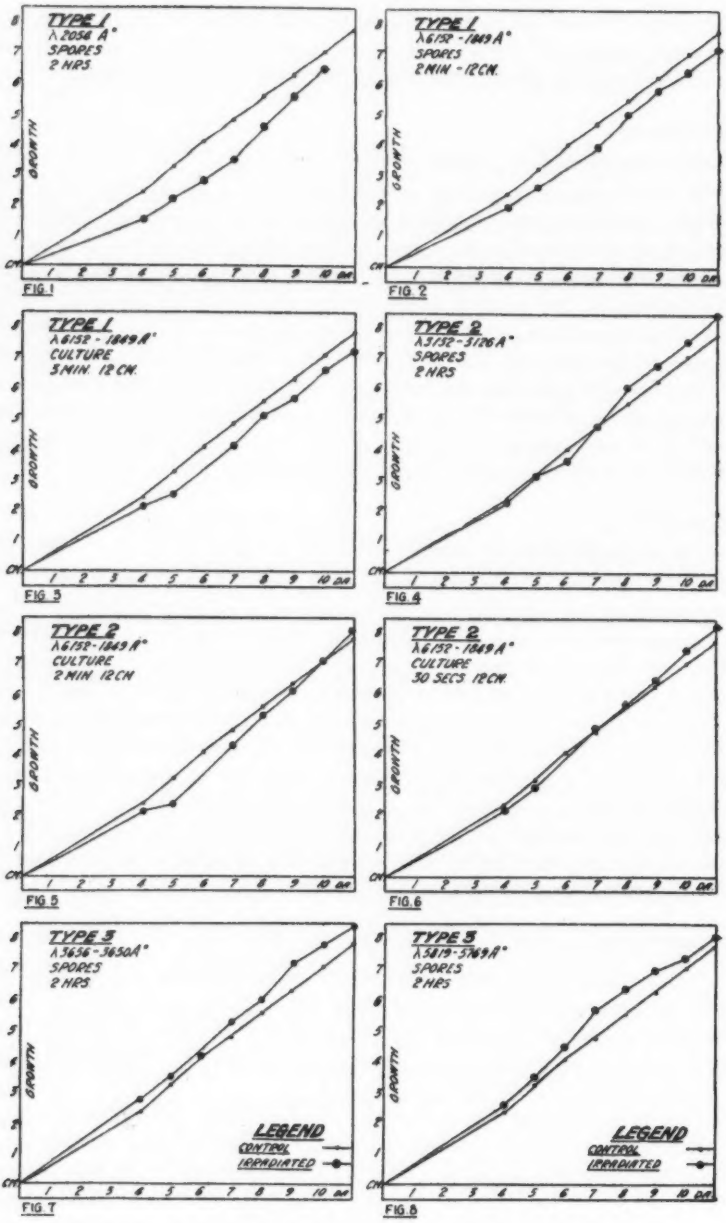

FIG. 1-8. *The three types of effect in Colletotrichum caused by the irradiation of spores and of cultures.*

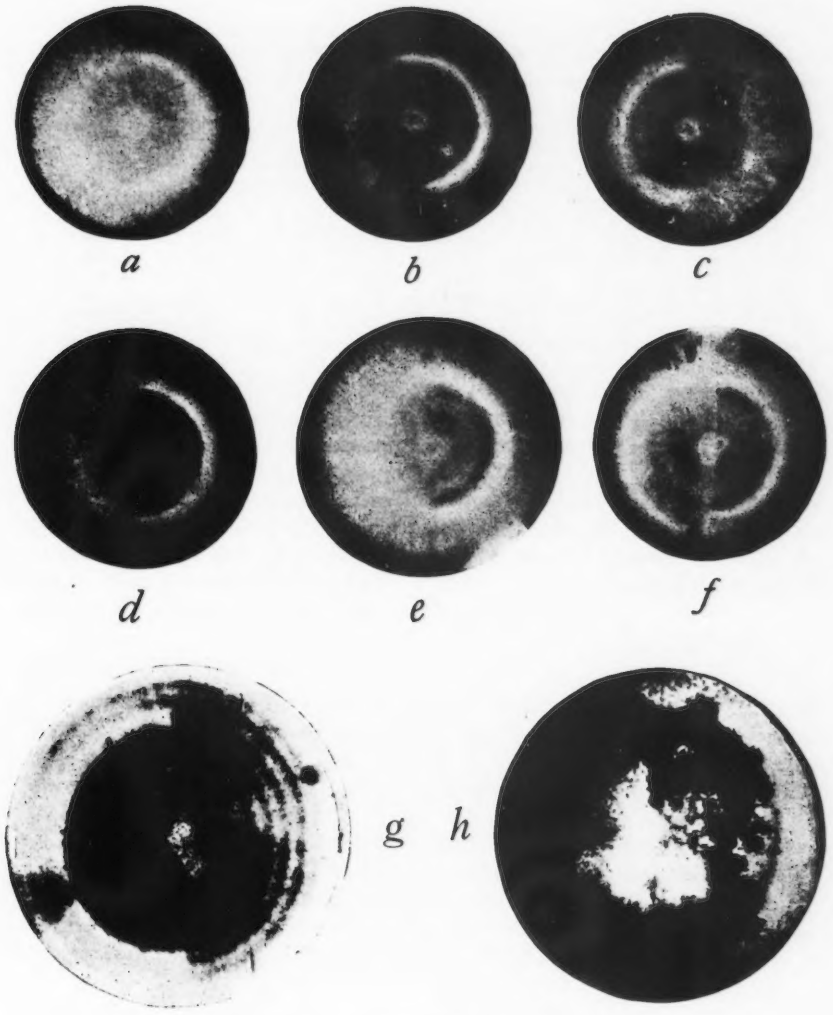

Effect on sporulation and growth of irradiating half of three-day cultures with the mercury vapor arc spectrum, right side exposed, left normal.

(*a*) *Culture, 3 days after 2 min. exposure.*
(*b*) *Culture, 3 days after 3 min. exposure.*
(*c*) *Culture, 3 days after 4 min. exposure.*
(*d*) *Culture, 3 days after 5 min. exposure.*
(*e*) *Culture, 3 days after 6 min. exposure.*
(*f*) *Culture, 3 days after 15 min. exposure.*
(*g*) *Culture, 6 days after 4 min. exposure.*
(*h*) *Culture, 14 days after 4 min. exposure.*

TABLE I

EFFECT OF FULL ILLUMINATION WITH THE MERCURY VAPOR ARC SPECTRUM UPON THE GROWTH OF *Colletotrichum*, (THREE-DAY CULTURES)

Exposure	Size of culture in cm.							
	4th day	5th day	6th day	7th day	8th day	9th day	10th day	11th day
3 min.	2.1	2.5	—	4.1	5.1	5.6	6.6	7.2
2 min.	2.15	2.4	—	4.3	5.35	6.1	7.1	8.2
1 min.	2.1	2.9	—	4.7	5.6	6.3	7.3	7.9
30 sec.	2.25	3.0	—	4.9	5.7	6.5	7.5	8.3
15 sec.	2.3	3.1	—	4.8	5.7	6.5	7.4	7.9
Control	2.4	3.28	4.1	4.8	5.6	6.3	7.1	7.8

It was found that the first effect of all irradiation during periods of more than 30 sec. was a temporary collapse of the aërial mycelium. With more prolonged irradiation of four or more minutes the aërial mycelium in many cases did not recover its original appearance.

If only half of the culture is irradiated for periods of 30 sec. to 3 min. the irradiated half is stunted and the non-irradiated half continues to grow normally, a clear line of demarcation being noticeable between the two; this demarcation is caused by the collapse of the aërial mycelium and the difference in the areas of growth on each side (See Plate I).

Effect on Development of Acervuli

Direct irradiation of the entire three-day culture results, after about 24 hr., in the formation of numerous acervuli, mostly in clumps. Maximum development of acervuli takes place as a result of exposure for 30 sec. to 1 min.; longer periods of irradiation accelerate development of acervuli, but in smaller quantities.

When one-half of the colony is irradiated, early development of acervuli can clearly be seen, one-half of the culture appearing darker than the other, while the non-irradiated half of the culture remains free from acervuli until the culture is about eight days old. Even after that time the acervuli are less numerous in the non-irradiated control (See Plate I).

Experiment 3

Irradiation of Spore Suspension

(a) With full illumination from the Lab-arc, *i.e.*, λ 6152-1849 Å.

Suspensions of the spores of *C. phomoides* in sterile water were irradiated in the full illumination of the lab-arc at a distance of 12 cm. for varying periods of time. These suspensions were then plated out on bacto potato dextrose agar, and from these plates single spore cultures were obtained, their growth and development being noted. In this experiment any effect of the ultraviolet light on the culture medium was eliminated.

TABLE II

EFFECT OF THE FULL ILLUMINATION WITH THE MERCURY VAPOR ARC SPECTRUM ON *Colletotrichum* SPORE SUSPENSIONS

Exposure	Size of culture in cm.							
	4th day	5th day	6th day	7th day	8th day	9th day	10th day	11th day
2 min.	2.0	2.7	—	4.0	5.1	5.9	6.5	7.2
1 min.	1.95	2.7	—	4.4	5.1	5.9	6.6	7.4
30 sec.	2.1	2.9	—	4.6	5.2	6.1	6.7	7.5
15 sec.	2.1	3.1	—	4.7	5.5	6.2	7.0	7.7
Control	2.4	3.28	4.1	4.8	5.6	6.3	7.1	7.8

TABLE III

SPECIFIC EFFECTS OF MONOCHROMATIC LIGHT UPON THE GROWTH OF *Colletotrichum* SPORE SUSPENSIONS

λ in Å	Exposure in hr.	Size of culture in cm.							
		4th day	5th day	6th day	7th day	8th day	9th day	10th day	11th day
Control	1	2.4	3.28	4.1	4.8	5.6	6.3	7.1	7.8
6152	1	2.2	3.1	4.1	4.8	5.6	6.3	7.1	7.8
	2	2.3	3.0	4.1	5.0	5.8	7.2	8.0	8.5
5819–5769	1	2.4	3.2	4.0	5.0	5.7	6.3	7.2	8.0
	2	2.6	3.5	4.5	5.7	6.4	7.0	7.4	8.1
4960–4916	1	1.9	2.9	3.8	4.8	5.6	6.3	7.0	7.7
	2	1.9	2.7	3.6	4.8	5.5	6.1	6.9	7.6
4078–3984	1	2.6	3.2	4.0	4.9	5.6	6.9	7.5	8.1
	2	2.6	3.1	4.1	5.2	6.6	7.6	8.2	—
3821	1	2.3	3.1	4.5	4.9	5.4	5.8	7.0	7.8
	2	2.3	3.1	4.2	5.0	6.0	6.8	7.6	8.5
3656–3650	1	3.0	3.6	4.3	4.7	5.6	6.3	7.1	7.8
	2	2.8	3.5	4.2	5.3	6.0	7.3	7.8	8.4
3342	1	2.9	3.4	3.9	4.8	5.8	6.3	7.1	7.9
	2	3.0	3.6	4.5	5.2	5.9	6.7	7.5	8.5
3132–3126	1	2.1	2.8	4.0	4.9	5.9	6.7	7.5	8.1
	2	2.3	3.2	3.7	4.8	6.1	6.8	7.6	8.5
3022	1	1.5	2.1	3.6	4.2	5.2	5.5	6.0	7.0
	2	1.4	2.1	2.8	3.5	4.2	5.7	6.3	7.2
2967	1	2.2	3.1	3.9	4.8	5.7	6.7	7.4	8.1
	2	1.9	2.8	4.0	5.0	5.5	6.6	7.4	8.4
2804	1	1.65	2.2	2.8	3.3	4.4	5.4	6.1	7.7
	2	1.2	2.1	2.6	3.4	4.2	4.7	5.7	6.5
2700	1	2.2	3.25	4.0	4.7	6.1	6.4	7.2	8.3
	2	2.2	3.2	4.0	4.7	6.1	6.5	7.3	8.5
2535	1	2.2	3.3	4.0	4.7	5.5	6.2	7.4	8.6
	2	2.0	3.1	4.0	4.7	5.4	6.2	7.1	7.9
2054	1	1.5	2.5	3.4	4.0	5.0	5.9	7.0	7.8
	2	1.5	2.2	2.8	3.5	4.6	5.1	6.0	—
1849	1	2.0	3.1	3.8	4.4	5.5	6.1	7.1	7.9
	2	1.8	2.5	3.3	4.2	5.1	6.1	7.0	7.7

It will be noticed that irradiation of the spores for periods of more than 30 sec. caused an intensive initial stunting from which the culture did not regain normal growth rate. Irradiation for 15 sec. also caused initial stunting but the rate of growth gradually approached normal.

It appears from these results that the effect of full illumination directly on the spores is greater than that of irradiation on a growing culture; in the case of the spores the culture never reaches normal growth, whereas in the case of the growing culture stimulation may result ultimately.

The effect on germination of irradiation for periods of time up to 5 and 6 min. was in no case complete inhibition. It was found, however, that as the time of irradiation was increased the proportion of germinating spores was decreased.

In all cases development of acervuli was hastened and they were observed in the irradiated culture several days before their development in the control; maximum development seemed to take place in cultures irradiated for 30 sec.

(b) With monochromatic light.

In this series of experiments a suspension of spores in sterile water was exposed, in the slot of the monochromatic illuminator, to light of different wave-lengths, and the specific effects of each individual wave-length noted.

The effects of monochromatic irradiation may be grouped into four classes:

Class I—Continued retardation.

This effect is caused by the following wave-lengths:—λ 4960-4916 Å, λ 3028-3022 Å, λ 2804 Å, λ 2054 Å, and λ 1849 Å. The initial retardation is great, while the final retardation is less except in the cases of λ 2804 Å and λ 2054 Å, where it is greater. (See Table III, and Fig. 1, 10 and 11.)

Class II—Retardation followed by stimulation.

Irradiation by lines in this class results in a primary retardation of small degree followed by stimulation, which is generally in inverse proportion to the initial retardation (Fig. 4, 9, 10 and 11). This effect is caused by wave-lengths: λ 6152 Å, λ 3132-3126 Å, λ 3821 Å, λ 2700 Å and λ 2967 Å.

Class III—Stimulation general.

The following lines cause this effect:— λ 5819-5769 Å, λ 3656-3650 Å, λ 3342 Å and λ 4078-3984 Å. The stimulation of growth continues to increase throughout the 11-day period, except in the case of λ 3342 Å, which reaches its maximum stimulation at the fourth day (Fig. 8-11).

Class IV—No effect.

λ 4359 Å does not affect the rate of growth to any appreciable extent.

Comparison of the effects of irradiation of cultures and of spores for varying periods of time

Three classes of effects of the irradiation of spores by monochromatic light for periods of two hours have been described above; the effects of direct irradiation of the culture with full mercury arc spectrum represent two of these classes, namely, class I and class II. When the three-day culture is irradiated at a

distance of 12 cm. for three minutes continued retardation results throughout the 11-day period of growth (Fig. 3). When the irradiation is for 30 sec. only, initial retardation is followed by final stimulation (Class II, Fig. 6).

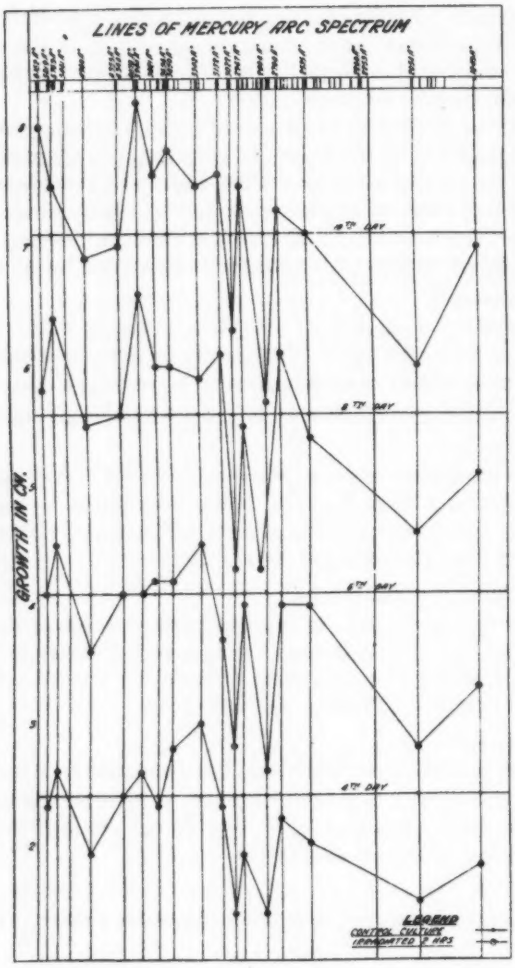

FIG. 9. *The progressive effect of various lines of the mercury arc spectrum on the growth of Colletotrichum at various time intervals.*

These results show conclusively that the effect of irradiation is upon the protoplasm and not upon the culture, since the results obtained by irradiating cultures are similar to those obtained by irradiating spores, and in the latter case the culture was at no time exposed to irradiation. The absence of instances of stimulation by full irradiation of cultures may be explained by the fact that there are in the mercury arc spectrum a greater number of lines which are inhibitory than stimulatory; consequently the total effect in each case might be expected to be that of retardation. The effect of irradiation of spores by full mercury arc spectrum at a distance of 12 cm. is one of retardation even when the time is 15 sec. (Table II, Fig. 2).

It is apparent that the irradiation of spores has a more marked effect than the irradiation of the culture, since the effect of a 15 sec. exposure of spores is similar to that of a three-minute exposure of a culture, with the same illumination, at the same distance. This again emphasizes the nature of the effect as being protoplasmic.

Comparison of the effects of monochromatic light upon the growth of Colletotrichum

Fig. 9 illustrates the growth in cm. of diameter for cultures irradiated by means of the monochromatic illuminator with specific lines of the mercury arc spectrum. Readings are illustrated for the control cultures and for the irradiated cultures at the fourth, sixth, eighth and tenth days. The complete results are given in Table III.

Comparison of the diameters at the intervals mentioned above show that there are three classes of effects, as already described, namely: (1) continued retardation, (2) primary retardation followed by stimulation, (3) continued stimulation. From a study of Fig. 9, the presence of sub-groups becomes evident.

Class I

λ 2804 Å and λ 2054 Å cause increased retardation throughout the 10-day period, while λ 4960 Å, λ 3022 Å and λ 1849 Å show continued retardation which decreases in degree from the fourth day, until the final growth at the tenth day in some instances approaches that of the control; in the case of λ 3022 Å, retardation increases until the sixth day, after which it decreases.

Class II

Retardation is caused by wave-lengths λ 3821 Å and λ 6152 Å only until the fourth day, by λ 2700 Å and λ 3132 Å until the sixth day and by λ 2967 Å until the eighth day. After the periods specified, stimulation takes place.

Class III

Wave-length λ 5819 Å shows an increasing stimulation until the end of the eighth day; λ 4078 Å and λ 3656 Å show decreasing stimulation to the sixth

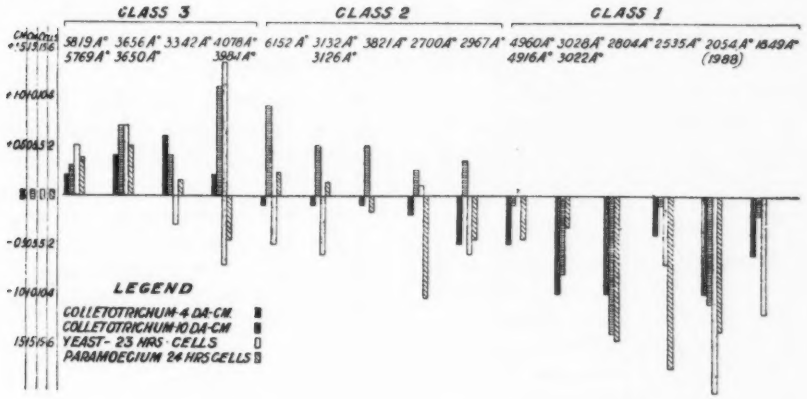

FIG. 10. *Diagram of the comparative effects of monochromatic light on Colletotrichum, Yeast and Paramoecium, the control represented as zero.*

day followed by a secondary increase. Wave-length λ 3342 Å stimulates during the first four days of growth and thereafter the growth is at the same rate as the control.

Class IV

λ 4359 Å at no time shows any appreciable effect upon growth.

Comparison of the effects of monochromatic light on Colletotrichum, Yeast and Paramoecium

The three classes of mercury arc spectral lines, according to their effect upon the growth of *Colletotrichum* described above, may be used for comparison with the effects on *Yeast* and *Paramoecium* (4, 5).

TABLE IV

COMPARISON OF THE EFFECTS OF MONOCHROMATIC LIGHT UPON THE GROWTH OF *Colletotrichum*, *Yeast* AND *Paramoecium*

λ in Å	Duration	*Colletotrichum*	*Yeast*	*Paramoecium*
Class I				
4960–4916	4th day	−0.5	17	−1.8
	10th day	−0.1		
3022–3028	4th day	−1.0	—	−1.0
	10th day	−0.8		
2804	4th day	−1.0	—	−3.9
	10th day	−1.4		
2535	4th day	−0.4	−7	−7
	10th day	−0.1		
2054	4th day	−1.0	−11	−5.5
	10th day	−1.1		
1849	4th day	−0.6	−10	—
	10th day	−0.2		
Class II				
6152	4th day	−0.1	−5	0.9
	10th day	0.9		
3132–3126	4th day	−0.1	−6	0.5
	10th day	0.5		
3821	4th day	−0.1	—	−0.7
	10th day	0.5		
2700	4th day	−0.2		
	10th day	0.2	1	−4.2
2967	4th day	−0.5	−6	−1.8
	10th day	0.3		
Class III				
5819	4th day	0.2	5	1.5
	10th day	0.3		
3656	4th day	0.4	7	2.0
	10th day	0.7		
3342	4th day	0.6	−3	0.6
	10th day	0.4		
4078	4th day	0.2	−7	−1.8
3984	10th day	1.1	(13)	

NOTE:— *Readings for Colletotrichum denote stimulation or retardation of cultures from spores irradiated for two hours. Yeast and Paramoecium data show the number of cells greater or less than the control after irradiation for 23 or 24 hr.*

Class I

λ 4960-4916 Å, λ 3022 Å, λ 2804 Å, λ 2535 Å, λ 2054 Å and λ 1849 Å, which give constant retardation of growth in *Colletotrichum*, also retard growth in both *Yeast* and *Paramoecium*, and approximately in the same proportion. It may be noticed, however, that λ 2535 Å which produces only slight retardation with *Colletotrichum*, results in marked retardation with *Yeast* and extreme retardation in *Paramoecium*; also that λ 4960 Å produces a somewhat variable result with *Yeast*.

Class II

λ 6152 Å, λ 3132 Å, λ 3821 Å and λ 2967 Å give rise to retardation followed by stimulation in *Colletotrichum*. They all produce retardation in *Yeast* with the exception of λ 2700 Å, which as in *Colletotrichum*, first causes retardation followed by final stimulation. Apparently the experiments with *Yeast* were not carried far enough to give the final effect except in the case of λ 2700 Å. λ 6152 Å and λ 3132 Å, which produce final marked stimulation with *Colletotrichum*, and slight stimulation in *Paramoecium;* λ 3821 Å and λ 2967 Å, which show marked initial retardation in *Colletotrichum*, also show retardation in *Paramoecium*.

Class III

λ 5819-5769 Å, λ 3656 Å, λ 3342 Å and λ 4078-3984 Å show continued stimulation of *Colletotrichum*. Of these, the first two show similar stimulation of *Paramoecium* and *Yeast*, while λ 3342 Å also produces stimulation of *Paramoecium* but retardation in *Yeast*, and λ 4078 Å gives rise to retardation in *Paramoecium* and varied results with *Yeast*. The latter region seems to be a transitional region and consequently varied results with different organisms may be expected.

Comparison of the effects of monochromatic light on the growth and sporulation of Colletotrichum

These effects are graphically illustrated in Fig. 11 and recorded in Table V. The growth of *Colletotrichum* is represented as stimulation or retardation at the fourth and at the tenth day of growth; the effect on sporulation is indicated by the number of days by which the appearance of acervuli in the irradiated cultures precedes that in the control.

When the retardation of growth extends over the 10-day period, sporulation is ordinarily hastened. It may be noted, however, that when the full mercury arc spectrum was used for irradiation, although sporulation increased with exposures of from 15 sec. to 2 min., it decreased when exposures were more than two minutes in duration. This seems to indicate that sporulation is an inverse expression of growth rate only within certain limits, and that there is an optimum amount of irradiation causing sporulation. In the case of λ 3022 Å, λ 2804 Å, λ 2054 Å and λ 1849 Å, spores appear at the fifth day in the irradiated cultures as compared with the eighth day in the control. Wavelengths λ 4960 Å and λ 2535 Å cause acervuli development two days sooner

than in the control. The latter lines retard growth to a less degree and also stimulate sporulation to a less degree. With λ 3132 Å, λ 2700 Å and λ 3821 Å there is an initial retardation of growth followed by stimulation and also sporulation is hastened by two days and one day respectively. λ 3656 Å, λ 3342 Å, which constantly stimulate growth, and λ 6152 Å, which gives a

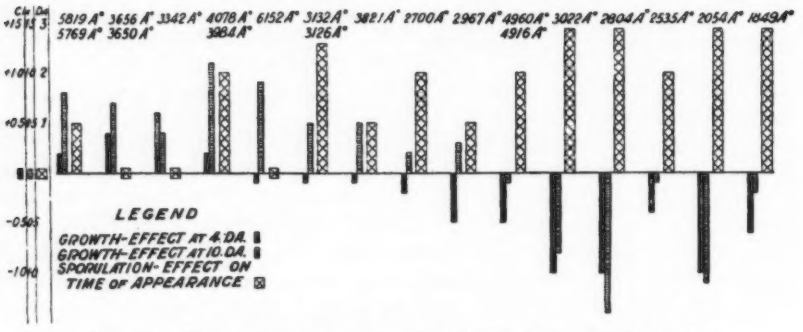

FIG. 11. *The relations between the effect of monochromatic light on the growth and sporulation of Colletotrichum, the control represented as zero.*

slight retardation followed by a marked stimulation, have no apparent effect upon the time of development of spores. On the other hand, λ 4078 Å and λ 5819 Å, which produce the most marked stimulation, also cause early development of acervuli. It would seem that retardation and extreme stimulation of growth are accompanied by early sporulation, while irradiation causing intermediate stimulation of growth has no apparent effect on the development of acervuli.

TABLE V

EFFECT OF MONOCHROMATIC LIGHT ON SPORULATION IN *Colletotrichum*

Wave-length in Å	Acceleration in days	Wave-length in Å	Acceleration in days
6152	0	3022	3
5819	1	2967	1
4960	2	2700	2
4359	2	2804	3
4078	1	2535	2
3821	0	2054	3
3342	0	1849	3
3132	3		

Acknowledgments

The authors wish to express their appreciation to Dr. Frank Dickson, who made the primary isolations of *Colletotrichum phomoides*, and who suggested it as a suitable form for experimentation.

References

1. Bovie, W. T. The action of light on protoplasm. Am. J. Trop. Diseases Prev. Med. 2: 506-517. 1915.
2. Bovie, W. T. The action of Schumann rays on living organisms. Botan. Gaz. 61: 1-29. 1916.
3. Fulton, H. and Coblentz, W. W. The fungicidal action of ultra-violet light. J. Agr. Research. 159-160. 1929.
4. Hutchinson, A. H. and Ashton, M. R. The specific effects of monochromatic light on the growth of *Paramoecium*. Can. J. Research. 1: 292-304. 1929.
5. Hutchinson, A. H. and Newton, D. The specific effects of monochromatic light on the growth of *Yeast*. Can. J. Research. 2: 249-263. 1930.
6. Priestley, J. H. and Pearsall, W. H. Growth studies II. An interpretation of some growth curves. Ann. Botany 36 (142): 239-249. 1922.
7. Ramsay, G. B. and Bailey, Alice. Effects of ultra-violet radiation upon sporulation in *Macrosporium* and *Fusarium*. Botan. Gaz. 89 (2): 113-137. 1930.
8. Robertson, T. B. The chemical basis of growth and senescence. Monographs of Experimental Biology, 1923.
9. Stevens, F. L. Effects of ultra-violet radiation on various fungi. Botan. Gaz. 86 (1): 210-226. 1928.
10. Stevens, F. L. The sexual stage of fungi induced by ultra-violet rays. Science, n.s. 67: 514-515. 1929.

FEED FLAVOR OR STABLE ODOR IN MILK CAUSED BY AN ATYPICAL STRAIN OF *AEROBACTER OXYTOCUM*[1]

By Wilfrid Sadler[2] and M. Lenora Irwin[3]

Abstract

A cultural study was made of an organism of the *Escherichia-Aërobacter* group in connection with the production of an alleged feed flavor or stable odor in milk. A tentative classification of the organism as an atypical strain of *Aërobacter oxytocum*, (Migula) Bergey et al., is based on the sum of its characteristics. The suggestion is made that the organism may be defined as a new species within the genus *Aërobacter*, but until other characteristically identical strains have been isolated, this is merely tentative.

Introduction

In a recent paper Sadler, Irwin and Golding (5) have shown that a common so-called feed flavor or stable odor in milk is to be attributed to organisms of the *Escherichia - Aërobacter* group. The typical organism responsible was isolated from corn silage, but no evidence that it was to be found in all corn silage was presented. The flavor produced by the culture is difficult to define, but it is not necessary to detect the organism by means of flavor owing to the characteristic odor developed. Cheese made from milk infected with the organism is unsuitable for the market, and cultures developed from colonies picked from such cheese proved to be characteristically identical with the original strain with which the milk had been inoculated. The paper referred to (5) contained a rather full account of the inquiry, particular attention having been given to establishing proof that the organism isolated was the cause of the alleged feed flavor. The present paper confines itself primarily to recording the cultural characteristics of the organism.

The Cultural Study

Media Employed

Agar gelatine, and the various differential media used in the study were prepared from the desiccated media of The Digestive Ferments Company of Detroit, Michigan, and were sterilized under 14 lb. pressure for 20 min.

Glucose gelatine: Difco nutrient gelatine to which 1% glucose was added before sterilizing.

Milk: Skim milk was placed in test tubes and sterilized under 14 lb. pressure for 20 min.

Litmus milk: Skim milk, to which sufficient azolitmin solution to give the required color had been added, was employed and was sterilized as described for milk.

[1] *Manuscript received May 22, 1930.*
Contribution from the Department of Dairying, University of British Columbia.
[2] *Director of the Department of Dairying, University of British Columbia.*
[3] *Research Assistant, Department of Dairying, University of British Columbia.*

Milk: In flasks for smelling and tasting, steamed for one, two or three days as the particular trials demanded.

Carbohydrates: Of the carbohydrates used in the fermentation determinations, glycerol, adonite, trehalose, inosite, glycogen, and aesculin were obtained from various sources. All other carbohydrates employed were products of The Digestive Ferments Company. The method of preparing the media for the fermentation studies and the procedure followed in using them is given in a subsequent section.

Morphology

Microscopically, from a 17-hour old nutrient agar culture at 37° C., the organism appears as short, thick rods, varying in length; the majority are slightly longer than broad, some long forms being noted. It appears non-motile when the condensation water from young nutrient agar slopes is used after frequent transfers at 3-hour periods, and it is grown at 37° C. The reaction to the Gram stain was variable but, following strictly Hucker's modification of the Gram procedure, the organism was shown satisfactorily to be Gram negative.

Nutrient Agar Colonies

Kept 48 hr. at 23° C., the colony was raised, particularly at the centre, and thick, edges entire, colony dirty white by transmitted light, many colonies 1 mm. diameter, some 5 mm. diameter, some colonies punctiform. A putrid nauseating odor came from the plates.

Peptonized Milk Gelatine Colonies

After 24 hr. at 23° C., some surface colonies 2 mm. diameter, many 1 mm. diameter; in the more crowded plates, gas pockets and bubbles formed around colonies.

McConkey's Bile Salt Lactose Agar Slope

After 36 hr. at 37° C., growth raised, thick luxuriant pink; outer part dirty white to cream, by reflected light.

Eosin Methylene Blue Agar Slope

After 24 hr. at 37° C., growth luxuriant and raised; centre part of slope pink, merging into purple, then translucent white; by transmitted light medium pink-eosin; lower part of slope eosin to blue; by reflected light, growth along track of needle royal purple but grey at side. Medium glistening but not metallic, forced up in the tube by the gas evolved.

Simmons Citrate Agar

After 24 hr. at 37° C., blue along track of needle, raised luxuriant growth; by reflected light medium and iridescent blue.

Nutrient Gelatine Stab

After 24 hr. at 23° C., growth in stab and on surface, no liquefaction even after 59 days.

Glucose Gelatine

After 24 hr. at 23° C., growth in stab and on surface, gas bubbles along track of needle, surface growth heavy, iridescent, porcelain to dirty white; after 12 days good growth in stab and on surface, no liquefaction; after 59 days no liquefaction.

Litmus Milk

After 24 hr. at 30° C., litmus bleached, no clot, gas produced on surface and much gas on tilting the tube.

After 24 hr. at 37° C., litmus bleached, clot formed, and much gas on surface of clot, curd broken by gas production; evolution of gas may be observed after 5 hr. incubation, and bleaching of litmus takes place within 12 hr.

Milk

After 24 hr. at 30° C., no clot, gas on surface and much gas observed on tilting the tube.

After 24 hr. at 37° C., clot, curd slightly broken by gas, much gas observed on tilting the tube. Inoculations from a young milk culture to the extent of 1% produced the odor characteristic of the so-called feed flavor in 1.5 hr.—the milk having been warmed to the temperature of the incubator prior to being inoculated. In three to four hours the odor was strong and penetrating.*

Biochemical Reactions

Indol production	:	Indol not produced
Reduction of nitrates	:	Nitrates reduced to nitrites
Voges-Proskauer reaction	:	Positive**
Methyl Red reaction	:	Negative
Catalase Production	:	(after Orla-Jensen (4)) Catalase produced: reaction rapid and violent.

Fermentation of Carbohydrates

Fermentation of Carbohydrates

For the determination of the acid and gas formed from the various substances used, the shake agar method was employed. With the exception of adonite on account of its cost, and of aesculite, because of the difficulty of using a greater concentration, which were added to the extent of 0.5%, the carbohydrates were added to nutrient agar to the extent of 2%. Brom-cresol-purple was used as an indicator. Portions of about 8 cc. of the various sugar media were placed

* *The action of the organism in milk of various temperatures has been reviewed previously and reference made to the alleged feed flavor as well as to the significance of the organism in cheese-making (5).*

** *The production of acetyl-methyl-carbinol as defined by the Voges-Proskauer test is characteristic. The results are positive both at 30° and 37° C., when using broth cultures incubated for 18, 24, 36, and 48 hr. respectively. After three days incubation the positive result is barely noticeable, and after four days the reaction is negative. The test is more clearly defined when applied to cultures grown at 30° C., than to those grown at 37° C.*

in tubes 6 in. long and 0.6 in. in diameter, and these placed in an autoclave for 20 min. under 13 lb. pressure. A 17-hr. old nutrient broth culture grown at 37° C., was used for inoculating. In order to get results as closely comparable as possible, a similar amount of the broth—the quantity held by a loop 2 mm. in diameter—was added to each melted sugar agar. Each agar tube was immediately rotated in such a manner that the medium was not distributed around its walls, and it was placed in cold water. After setting, the inoculated tubes were placed in a water-bath so as to reach as rapidly as possible the approximate temperature of incubation; they were then transferred to the incubator kept at 37° C. The tubes were examined after an incubation of four hours and at regular intervals to 10 and 12 hr. incubation. All inoculated media were again examined after 24 hr. Each tube being removed from the autoclave to be examined was held in a water-bath at a suitable temperature.

The following carbohydrates and higher alcohols were used: xylose, arabinose, rhamnose, glycerol, adonite, sorbite, dulcite, mannite, inosite, laevulose, glucose, mannose, galactose, saccharose, maltose, lactose, raffinose, inulin, dextrin, soluble starch, glycogen, salicin, aesculin, trehalose.

Gas was produced to a greater or lesser extent in every case within 24 hr. at 37° C., but the organism showed distinct preferences and was much more rapid and violent in its action on some sugars than on others.

Acid and gas formation was evident in laevulose, saccharose, maltose and trehalose after four hours incubation. After 12 hr. the saccharose-agar and mannite-agar were violently split, and the media blown up in layers almost to the top of the tube. After 24 hr. the agar containing glycerol, arabinose, dulcite, sorbite, mannite, laevulose, glucose, mannose, saccharose, maltose, raffinose and salicin was split in layers by the gas evolved and blown to the top of the tube, the gas spaces resembling a spider's web. Of the disaccharides, saccharose was most readily attacked; both saccharose and maltose were more readily attacked than lactose, the change to acid of the latter being slow. In arabinose-agar the organism was much more active than in xylose-agar. Of the alcohols, mannite is preferred by the organism. Activity, with the higher polyoses was less evident than with the foregoing; gas bubbles appeared within six hours in starch-agar, inulin-agar and glycogen-agar, but later in dextrin-agar. In the case of the higher polyoses, the acid formed was insufficient to change the indicator completely, and there was no splitting and blowing up of the media.

Classification

The organism studied relates itself to certain strains reported upon by Levine (3); more especially with respect to the production of acetyl-methyl-carbinol, the preference shown for saccharose and the action on starch. The sum of its characteristics places the organism within the genus *Aërobacter*, and it is to be considered as a strain allied to *Aërobacter oxytocum* (Migula) Bergey et al. (1). Certain cultural differences are to be noted however. *Aërobacter oxytocum* produces indol, and fails to give any characteristic odor in

culture media. The organism under study fails to produce indol, but gives a characteristic odor in milk and a disagreeable odor on nutrient agar. The optimum temperature for *Aërobacter oxytocum* is 37° C. (5), whereas for the present culture 30° C. appears to be as suitable as 37° C. for the production of acetyl-methyl-carbinol.

Should more strains, in a study now under way,* be shown to ally themselves characteristically with the organism discussed in this paper, the definition of this organism as a new species within the genus *Aërobacter* may be suggested. The conclusion based on the present results, however, is that the organism as an atypical strain of *Aërobacter oxytocum*, (Migula) Bergey et al., (1) is responsible for the production of an alleged feed flavor in milk.

Acknowledgment

The authors wish to acknowledge with thanks the kind assistance of Miss Gladys Pendray in certain of the fermentation studies.

References

1. BERGEY, D. H. Manual of Determinative Bacteriology, 3rd ed. Baltimore, 1930.
2. JOHNSON, B. R. and LEVINE, M. Characteristics of Coli-like Microörganisms from the Soil, 1917.
3. LEVINE, M., WEEDIN, J. C. and JOHNSON, B. R. The Voges-Proskauer and Correlated Reactions of Coli-like Bacteria, 1917.
4. ORLA-JENSEN, S. Dairy Bacteriology, translated by Arup. London, 1921.
5. SADLER, W., IRWIN, M. L. and GOLDING, N. S. The Milk Dealer, 1929.

* *Following the work previously reported (5) and the present work, a grant was made by the National Research Council of Canada so that the inquiry might be expanded. The investigation is being undertaken jointly by the Department of Animal Husbandry and the Department of Dairying of the University of British Columbia.*

SPECIFIC HEATS AND LATENT HEAT OF FUSION OF ICE[1]

By W. H. Barnes[2] and O. Maass[3]

Abstract

Values for the heat capacities of ice and resulting water from initial temperatures of between 0° C. and −78.5° C. to a final temperature of +25.00° C. are measured to ±0.05% or better with an improved adiabatic calorimeter previously described. The specific heats of ice over the temperature range 0° C. to −80° C. are found and the latent heat of fusion of ice at 0° C. is obtained from these heat capacity determinations.

Introduction

In a recent paper (3) the authors have described a new adiabatic calorimeter involving the use of a radiation thermel. A series of measurements of the heat capacities and the latent heat of fusion of ice were included, to illustrate the method of procedure with this calorimeter and to find some measure of the accuracy of the results obtained. Using a Beckmann thermometer to determine the temperature changes in the calorimeter, it was found that results could be reproduced with an accuracy depending on the probable error in reading the thermometer, about 0.2% in the work described.

Due to the importance of these constants for ice it was considered of interest to repeat the measurements with a view to obtaining the highest accuracy possible with the calorimeter. For this purpose the Beckmann was replaced with a platinum resistance thermometer as described in the paper referred to (3) and the results obtained for the specific heats and latent heat of fusion of ice are presented in the present paper.

Apparatus and Experimental Procedure

The apparatus employed was the adiabatic calorimeter in its latest form with radiation thermel and platinum resistance thermometer as described in detail in the previous paper (3).

Ordinary distilled water was redistilled in an all-platinum still and subsequently boiled in platinum before filling the container.

The procedure adopted was the same as that already described with certain obvious changes necessitated by the presence of the platinum resistance thermometer.

A typical time-temperature curve is shown in Fig. 1 where R is the reading of the platinum resistance thermometer in the outer bath and T is the time. In this particular example the initial temperature of the container was −4.60°C. and the final temperature (corresponding to 2.86378 ohms) was 25.04° C. The time at which the container was introduced was 12.37½ p.m. and the

[1] *Manuscript received July 19, 1930.*
Contribution from the Laboratory of Physical Chemistry, McGill University, Montreal.

[2] *Sessional Lecturer in Physics, McGill University, and holder, at the time, of a fellowship under the National Research Council.*

[3] *Professor of Physical Chemistry, McGill University.*

drop in the curve at this time is (3.05155-2.86378) or 0.18777 ohms, which corresponds to 1.8907° C. The total water equivalent of the inner calorimeter (including water) is 854.65 cal. per degree, so that the heat absorbed by container and contents from −4.60° C. to +25.04° C. is equal to (854.65×1.8907) or 1615.9 cal. The heat capacity of container and water near +25° C. is 15.906 cal. per degree so that the correction to be applied to the total heat taken up by container and contents for a final temperature of 25.00° C. is 0.6 cal. The total heat from −4.60° C. to +25.00°C. therefore is equal to 1615.3 cal. This is the result for experiment No 18 in Table I page 207.

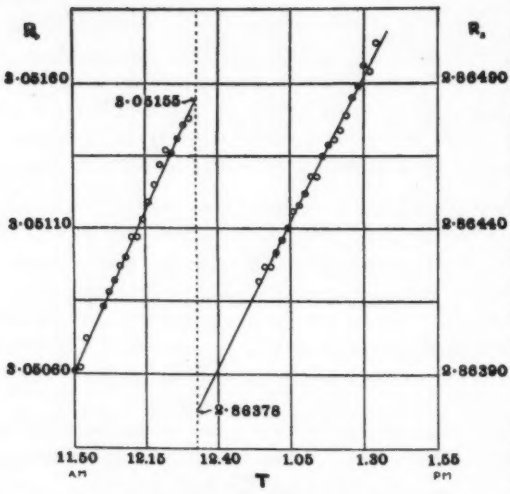

FIG. 1. *Time-temperature curve.*

Determinations of heat capacities were made with initial temperatures between the sublimation point of solid carbon dioxide (about −78.5° C.) and 0° C. The temperatures of thermostats between 0° C. and −25° C. were determined by means of standard Beckmann thermometers and were kept constant to ±0.05° or better. For those at about −30° C. and −50° C. a calibrated platinum resistance thermometer was employed and temperatures were kept constant to within ±0.1°. The temperature of the sublimation point of carbon dioxide was found from the formula, $t = -78.51 + 0.01595\,(p-760) - 0.000011\,(p-760)^2$ (6) by substitution of the barometric pressure (p). The mean temperature of −78.57° C. has been taken for this point because in no experiment did the calculated value differ by more than 0.1° from this figure.

Experimental Results

The results of all the experiments, for the container filled, are set forth in Table I where column 1 gives the number of the experiment, column 2 the initial temperature and column 3 the value obtained for the total heat of ice and container from the initial temperature to +25.00 °C.

In the calculations which follow, the results of experiments 1 to 4 inclusive have been discarded because they represent the first tests made with the new apparatus and the technique of reading the temperatures of the outer bath with the platinum resistance thermometer had not been perfected. Of the remaining experiments the following have been selected as the best values at the temperatures indicated: at −2.60° C., experiments 11, 12, 14; at −4.60° C.,

TABLE I

TOTAL HEATS OF ICE AND CONTAINER

Experiment	Initial temperature (° C.)	Total heat (cal.)	Experiment	Initial temperature (° C.)	Total heat (cal.)
1	−78.5	2154.4	25	−15.17	1702.2
2	−78.5	2156.2	26	−15.17	1700.3
3	−78.5	2158.6	27	−15.17	1699.8
4	−78.5	2155.1	28	−15.17	1700.3
5	−78.54	2145.4	29	−19.99	1737.2
6	−78.59	2142.7	30	−19.99	1737.2
7	−78.57	2156.4	31	−19.99	1737.7
8	−78.50	2154.1	32	−25.01	1777.2
9	−78.62	2155.7	33	−25.01	1775.9
10	−78.60	2157.2	34	−25.01	1776.9
11	− 2.60	1598.1	35	−25.01	1777.3
12	− 2.60	1598.3	36	−30.05	1817.7
13	− 2.60	1596.7	37	−30.05	1815.8
14	− 2.60	1597.7	38	−30.05	1815.0
15	− 4.60	1615.9	39	−30.05	1816.8
16	− 4.60	1612.2	40	−30.05	1816.8
17	− 4.60	1614.9	41	−30.05	1817.0
18	− 4.60	1615.3	42	−50.15	1963.8
19	−10.15	1660.3	43	−50.15	1962.7
20	−10.15	1660.7	44	−50.15	1966.4
21	−10.15	1658.1	45	−50.15	1965.2
22	−10.15	1658.4	46	−50.15	1963.2
23	−10.15	1659.8	47	−50.15	1960.8
24	−10.15	1660.4			

experiments 15, 17, 18; at −10.15° C., experiments 19, 20, 23, 24; at −15.17° C., experiments 26, 27, 28; at −19.99° C., experiments 29, 30, 31; at −25.01° C., experiments 32, 34, 35; at −30.05° C., experiments 36, 39, 40, 41; at −50.15 °C., experiments 42, 43, 44, 45, 46, 47; at −78.57° C., experiments 7, 8, 9, 10.

With regard to these selections the following remarks obtain. In all cases three out of four, or four out of six, results have been chosen which agree with one another to better than one part in 1,000. In only one set, namely at −15.17° C. is a discarded result higher than the selected ones. It will appear later that the greatest sources of error involve a gain in heat by the container, tending to decrease the measured heat capacity, so that the highest values obtained should be more nearly correct. No selection is possible among the six results at −50.15° C. because the values are distributed evenly over the range between the highest and lowest figures.

Values for the total heats of the container filled with dry air and sealed with DeKhotinsky cement (as in the experiments with ice) are tabulated below in Table II where the first column gives the number of the experiment, column 2, the initial temperature, and column 3, the total heat in calories required to warm the container from the initial temperature to +25.00° C. Of the results included in this table, only that for experiment 1 was discarded.

TABLE II

TOTAL HEATS OF CONTAINER

Experiment	Initial temperature (° C.)	Total heat (cal.)	Experiment	Initial temperature (°C.)	Total heat (cal.)
1	0.0	23.73	7	−30.05	53.10
2	0.0	24.25	8	−50.15	71.10
3	0.0	24.59	9	−50.15	70.31
4	−15.0	39.28	10	−78.43	101.48
5	−15.0	38.46	11	−78.46	100.74
6	−30.05	52.47			

In the case of the container alone the heat drop in the calorimeter was very much less than in the experiments with the container and ice, so that the agreement among the results at the various temperatures is not so high as for the latter determinations. Since a subtraction is involved, however, a difference of one calorie in the total heats of the container represents less than one part in 1,000 difference between values for the total heats of ice.

The values for the total heats of ice and container given in Table I are subject to a number of corrections:

1. Correction for heat capacity of air in container.

The volume of the air was 6.31 cc. and hence its mass was 0.00816 gm. Taking the specific heat (C_v) as 0.2 cal. per gm. (11) the heat capacity per degree is 0.001632 cal. so that the heat capacity (for example) from −78.57° C. to +25.00° C. is equal to 0.2 cal.

2. Correction for deposition of moisture during temperature drop in vapor-saturated space above the water in the closed inner calorimeter vessel.

The volume of the space was 275 cc. The mass of water vapor present in this space at the initial and final temperatures of the calorimeter was found from tables (7). The mass of water condensed during this temperature change was calculated and the number of calories involved was found by taking the latent heat of evaporation at about 25° C. as 582 cal. per gm. (5).

For example in the experiments at −78.5° C. the temperature drop in the calorimeter was of the order of 2.5°. Between 20° and 25° C. the number of grams of water vapor per cubic metre changes by about 1.14 gm. per degree. For a 2.5° drop in temperature this means the deposition of about 2.85 gm. from a space of one cubic metre or 0.000784 gm. from 275 cc. with an evolution in the latter case of about 0.5 cal. during the process.

3. Correction to the water equivalent of the calorimeter for the heat capacity of known weights of vaseline on flanges of cover.

Taking the specific heat of vaseline as of the same order of magnitude as that of petroleum, 0.511 cal. per gm. per degree (10) this correction was calculated for each experiment. The figures obtained were never more than 0.5 cal. and the average magnitude was 0.2 cal.

4. Corrections for the evaporation of water into the space above it in the container, and for the heat capacity of the water vapor in the air space in the closed inner calorimeter vessel.

These corrections have been neglected since their sum amounts to less than 0.1 cal. in all cases.

Table III gives the corrected values for the total heats of container and ice (column 5). For the sake of brevity the figures for correction factor 3 for each experiment are not shown. In this table column 1 contains the initial temperatures, column 2 the average values of the total heats after correction factor 3 was applied, columns 3 and 4 the values for corrections 1 and 2, respectively, and column 5 the figures for the corrected total heats.

TABLE III

CORRECTED HEAT CAPACITIES OF ICE AND CONTAINER

Initial temperature in deg. C.	Average total heats (uncorrected) (calories)	Correction		Total heats (corrected) (calories)
		1	2	
− 2.60	1598.2±0.3	0.0	0.4	1597.8
− 4.60	1615.5±0.6	0.0	0.4	1615.1
−10.15	1660.6±0.6	0.0	0.4	1660.2
−15.17	1700.3±0.4	0.1	0.4	1699.8
−19.99	1737.5±0.3	0.1	0.4	1737.0
−25.01	1777.3±0.2	0.1	0.4	1776.8
−30.05	1817.2±0.6	0.1	0.4	1816.7
−50.15	1964.0±2.7	0.1	0.5	1963.4
−78.57	2155.5±1.8	0.2	0.5	2154.8

Table IV gives the same data for the container alone as is included in Table III. In addition to the two correction factors (1 and 2) the difference in the heat capacities of the amounts of DeKhotinsky cement used in sealing the container empty and full respectively is included as correction 5. Since the amount was greater for the empty container, the difference can be considered as a negative correction to the total heats of container. The weights of cement were 0.0175 gm. and 0.0142 gm. for the empty and full container respectively and the specific heat was taken as 0.48 (the value for rubber) (7, p. 793). The heat capacity of the vaseline on the calorimeter cover in these experiments (correction factor 3) was always less than 0.01 cal. and consequently has been neglected.

From a curve plotted with the values for the corrected total heats of container given in the last column of Table IV the corresponding values from the initial temperatures employed in the ice determinations were obtained.

Table V gives the final results. Column 1 contains the initial temperatures, column 2 the corrected total heats of the container from the initial temperatures to a final temperature of +25.00° C. obtained from the curve mentioned above, column 3 gives the total heats of ice found by subtracting the values in the

TABLE IV

CORRECTED HEAT CAPACITIES OF CONTAINER

Initial temperature in deg. C.	Total heats (uncorrected) (calories)	Correction			Total heats (corrected) (calories)
		1	2	5	
0.0	24.42±0.17	0.14	0.00	0.04	24.24
−15.0	38.87±0.41	0.22	0.01	0.07	38.57
−30.05	52.79±0.32	0.30	0.01	0.09	52.39
−50.15	70.71±0.40	0.41	0.02	0.12	70.16
−78.45	101.11±0.37	0.57	0.06	0.17	100.31

preceding column from the corresponding values in the last column of Table III, and column 4 records the heat capacities per gram of ice obtained by dividing the figures in column 3 by the weight of ice (14.864 gm. corrected to standard brass weights in vacuo).

The following equation represents the heat capacity curve of ice over the entire range of temperatures:

$$H=135.94+0.50107T-0.0031516T^2+0.000003276T^3 \quad \ldots\ldots 1$$

where H is the heat capacity per gram from the initial temperature (T) to +25.00° C. and T is the initial temperature in degrees absolute (0° C. = 273.1° abs.).

Values for the heat capacities calculated with equation 1 are shown in Column 5 of Table V and the differences between heat capacity values observed and calculated are given in column 6.

TABLE V

HEAT CAPACITIES OF ICE

Initial temperature in deg. C.	Total heats (calories)		Heat capacities of ice (cals. per gm.)		
	Container	Ice	(Obs.)	(Calc.)	(Difference)
− 2.60	26.8	1571.0	105.69	105.72	−0.03
− 4.60	28.7	1586.4	106.73	106.69	+0.04
−10.15	34.0	1626.2	109.40	109.35	+0.05
−15.17	38.7	1661.1	111.75	111.72	+0.03
−19.99	43.2	1693.8	113.95	113.98	−0.03
−25.01	47.9	1728.9	116.31	116.29	+0.02
−30.05	52.4	1764.3	118.69	118.59	+0.10
−50.05	71.4	1892.0	127.28	127.31	−0.03
−78.57	100.4	2054.4	138.21	138.24	−0.03

From equation 1 the heat capacity per gram at 0° C. is equal to 104.45 cal. Taking the average specific heat of water between 0° C. and +25.00° C. as 1.0020 (1) the heat capacity per gram of water over this temperature range is equal to 25.05 cal. Hence the latent heat of fusion of ice at 0° C.

$$= 104.45 - 25.05$$
$$= 79.40 \text{ cal. per gm.}$$

Differentiation of equation 1 with respect to T yields the following result for the specific heats of ice

$$-\frac{dH}{dT} = C_v = -0.50107 + 0.0063032T - 0.000009828T^2 \quad \ldots\ldots\ldots\ldots \quad 2$$

where C_v is the specific heat in calories per gram per degree at temperature T, and T is the temperature in degrees absolute.

Values for the specific heats calculated from equation 2 are given in column 2 of Table VI together with corresponding values obtained by Maass and Waldbauer (column 3) (8), Nernst (column 4) (9) and Dickinson and Osborne (column 5) (4).

TABLE VI

SPECIFIC HEATS OF ICE

Temperature, in deg. C.	M. & B.	M. & W.	Nernst	D. & O.
0	0.4873	0.485	....	0.5057
−10	0.4770	0.475	0.533	0.4871
−20	0.4647	0.465	0.478	0.4684
−30	0.4504	0.453	0.451	0.4498
−40	0.4340	0.440	....	0.4312
−50	0.4160	0.426	0.410	....
−60	0.3958	0.411	....	....
−70	0.3737	0.394	0.374	....
−80	0.3496	0.377	0.367	....

Discussion

In view of the good agreement among the various measurements given in Table I and of the small differences recorded in Table V between observed heat capacities and those calculated with equation 1, the accuracy with which this equation represents the heat capacity of ice over the initial temperature range from 0° C. to −80° C. is probably of the order of ±0.05% or better.

The value of 79.40 cal. per gm. for the latent heat of fusion agrees almost exactly with the figure (79.42) published by Maass and Waldbauer (8). It is about 0.1% or 0.2% lower than most of the more accurate values previously obtained by other investigators (2).

A contributing factor to the increasing divergence of the specific heat values given in Table VI from those of Maass and Waldbauer may arise from the fact that in plotting the heat capacity curve the latter took −78.2° C. as the sublimation point of solid carbon dioxide instead of −78.5. This has the effect of increasing the slope of their heat capacity curve and consequently leads to higher values for the specific heats.

The measurements of the heat capacities of ice were not carried out below −78.5° C. because at lower temperatures a source of error due to the method of introducing the container may become appreciable. The container filled with water was brought to the desired initial temperature in a thermostat and

was then transferred by hand to the calorimeter. During this transfer the container may gain heat by conduction, convection and radiation and a small amount of water vapor may condense on it.

The effect of these factors is to reduce the heat capacities of the container, full and empty respectively, by uncertain amounts. All of them are proportional, among other things, to a function of the temperature gradient between the container and the air through which it passes from the thermostat to the calorimeter, and to the time required to make this transfer. In the case of the deposition of water vapor the absolute humidity also becomes an important item.

In the experiments described in this paper humidity played a negligible part. This is shown by the fact that with moderately constant room temperatures, but very different relative humidity figures, no relationship is shown between relative humidity and differences in heat capacities from the same initial temperatures.

None of these factors will affect the absolute values for the heat capacities of ice, providing the times for the transference of the container when full and empty respectively are always the same. Any differences in these times will have a greater effect on the heat capacity measurements the greater the temperature gradients involved.

In Table I, with one exception (from $-15.17°$ C.), the best agreement among the experimental results from any temperature is found among the highest figures. Since all the factors involved in transferring the container entail a decrease in the heat capacity, this is to be expected from the foregoing argument, and these are the figures to which greatest weight must be attached.

Further investigation of Table I shows that, in general, it was more difficult to obtain repetition of results to better than 1 part in 1,000 from the lower initial temperatures, although these experiments involved the largest temperature drop in the calorimeter and should have been susceptible to higher accuracy of measurement. As a matter of fact the times of transference from the thermostat baths at $-30°$ C. and $-50°$ C. (the experiments which show the greatest divergency among individual results in Table I) were somewhat more uncertain than those from the baths at the other temperatures due to the arrangement of the apparatus for these particular experiments.

The accuracy of $\pm 0.05\%$ attained in these heat capacity measurements thus appears to be dependent on the method of removing the container from the thermostat to the calorimeter. At some future time it is hoped to develop the calorimeter to a stage where these effects will be eliminated or at least reduced to a measurable minimum.

References

1. BARNES, H. T. Trans. Roy. Soc. (A) 199: 149-263. 1902.
2. BARNES, H. T. Ice Engineering, p. 30. 1928.
3. BARNES, W. H. and MAASS, O. Can. J. Research. 3: 70-79. 1930.
4. DICKINSON, H. C. and OSBORNE, N. S. U.S. Bur. Standards Sci. Paper 248. 1915.
5. GRIFFITHS, E. H. Trans. Roy. Soc. (A) 186: 261-341. 1895.

6. HENNING, F. Ann. Physik, 43: 282-294. 1914.
7. HODGMAN, C. D. and LANGE, N. A. Handbook of Chemistry and Physics, p. 843. 1928.
8. MAASS, O. and WALDBAUER, L. J. J. Am. Chem. Soc. 47: 1-9. 1925.
9. NERNST, W. Theory of the Solid State, p. 90. 1914.
10. PAGLIANI, S. Atti accad. sci. Torino, 17: 97. 1881-82.
11. WOMERSLEY, W. D. Proc. Roy. Soc. (A) 100: 483-498. 1922.

THE INFLUENCE OF HYDROGEN IONS ON THE FENTON REACTION[1]

By W. H. Hatcher[2] and M. G. Sturrock[3]

Abstract

In the preparation of dihydroxy maleic acid from tartaric acid by hydrogen peroxide in the presence of ferrous sulphate, the very small yields are the result of inactivation of the catalyst by the production of the relatively strong dihydroxy maleic acid; this reaction product undergoes such rearrangement to an isomer as prevents quantitative separation. By means of conductivity measurements of the reaction mixture, the course of the reaction is accurately followed.

The existence of the tautomeric keto form of dihydroxy maleic acid, first suggested by Nef as an alternative formula, has been clearly indicated.

The search for a procedure which will improve the yield of dihydroxy maleic acid is now restricted to the discovery of some compound which will at the same time reduce the hydrogen ion concentration and shift the equilibrium in favor of the enol form.

Historical

In connection with an investigation of dihydroxy maleic acid it was necessary to prepare this substance in quantity. The method used was that devised by Fenton (3), of which further details are given by Nef (7), and the very low yields immediately attracted attention, *viz.*, approximately 20%. This method involves the treatment of tartaric acid with hydrogen peroxide in the presence of ferrous sulphate. Fenton showed the action of the ferrous ion to be purely catalytic. Von Bertalan (9) and Bohnson (1) and Bohnson and Robertson (2) have studied the action of iron salts on hydrogen peroxide, the latter proving the presence of ferric acid by ultra-violet absorption data.

These studies did not, however, account for the low yields characteristic of Fenton's reagent. It is with this phase of the reaction that this paper deals.

Experimental

The directions given by Nef call for 320 cc. of 3.5% hydrogen peroxide per 50 gm. of tartaric acid, this being almost the amount demanded by theory. Over a series of many experiments in no single case could the yields obtained by Nef be approximated when this amount of peroxide was employed. Preliminary tests showed that a decrease in the proportion of peroxide does not decrease the yield but actually increases it up to a certain point; Fenton advised using but 10% of the theoretical peroxide because he found dihydroxy maleic acid easily oxidized. It was found that the best yields were obtained by using about 4.9 gm. of peroxide per 50 gm. of tartaric acid.

Following this a great many experiments were performed with the object of improving the yield, or at least of determining the cause of the great loss. The difficult part of the procedure employed by Nef lies in the very careful

[1] *Manuscript received August 5, 1930.*
Contribution from the Chemistry Department, McGill University.

[2] *Associate Professor of Chemistry, McGill University.*

[3] *Demonstrator in the Department of Chemistry, McGill University, and formerly holder of a bursary under the National Research Council of Canada.*

addition of the dehydrating agent. Moreover, since it requires over 10 days in which to crystallize out all the dihydroxy maleic acid, the acid sodium salt was prepared in all subsequent experiments. This salt is obtained by adding a quantity of saturated sodium sulphate solution to the reaction mixture about three hours after all the peroxide has been run in. Within six or seven hours from the addition of the sodium sulphate solution all the product has separated out. Since it is much less soluble than the free acid it may be recrystallized with much less loss. Results showed as before that no greater yields were obtained when the theoretical amount of hydrogen peroxide was added than when but 22% of this amount was employed.

The several attempts to improve the yield are briefly treated in the following paragraphs.

(*A*) *Cooling of the Reaction Mixture.* Dihydroxy maleic acid decomposes easily at 60° C. and a sudden rise in temperature locally might be expected to cause decomposition. Consequently an ether-carbon dioxide mixture was used to replace the ice-salt bath: the resulting increase of only 8% did not justify continuing this procedure.

(*B*) *Racemization of the Tartaric Acid.* The tartaric acid, being the C.P. dextrorotatory variety, was first boiled for two hours with caustic soda; on neutralization with sulphuric acid and subsequent treatment no increase was noted in the desired product although it was contaminated with much sodium sulphate.

(*C*) *The Effect of More Concentrated Mixtures.* It was thought that a decrease in the total volume of the reaction mixture might result in an increase in yield. This might be brought about by a shift of the equilibrium of the two forms if there is tautomerism, or simply by decreasing the total amount of the product held in solution. Accordingly an experiment was made using 30% hydrogen peroxide solution.

When the figures found most satisfactory with the 3% solution were employed, it was discovered that the yield was but very slightly increased.

However, using one-tenth the total volume of sulphuric acid to cause separation of the free acid and 22.5 gm. of peroxide in 30% solution, 14.6 gm. of the product was obtained; this was slightly better than Nef's yield.

It was also found with this concentrated peroxide that the addition of sulphuric acid was unnecessary, the product separating out of its own accord. Accordingly in all subsequent preparations this concentration of peroxide was employed.

(*D*) *Change in the Order of Addition of Reagents*

1. Tartaric, peroxide—the whole added to the catalyst in solution: no change in yield.

2. Tartaric, sulphuric, the catalyst, and the peroxide—no reaction at all other than decomposition of the hydrogen peroxide. Obviously the hydrogen ion concentration of the mixture at the start was important.

(*E*) *Influence of Acidity.* In order to illustrate the effect of the original hydrogen ion concentration the following experiment was performed:— 100 gm. of tartaric acid was dissolved in water and the total volume made up to 160 cc. This solution was divided into eight equal parts and placed in small wide-mouthed flasks. Increasing amounts of sulphuric acid were added to the solutions as shown below (Table I). The flasks were then placed in the freezing mixture and 7.66 cc. H_2O_2 slowly added to each. (1 cc. peroxide solution = 0.358 gm. H_2O_2.)

TABLE I

INFLUENCE OF ACIDITY ON YIELD

No.	5% H_2SO_4 in cc.	H_2O in cc.	Color of final solution	Yield in gm.
a	0	20	black	1.76
b	1	19	lighter than *a*	0.37
c	2	18	lighter than *b*	0.25
d	3	17	faintly colored	—
e	5	15	colorless	none
f	10	10	colorless	none
g	5 cc. 20%	15	colorless	none

Acetic acid was found to have the same disastrous effect on the yield.

As stated above the active agent in Fenton's reagent is unstable ferric acid, ferrates being stable only in alkaline solution and decomposing in acid solutions.

Tartaric acid is a weak acid (its ionization constant at 10° C. $K_a \times 10^{-4} = 5$) (4). Dihydroxy maleic acid is a relatively strong acid, its ionization constant being approximately 100 times as great as that of tartaric ($K_a \times 10^{-2} = 7.2$) (8). It was thought possible that, as this stronger acid is prepared from the weak one, the hydrogen ion concentration so increases that the catalyst becomes inactivated. The reaction then proceeds up to the point where the ferric acid decomposes, or, as is more likely, ionizes as a base in this very acid medium, and can no longer function. At this point the reaction ceases.

In another experiment it was planned to add only one-third of the peroxide, remove the dihydroxy maleic acid and thus decrease the hydrogen ion concentration, add more catalyst and then the second third of the peroxide. The yield for the first third of the peroxide was 9.3 gm. Addition of further catalyst and peroxide produced no more of the product. The mixture apparently was still too acidic.

It was then decided to follow the change in the hydrogen ion concentration during the course of the oxidation. The hydrogen electrode is of course inapplicable and so it was decided to try the quinhydrone electrode. The ultimate object of the experiment was to find the optimum pH of the reaction solution, buffer it to this pH by means of a sodium salt and finally dissolve the salt in concentrated sulphuric acid from which the free acid itself might be crystallized.

The details of the reason for the failure of the quinhydrone electrode for this work form the substance of another publication; it is sufficient to say here that dihydroxy maleic acid is rapidly reduced to tartaric acid, thus rendering the determination of pH by this method impossible. Such intriguing consideration arose with respect to the Fenton reagent in this instance that it was decided to study this reaction thoroughly from the point of view of the influence of the hydrogen ion concentration.

The conductivity of the solution of acids which had to be dealt with in this work is due, in the main, to hydrogen ions, the relatively large and slow-moving anions and the neutral salts playing very little part in the transportation of the current. For this reason a consideration of the conductivity changes would be essentially the same as that of changes in pH.

Ordinary conductivity apparatus cannot be used because of decomposition and polarization which take place at the electrodes in hydrogen peroxide solutions. Until recently no method for conductivity measurements in the presence of hydrogen peroxide was available. Maass and Cuthbertson (5) have found that excellent results may be obtained by measuring the drop of potential across two tin electrodes inserted at fixed distances in the solution through which a current is flowing. It is their method for conductivities in hydrogen peroxide solutions which has been used in this research.

The apparatus used was the same except that a straight scale was substituted for the previous semi-circular one, and the most suitable cell was found to be one whose arms were constructed of 2 mm. bore pyrex tubing. After calibration of the scale and measurement of the cell constant it was found possible to obtain values which showed agreement better than 0.2% of the established figures.

The Static Method for Conductivities Applied to the Oxidation of Tartaric Acid by Fenton's Reagent

Preliminary experiments showed that the addition of hydrogen peroxide to tartaric acid in the presence of ferrous ions caused a steady rapid increase in the conductivity of the solution.

In this experiment no account was taken of the change in volume resulting from the addition of the peroxide solution. In subsequent experiments the solutions were made up to equal volumes after the addition of the peroxide. The results of this preliminary experiment, however, were sufficient to justify a detailed investigation of the reaction from the standpoint of conductivity changes.

As has been shown, dihydroxy maleic acid can never be obtained in anything even approaching quantitative yields and this difficulty is associated with hydrogen ion concentration. Since there is no possibility of salt formation, any increase in conductivity during the course of the reaction must be due to the production of dihydroxy maleic acid, or a mixture of dihydroxy maleic and some other acid or acids which are relatively more dissociated than tartaric. Fortunately, it was found possible to determine whether such a partition actually takes place. This is done in the following way:—

Dihydroxy maleic acid at 60° C. in aqueous solution is decomposed almost quantitatively into glycollic aldehyde and carbon dioxide (3). The former is a non-electrolyte and the latter may be removed by boiling. The conductivity of the reaction solution after boiling would be due, therefore, to the unattacked tartaric acid, to the neutral salts which play the rôle of catalysts and would be constant, and to any acids produced in the oxidation and not decomposed by the heat treatment. Dihydroxy maleic acid is the only acid whose production is possible in this reaction and which is decomposed in aqueous solution at this relatively low temperature.

Knowing the amount of hydrogen peroxide added and the amount of tartaric acid theoretically converted to dihydroxy maleic acid, the amount of tartaric remaining may be readily calculated. If no partition has taken place the conductivity of a solution containing the catalyst and this amount of tartaric acid should very nearly coincide with the conductivity of the solution after boiling.

Nef used 50 gm. of tartaric acid and one gram of ferrous sulphate in 50 cc. of water and to this added 320 cc. of 3.5% hydrogen peroxide solution, *i e*, approximately 50 gm. of tartaric acid in 400 cc. of solution. In this work solutions containing 12.5 gm. of tartaric acid, 0.3527 gm. of ferrous ammonium sulphate and increasing amounts of peroxide up to the theoretical, were diluted to 100 cc. total volume. Approximately the same concentrations, therefore, were used in both researches.

The reaction solutions were prepared by dissolving the tartaric acid and catalyst in a very little water contained in a standard 100 cc. volumetric flask. The peroxide was added as rapidly as possible and the volume increased to the mark by the addition of boiled and cooled distilled water. During the addition of the peroxide it was found necessary to keep the solution cooled by surrounding the volumetric flask with an ice-salt mixture. After thorough mixing the solutions were transferred to large pyrex test tubes kept in an ice-water bath. The cell and a standard thermometer were then inserted and when the solution had cooled uniformly to 0.5° C. conductivity readings were taken against time.

After the conductivity had shown no further change over a period of several hours, the solutions were allowed to stand over night in contact with platinum foil at 0° C. This precaution was taken to ensure against further oxidation during the heat treatment, which might result should there be any residual peroxide. The following morning the platinum was removed and the solutions warmed to 65° C. on a water bath for a period of about 90 min., and then finally boiled. The contents of the tubes were washed into the original volumetric flask, cooled to 0.5° C., diluted to the mark and the conductivities taken as before.

It might be mentioned here that standard volumetric apparatus and thermometers were used exclusively throughout this entire work. The apparatus was dried by means of specially purified alcohol and ether. The hydrogen peroxide employed was specially distilled.

A preliminary experiment, in which the requisite peroxide was added by degrees to the mixed tartaric acid-catalyst solution and readings of the resistance taken after each addition, showed an increase of nearly 70% in the specific conductivity of the solution.

Table II shows the conductivity C of solutions of tartaric acid and ferrous ammonium sulphate mixed.

TABLE II

CONDUCTIVITY OF TARTARIC ACID SOLUTIONS

Tartaric acid (in gm.)	Ferrous ammonium sulphate (in gm.)	$C \times 10^{-3}$
12.500	0.3527	7.17
10.000	0.3527	6.82
7.500	0.3527	6.28
5.000	0.3527	5.54
3.750	0.3527	5.08
2.500	0.3527	4.47

NOTE:—*Temp. = 0.5° C. Volume of solutions, 100 cc. These values are plotted in Fig. 2; Curve III, will be referred to as the "Tartaric acid reference curve".*

Table III shows briefly the values obtained when constant quantities of tartaric acid and ferrous ammonium sulphate are treated with varying quantities of hydrogen peroxide in a constant volume at 0.5° C. The technique consisted in making up a solution to contain 12.500 gm. of tartaric acid, 0.3527 gm. of ferrous ammonium sulphate, and the required quantity as shown of hydrogen peroxide, diluting the whole to 100 cc., and measuring the resistance at frequent intervals at 0.5° C. When the resistance had become constant, this mixture was subjected to the heat treatment previously mentioned; its resistance, after suitable dilution to 100 cc., was again measured at 0.5° C. Fig. 1 contains the time-resistance curves for those mixtures labelled A, B, C and D. No resistance values could be obtained for E and F since the conductivity was so high that electrolysis set in; the values after heat treatment, however, were obtained.

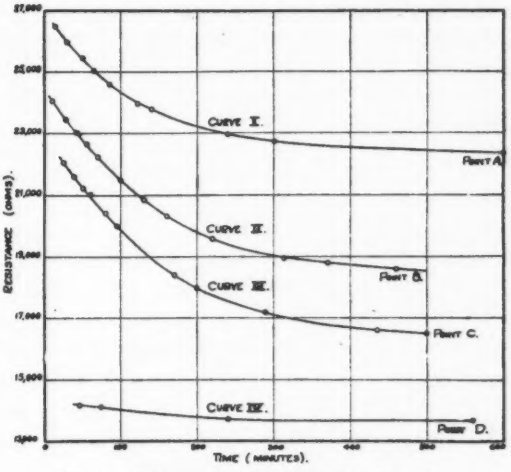

FIG. 1. *The influence of hydrogen ions on the Fenton reaction. Time-resistance curves.*

TABLE III

CONDUCTIVITY OF TARTARIC ACID SOLUTIONS IN PRESENCE OF VARIOUS AMOUNTS OF HYDROGEN PEROXIDE

Experiment No.	Point	Theoretical amount of peroxide, in %	Resistance at end of reaction (ohms)	Resistance after heat treatment (ohms)	$C\times10^{-3}$ at end of reaction	$C\times10^{-3}$ after heat treatment
1		0	28,770	—	7.17	—
2	A	17.0	22,302	29,995	9.24	6.87
3	B	33.5	18,547	28,993	11.12	7.11
4	C	49.9	16,542	28,107	12.46	7.34
5	D	66.5	13,683	24,118	15.17	8.55
6	E	83.6	—	15,078	—	13.67
7	F	98.8	—	14,489	—	14.22

These results are illustrated in Fig. 2 where curve I shows the conductivity at the point in the table which corresponds to a certain hydrogen peroxide content after reaction, as determined by change in resistance, had ceased; curve II shows the conductivity for the same point after heat treatment. Curve III is the tartaric acid reference curve.

Discussion of Results

A consideration of the work of Bohnson (1), who showed that the catalyst acting in oxidations by Fenton's reagent is ferric acid, led to the belief that the catalyst is inactivated and the reaction stopped when a certain critical hydrogen ion concentration is attained. This was inferred from the fact that ferrates are stable only in alkaline solution (6), and that the acidity of the solution in this case must rapidly increase with the formation of the relatively strong product. The results obtained substantiate this assumption to a remarkable degree.

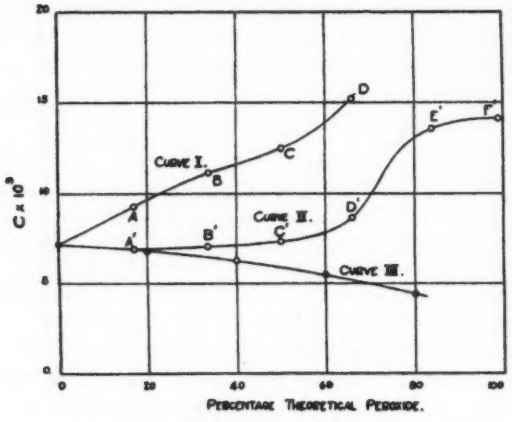

FIG. 2. *The influence of hydrogen ions on the Fenton reaction.*

The yields of dihydroxy maleic acid vary up to about 30% of the theoretical. It was expected, therefore, that the conductivity curve would rise sharply up to the point where 30% of the theoretical amount of hydrogen peroxide had been allowed to react. At this point it was expected that the curve would fall off to a constant level.

Curve I in Fig. 2 represents the results of experiments which show a steady increase in hydrogen ion concentration up to the point where 60% peroxide had been added. At this point there is a remarkable rise rather than a falling off to a constant level as was expected.

Curve II, Fig. 2, represents the points "A", "B", "C", etc. after the dihydroxy maleic acid had been removed by heat. Curve III, Fig. 2, is called the "Tartaric acid reference curve." It represents the theoretical position of the points of the curve immediately above, providing only dihydroxy maleic acid is produced in the reaction and this subsequently removed by heat. The fact that Point "A" falls at its theoretical position on the "Reference curve" is important. This shows primarily that the wide spread between curves I and II is due to dihydroxy maleic acid. It also shows that up to the point where 30% of the peroxide has been added, only dihydroxy maleic acid was produced.

The most striking observation which results from a consideration of the three curves in Fig. 2 is the remarkable increase in conductivity which takes place in the two reaction curves at 60% peroxide. This definitely proves a sharp change in the course of the reaction at this point where it must be assumed that some acid unaffected by the heat treatment has been produced. This acid is difficult of identification, but oxalic acid is suggested as the most likely. Thus are the low yields partially accounted for by the sudden deviation in the course of the reaction. The yields are 30%, the loss 70%. Forty of this 70% is accounted for by the shift in the course of the reaction which takes place at 60% peroxide. The other 30 remains to be accounted for.

It is significant that the darkening of the reaction mixture, characteristic of this oxidation, first manifests itself at the same point as the sudden rise in the conductivity curve. This darkening may be due to colloidal iron salts resulting from the decomposition of the catalyst, or it may be due to a combination of the iron salts and some product of the reaction. The color reaction of iron salts with compounds containing hydroxyl groups is well known.

Possible explanations for the unsatisfactory yields may be advanced because of the tautomerism and geometrical isomerism which may be applied to dihydroxy maleic acid. To these must be added the possibility of steric isomerism of the keto tautomer. This last is but a minor consideration, since it is very unlikely that there would be a difference in solubility of the two optically active forms sufficient to account for anything but a fraction of the loss which has not already been explained.

The evidence outlined which gave rise to the idea of a tautomeric change becomes more important now that all the loss cannot be accounted for on the basis of inactivation of the catalyst or change in the course of the reaction. This evidence is, therefore, repeated here and is as follows:—

(1) The extremely poor yields indicate a partition, an equilibrium or an incomplete reaction. It is shown that the partition occurs when the reaction is 60% complete. Since the yields are but 30%, there must be both a partition and an equilibrium.

(2) The decomposition of dihydroxy maleic acid in aqueous solution by heat is not quantitative, and the completeness of the reaction estimated by CO_2 absorption is dependent on the medium in which the acid is decomposed more than on such factors as temperature and concentration.

(3) The main product besides glycollic aldehyde and carbon dioxide is glyoxylic acid.

The mechanism suggested by Fenton for the decomposition of dihydroxy maleic acid into glycollic aldehyde and carbon dioxide depends on the previous addition of water across the double bond with the production of trihydroxy succinic acid. This latter then gives up two molecules of CO_2 and one molecule of water, and the aldehyde remains. Represented graphically these changes are as follows:—

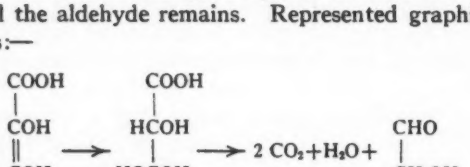

No mention is made of the mechanism by which the glyoxylic acid is produced.

The glyoxylic acid might very possibly arise from a decomposition of the keto form of dihydroxy maleic acid in accordance with the following equations:

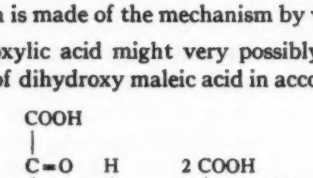

Additional evidence, however, appears in support of this idea, and the further study of this very complicated reaction from the standpoint of tautomerism is here strongly recommended.

Assuming that the conception of a tautomeric change is correct, it is quite within reason to expect that this equilibrium will be more or less dependent on the hydrogen ion concentration of the solution. It would make a very interesting investigation if the decomposition of the reaction mixture were followed by means of CO_2 absorption. This has been done by Fenton on solutions of the pure product but not on the reaction mixture itself.

If the equilibrium is dependent on the hydrogen ion concentration the explanation of the addition of the fuming sulphuric acid which "salts out" the product during its preparation is obvious.

It was stated above that the fact that Point "A" falls in its theoretical position on both curves II and III proves that up to this point only dihydroxy maleic acid, or some acid very closely related and equally readily removed by

heat, is produced. This means that at Point "A" on Curve I the reaction solution must be

$\frac{184}{150} \times \frac{12.5}{18.4} \times \frac{16.98}{4 \times 100} = 0.1415M.$ with respect to dihydroxy maleic acid alone.

Attempts to check the Point "A" on Curve I by the addition of the required amount of dihydroxy maleic acid to the solution represented by the Point "A" on Curve II were unsuccessful. It was found impossible to dissolve even a small fraction of the required quantity in the 100 cc. of solution, even after several hours shaking.

Again, Skinner (8) has found that solutions of dihydroxy maleic acid show a decrease in conductivity with time. He explains this on the basis of a slow decomposition of the acid into CO_2 and glycollic aldehyde. It was found that freshly prepared solutions of dihydroxy maleic acid in contact with excess of the solid showed conductivity increases with time. This is interpreted here as slow solution and a tautomeric change.

Still one more important consideration remains. It was shown that at the Point "A" on Curve I the solution must be $0.1415M.$ with respect to dihydroxy maleic acid. This acid is relatively strong, since its ionization constant as determined by Skinner approaches that of oxalic acid. Attempts to measure the conductivity of a $0.125M.$ solution of oxalic acid, using the conductivity cell employed throughout this whole research, were unsuccessful. Electrolysis commenced as soon as the primary circuit was closed.

Conductivity measurements prove that the product is removed completely by heat. They also prove that the product cannot consist entirely of dihydroxy maleic acid. These experimental facts point conclusively to the formation of some weak organic acid which is much more soluble, and, at the same time, much less ionized than dihydroxy maleic acid and yet so closely related that it is either converted to the latter acid or itself decomposed by mild heat treatment. The tautomeric keto-malic acid is suggested.

References

1. BOHNSON, V. L. J. Phys. Chem. 25: 19-54, 1921.
2. BOHNSON, V. L. and ROBERTSON, A. C. J. Am. Chem. Soc. 45: 2493-2503, 1923.
3. FENTON, H. J. H. J. Chem. Soc. 65: 899-910, 1894; 67:774-780, 1895; 87:804-818, 1905.
4. JONES, H. C. and GETMAN, F. H. Am. Chem. J. 32: 308-338, 1904.
5. MAASS, O. and CUTHBERTSON, A. C. J. Am. Chem. Soc. 52: 489-499, 1930.
6. MELLOR, J. W. Inorganic Chemistry, 1916, p. 498.
7. NEF, J. U. Ann. 357: 214-312, 1907.
8. SKINNER, S. J. Chem. Soc. 73: 483-490, 1898.
9. VON BERTALAN, J. Z. phys. chem. 95: 328-348, 1920.

THE HEATING OF ELECTROLYTES IN HIGH FREQUENCY FIELDS[1]

By J. C. McLennan[2], F.R.S., and A. C. Burton[3], M.A.

Abstract

In this investigation the heating of solutions of simple electrolytes of varying concentrations when irradiated by short electromagnetic waves from 10 to 200 metres in length was measured. It was found that for a given wave-length there is a maximum heating effect produced in a medium, the specific conductivity and dielectric constant of which are connected with the frequency by a simple law. This law, proved theoretically as well as shown experimentally to hold for dilute solutions is $\frac{2C}{nK} = 1$ where C = specific conductivity in absolute units, K = dielectric constant and n = frequency of wave.

"Skin effect" was shown theoretically and experimentally to be negligible for substances having the low conductivities studied and deep-seated heating effects were shown to be attainable with the radio waves used. The possibility of directed selective heating effects is suggested and illustrated by experiments on blood. The law shown to apply in these experiments was used to evaluate the dielectric constant of water.

Considerable interest has recently been aroused by the discovery that curious and unexpected physiological and biological effects are produced by short electromagnetic waves of wave-lengths 50 meters and under. Gosset, Cutmann, Lakhowsky and Magron (7) in 1924 reported an effect on plant tumors, whilst Schereschewsky (14) in 1926 noted their lethal effect on mice and inferred that certain wave-lengths had a specific effect on living cells. The production of fever in men has since been observed (2). Later experiments, however, by Wood and Loomis (15), Hosmer (8), Kahler, Chalkley and Voegtlin (9), and Christie and Loomis (3), have shown that all the phenomena observed so far can be explained as due to simple heating effects. No direct action on bacteria or living cells, other than that of heating, has yet been demonstrated.

The production of these heating effects by high frequency fields has, however, many far-reaching possibilities of application in medical science. In view of this, enabled by a National Research Council grant and the gift of a high frequency heater apparatus by the General Electric Company, the present research was undertaken to investigate the physical causes of the phenomena and what physical properties of the heated medium will condition them. During the progress of the work, publication of a research on somewhat similar lines was made by Loomis and Richards (13). Their method of attack differs from ours as explained below.

Method of Investigation

As a preliminary research, the heating of solutions of various concentrations of simple electrolytes when placed in the field of the oscillator was investigated.

[1] *Manuscript received May 30, 1930.*

Contribution from the Physical Laboratory of the University of Toronto, Canada, with financial assistance from the National Research Council of Canada.

[2] *Professor of Physics and Director of the Physical Laboratory, University of Toronto.*

[3] *Research student, University of Toronto.*

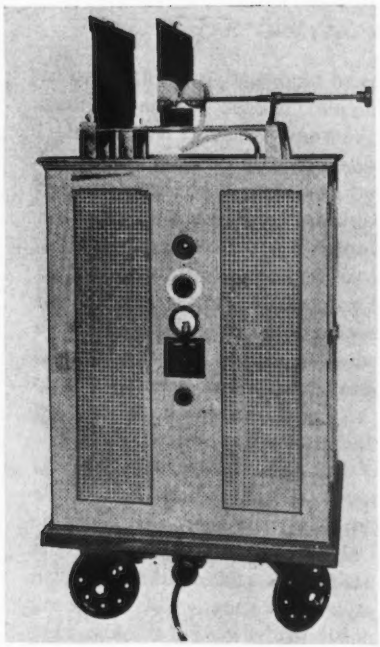

FIG. 1. *The oscillator used in the experiments.*

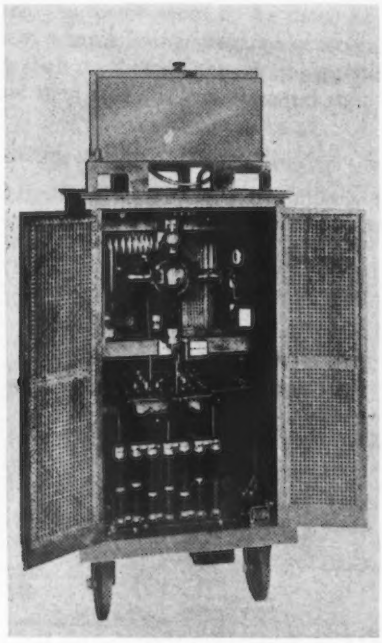

FIG. 2. *The oscillator used in the experiments, with the doors of the cabinet open.*

In order that results should be easily interpretable, and the variables be few in number and well defined, two methods of experimentation suggest themselves.

In the first case, the liquid under investigation may be made to fill the space between the plates of a condenser forming part of the oscillatory circuit, and the 'dielectric loss' measured by the rise in temperature of the liquid. This is the method used by Richards and Loomis. It seems to us that it has the disadvantage that when the liquid in the condenser is replaced by another, the constants of the oscillatory circuit are profoundly changed. The readjustment of the circuit, so that the frequency and at the same time the intensity of the field is the same as before, is an extremely difficult matter. Richards and Loomis (13) do not state how these variables were kept constant. The accurate measurement of potentials and current at these high frequencies is practically an impossibility.

The alternative is to arrange the apparatus so that, with the range of liquids studied, their introduction into the field does not materially affect the output of the oscillator. That is, though the field near the specimen is, of course, changed, the 'external' field at points distant from it is unaffected. (An analogous experiment is the placing of a piece of iron in the earth's magnetic field.) We have then a case that is capable of theoretical treatment as a 'field' problem. Moreover, the results of such treatment seem to be more easily applicable to the varied conditions realized when a living specimen of irregular shape and heterogeneity is being heated, than do those of the 'circuit' problem treated by Richards and Loomis. This then was the experimental method adopted.

Apparatus

Photographs of the oscillator supplied by the General Electric Company are shown in Fig. 1 and 2 (Plate I) with its circuit diagram in Fig. 3. It uses two U. V. 861 Radiotron tubes (having screen-grids) in a shunt feed Hartley circuit, and is capable of giving an output of one kilowatt at a frequency of 12,000 kilocycles (25 metres). The heater plates, between which the specimen is placed, have a maximum area of 53 cm.×53 cm. and may be used up to 35 cm. apart.

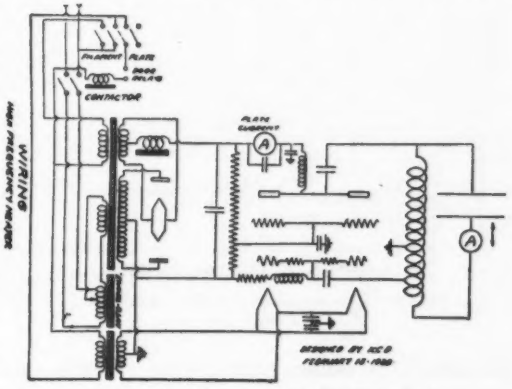

FIG. 3. *Circuit diagram of the oscillator used.*

A spherical bulb of capacity 140 cc. having an outer spherical jacket with an evacuated space between the walls, was used to contain the liquid. Thus the heat losses by radiation during an experiment were negligible, whilst the

heating by the field was still large. Heating of the containing vessel itself is of course a complicating factor, but as it occurs in all the measurements the conclusions reached are not invalidated. The vessel was supported by an ebonite rod of small capacity in the centre of the field between the plates of the oscillator. The size of the latter and their distance apart were adjusted until it was found that filling the flask with aqueous solutions of the salts up to the maximum strength used produced no appreciable change in the external field. This could be measured by the readings of a wave meter placed about one metre away from the oscillator. It was necessary that all adjustments of the wave meter should be made with the operator at a distance, since at these high frequencies the approach of any large capacity body within two or three feet has a large effect on the readings of instruments. Also any measuring instrument used to measure the current induced in the wave meter circuit must necessarily be of as low capacity and inductance as possible. To meet these requirements, the following arrangement was devised. The current in the wave meter lit a small two-volt bulb fixed to the case of the condenser. Its brightness could be compared with that of a similar 'standard' lamp which was lit by a measured current from a battery. The two lamps were at the opposite ends of an ebonite tube in the centre of which was a small 'paraffin-block and tin-foil' photometer which was viewed at right angles from a distance by a telescope. In operation, the capacity of the wave meter condenser was varied by rotation of a long insulated rod attached to a vernier until the lamp showed the position of resonance by its maximum brightness. The current through the standard lamp was then adjusted until the photometer showed that the two lamps were of equal brightness. The value of this current gave a measure of the intensity of the radiation picked up by the wave meter. With this arrangement the frequency and intensity of the field could be kept constant to within 1 or 2%.

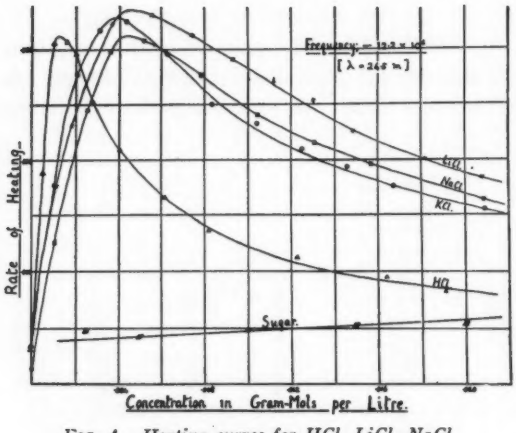

FIG. 4. *Heating curves for HCl, LiCl, NaCl, KCl and sugar solutions.*

The heating of the liquid in the cell was observed by the rise of the liquid itself in the vertical capillary tube attached to the stopper of the cell. The position of the meniscus could be read on a transparent scale fixed to the tube, viewed from a distance by a telescope. The rise of the liquid was found to be steady and uniform. In the majority of the experiments the specific heat and the coefficient of expansion of the most

concentrated solutions used differed so little from that of water that no correction had to be made. In no case was the rise of temperature in any experiment more than 1°C.

Results

Fig. 4 shows the heating curves for HCl, LiCl, NaCl, KCl and for sugar solutions at the frequency 12,000 k. c. The accuracy of measurements is about 2 or 3%. The heating in each case rises quickly from the value for pure water to a maximum, then falls away more gradually as the concentration is increased. Special experiments were made with solutions of NaCl up to four times normal and with very dilute solutions to see if further peculiarities occur. The results are given in Fig. 5 and 6. They show that the curve becomes a straight line near the origin, and that

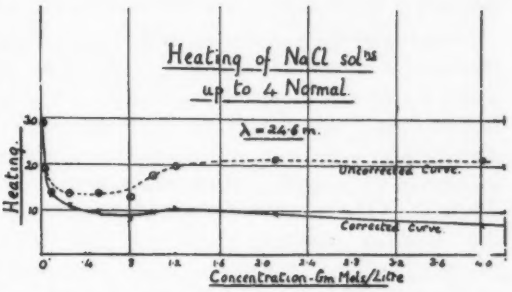

FIG. 5. *Heating curves of sodium chloride solutions at various concentrations.*

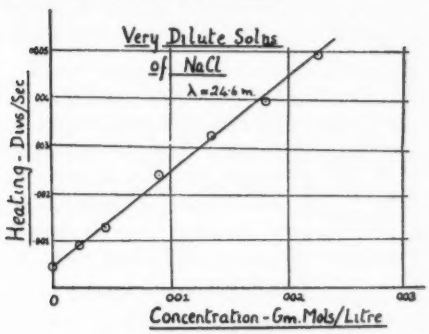

FIG. 6. *Heating curves of dilute solutions of sodium chloride.*

when corrections for specific heats and coefficients of expansion are made there is no indication of maxima other than the one in Fig. 4.

The concentrations at which the maxima occur for the salts are given in Table I.

It was noted that the specific conductivities of the solutions at these maxima were practically the same, though the concentrations were widely different. If the curves are plotted with conductivities as abscissae instead of concentrations,

TABLE I

CONCENTRATIONS OF SALTS AT WHICH MAXIMA OCCUR

Salts	HCl	LiCl	NaCl	KCl
Concentration giving maximum	.00125	.00395	.00450	.00465
Specific conductivity at this concentration in $10^{-4}\,\omega^{-1}$	5.25	5.64	5.47	5.14

the curves for the different electrolytes coincide. (In this region conductivity is very nearly proportional to concentration, so the curves have the same shape as in Fig. 4.) As Hosmer (8) and as Richards and Loomis (13) have found for a number of very different substances, the heating is a function of the resistance alone no matter what the nature of the ions present. As it is not possible to compare the heating produced at different frequencies in absolute value, and the heating due to the containing vessel is unknown, the units in which the heating is measured are unimportant, the shape of the curves and the position of the maxima being the significant results.

In the later more accurate work, it was desirable to replace the method of observation of the heating by the expansion of the liquid, by some method which would not require a knowledge of the coefficients of expansion of the liquids used. Accordingly the temperatures of the liquids in the flask were measured by a single copper-constantan thermocouple which could be inserted in place of the stopper of the flask immediately before and after the heating by the field. (The couple could not, of course, be left *in situ* owing to the currents that would be induced in it by the field.) With the vacuum jacketing described, this entails no serious error. Measuring the E.M.F. of the thermocouple—the other junction being in ice—on a Cambridge and Paul potentiometer with a sensitive Kipp and Zonen galvanometer the temperature could be rapidly and accurately determined to 1/50th of a degree centigrade. The specific heats of the liquids could be obtained by observing the rise in temperature when a small heater coil carrying a known current was inserted for a given time into the flask.

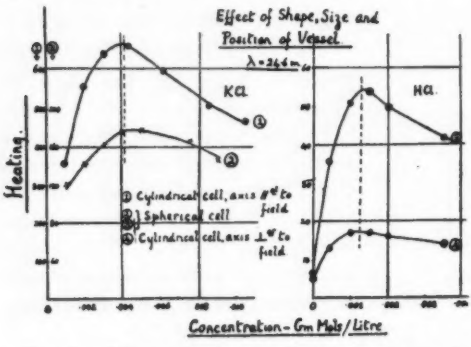

FIG. 7. *Effect on the heating of the shape, size and position of the liquid in the field.*

The effect on the heating of the shape, size, and position of the heated liquid in the field is shown in Fig. 7. Though the absolute value of the heating is very greatly affected by the shape and position of the heated liquid, it will be seen that the general shape of the curves and the position of the maximum is the same under widely different conditions. In general the heating is greater when the longer axis of the heated substance is parallel to the field than when across it. This is seen in the results for the cylindrical vessel. In the case of a vessel in the shape of a cylinder with rounded ends, of length 6.5 times its radius, the heating with the axis parallel to the field was found to be more than 50 times as great as when at right angles. The importance of maintaining the position of the specimen in the field accurately the same if consistent results are to be obtained, must be emphasized.

In order that experiments might be made at other frequencies an oscillator capable of covering a large range of wave-lengths by interchange of coils was constructed. Two V.X. 852 valves were connected in parallel in the familiar Hartley circuit shown in Fig. 8. By means of the interchangeable chokes and coils, experiments could be made at six different wave-lengths from 10 metres to 200 metres with an output of 150 watts, which could be maintained constant if precautions were taken to keep the filament emission steady. The filaments were lit half an hour before an experiment and the filament voltage was kept accurately constant throughout. The plate voltage was supplied by a 2000-volt direct current motor generator.

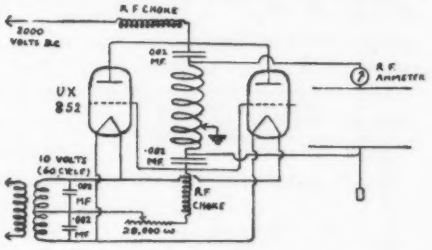

FIG. 8. *Circuit diagram.*

Frequencies were measured by a General Radio Company Precision wave meter, type 224. For the shorter wave-lengths a coil smaller than the smallest supplied had to be made, and the instrument was calibrated with the coil by the method of harmonics, using the known capacitance calibration of the condenser. The very short wave-lengths were checked by direct measurement on a Lecher wire system, 30 metres in length, the glowing of a neon discharge tube serving as an indicator of the position of the nodes.

Solutions were made to given strengths with 'conductivity' water redistilled in a tin-lined still. Their specific conductivities were measured by finding the resistance of a 'conductivity cell' on an alternating current bridge (frequency about 60 cycles). The experiments and conductivity determinations were made at a temperature of 22.5°C.

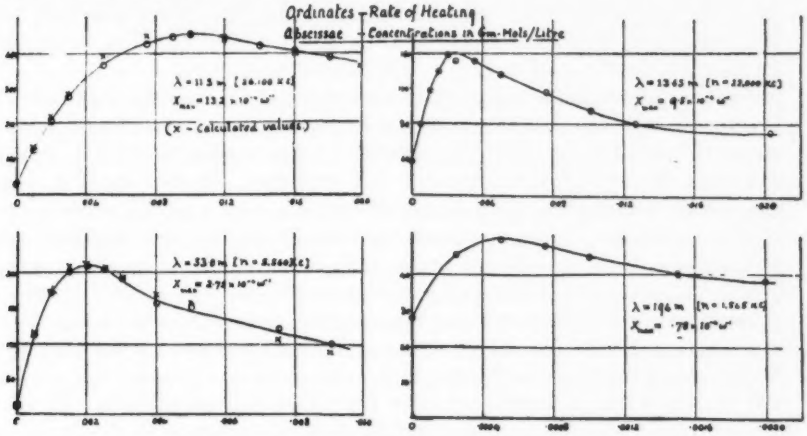

FIG. 9. *Heating of solutions of potassium chloride at different frequencies.*

The results for the various frequencies are illustrated in Fig. 9 which gives typical examples of the curves obtained. It will be seen that the concentration or the specific conductivity at which the maximum heating occurs is greater the greater the frequency of the field. Thus at 1,550 kilocycles (194 metres) a solution of KCl of $N/2000$ strength gives the maximum effect, whilst at 26,000 kilocycles (11.5 metres) it is a solution of $N/100$. The law of dependence of the conductivity giving the maximum heating, upon the frequency, is shown in Fig. 10 to be a simple linear one. The results included are for 11.5, 13.5, 24.5, 53.0 and 194.0 metres. Those at 24.5 metres include the results for the different electrolytes (HCl, LiCl, NaCl, KCl); the others are for KCl. The theoretical derivation of this law of dependence upon frequency will be given later in the paper.

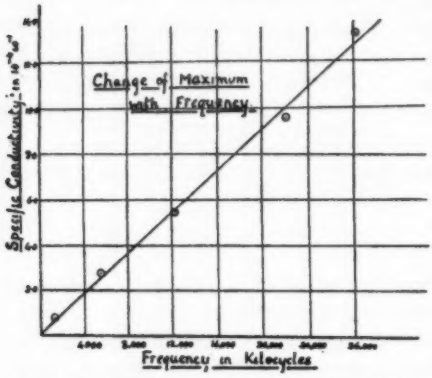

FIG. 10. *Relation of conductivity giving maximum heating to the frequency.*

The curves also show that the ratio of the maximum heating to that of pure water increases as the frequency is increased; that is, the selective heating effect is more marked at the higher frequencies. This too follows from the theory. That the selective effect is still of importance with wave-lengths as great as 200 metres is perhaps unexpected. Incidentally the curves show that the method used by Christie and Loomis (3) to compare the output of their oscillators at different frequencies, employing a thermometer filled with a salt solution placed in the field, is likely to lead to very wrong conclusions. With the same output and field, the heating of the electrolyte would vary with the frequency. The bearing of this on their conclusions as to the lethal effect on mice will be discussed later.

An attempt was made to show that the specific conductivity was the variable involved. Lithium chloride solutions have a maximum conductivity at a concentration of about five times normal, so that a solution of 12 *N*. has the same specific conductivity as one of 2 *N*. strength. It was hoped to prove that these two solutions, so different in concentration, gave the same heating effect. It was found, however, that the heating was so small that the rise in temperature of the containing vessel and the effect of air currents were of greater importance. These solutions heat much less in the field than does pure water. Accurate determinations were thus impossible, but an apparatus was developed that should be of use in the observations in the heating of liquids where the effect is small, as in the case of polar non-electrolytes (where the heating is due to a different cause from that dealt with here). For such work, a thin-walled containing vessel, holding a larger mass of the liquid and provided with a means of rapid continuous stirring, was prepared.

It was suggested that the so-called skin-effect which tends to confine high frequency currents to the surface of conductors might be responsible for the phenomena. The spherical, vacuum-jacketed cell was supported in the centre of the field inside a large beaker. The heating of the liquid in the cell was then compared with the heating under the same field when the surrounding space in the beaker was filled with the same liquid as in the cell. The results were that with the cell surrounded by the shielding liquid the heating was less than 1/20th of the heating when the surrounding liquid was absent. It was realized, however, that this is not an indication of the skin effect but is due to the shielding effect of the layer of different dielectric constant formed by the vacuum-jacketing of the cell. This effect will be discussed.

Other Experiments with the Apparatus

Some German workers have reported sterilization of milk by short wave treatment. Accordingly, experiments were made on the irradiation of milk by the waves to see if any effect on bacteria could be found. An effect first observed was found to be due to insufficient care in protecting the specimens from the air. When the proper precautions were taken, no difference in the aging of pasteurized or of unpasteurized milk between the irradiated and the control specimens was observed, even after treatment of half an hour's duration.

An experiment was made with the cell filled with liquid oxygen, to see if it were heated by the field. No consistent change in the rate of evaporation could be found when the field was switched on.

Experiments were repeated using a polar liquid, liquid sulphur dioxide, with again a negative result.

Theory of the Phenomena

The observed results can be explained by a simple theory, for which, however, no claim of great originality or of the strict validity of its assumptions is made.

Relative Importance of the Magnetic Field

Maxwell's theory predicted that, due to the magnetic fields set up and self-inductance at high frequencies the currents in a conductor would tend to be confined to the outer surfaces (10). Lord Rayleigh (12) calculated the consequent increase in the resistance of a cylindrical conductor to high frequency currents and his predictions were beautifully verified by the experiments of Fleming (5). For a copper wire of diameter 0.2 cm. the resistance at a frequency of 1,000 kilocycles is eight times that for steady currents, and the effect increases with frequency. It seems to have been taken for granted by many workers in high frequency electro-therapy that because of this skin effect the currents will be almost completely confined to the surface of the body and effects at any depth cannot be produced. Examination of Rayleigh's formula, however, shows that on the contrary for the conductivities encountered in the body, skin effect is negligible, and the path taken by high frequency currents is the same as that of steady currents.

Rayleigh's formula for the high frequency resistance of a cylindrical conductor is:

$$R' = R\left(1 + \frac{1}{12}\frac{p^2l^2\mu^2}{R^2} - \frac{1}{180}\frac{p^4l^4\mu^4}{R^4} + - - - -\right)$$

provided that $\frac{p^2l^2\mu^2}{R^2}$ is small compared to unity, where

R = resistance to steady currents
$p = 2\pi n$, n = frequency
μ = magnetic permeability
l = length of conductor.

Putting $\mu = 1$ and introducing the specific conductivity x, and A the cross sectional area, we get

$$R' = R\left(1 + \frac{1}{12}\left\{\frac{2\pi n.lAx}{l}\right\}^2 + - - - - - - -\right.$$

and the first correcting term is $\frac{1}{3}\left\{\pi nAx\right\}^2$.

The conductivities encountered in the body are of the order of $10^2\omega^{-1}$ (1), or $10^{-2} \times 10^{-9} = 10^{-11}$ e.m.u. Taking n as 3×107 ($\lambda = 10$ metres) and $A = \pi.2^2$ (the radius of our cylindrical vessel was 2 cm.) we get

$$\frac{1}{3}(\pi nAx)^2 = 5 \times 10^{-5}.$$

So that at the highest frequency used in our experiments the skin effect is negligible. It is only for good conductors, where the conductivity is of the order $10^6\omega^{-1}$ that it is of importance. That in electro-therapy skin effect need not be considered, is the conclusion reached experimentally by Pariseau (11). The fact, also, that we get the same shape of curve with the different vessels shown in Fig. 7 proves that it was inoperative in our experiments.

The fact that heating effects may be produced by these short waves, deep in the interior of the body as well as at the surface, while holding great possibilities of usefulness, also means that great caution will have to be exercised in experiments on living specimens. Internal injurious effects might be produced without the patient suffering any warning sensations.

We are justified, then, in disregarding the magnetic fields associated with the oscillations and those due to the currents induced in the specimen, and may treat the problem as one of a high frequency electrostatic field. Given such a field, considered for simplicity as a uniform one of known intensity and frequency, the idealized problem is to deduce the heating produced in a slightly conducting dielectric specimen placed in it.

Field Induced in the Specimen

The problem is amenable to mathematical calculation in the case where the dielectric is in the shape of an ellipsoid placed in a uniform field. Discussion of it will be found in Gray's Absolute Measurements in Electricity and Magnetism, Vol. II, Part I, pages 55-68. The result is that the field inside the ellipsoid is uniform and of magnitude $E' = E.f(K, \epsilon, \theta)$ where E is the external field, and $f(K, \epsilon, \theta)$ is a function depending on the dielectric constant, the ellipticity and the orientation of the ellipsoid in the field. In other cases, such as

with a cylinder, the field is not uniform and calculation would be very laborious, though straightforward, but the qualitative nature of the results can be deduced from those for an ellipsoid. Special cases of the function that are of interest to us are:

(a) For a sphere $E' = E.\ \frac{3K}{K'+2K}$ and for $\frac{K=1}{K'=80}$ $E' = E\ \frac{1}{27}$

(b) For a very elongated ellipsoid of revolution (approximating to a cylinder)
(1) with its long axis parallel to the field
$E' = E$
(2) with its long axis at right angles to the field
$E' = E\ \frac{2K}{K'+K}$ $\left(E' = \frac{E}{40}\right)$

(c) For a very oblate ellipsoid (approximating to a disc), with its axis parallel to the field
$E' = E\ \frac{K}{K'}$ $\left(E' = \frac{E}{80}\right)$.

We see that when the dielectric constant is high, as it is for water and substances in the body, the field inside the specimen and hence the currents produced by it are very greatly affected by its shape and position in the field. We understand how it is that, as was found in the experiments, the heating is much greater when the longer axis of the specimen is parallel to the field than when at right angles.

A single-walled glass vessel was made in the shape of an ellipsoid of revolution having the axes in the ratio of two to one. Taking $K' = 80$, $K = 1$, the theoretical ratio of the field inside, when the long axis is parallel to the field, to the same when it is at right angles, is 2.3:1, and the ratio of the squares of the fields 5.3:2, the experimental value of the ratio of the heating produced was found to be 2.75:1. The difference may be attributed to the effect of the glass of the containing vessel, whose dielectric constant is much less.

In a specimen of heterogeneous dielectric constant and irregular shape we may use the principle of minimum potential energy to predict that the lines of force will tend to crowd into the portions of higher dielectric constant, and will be denser there, if the longer axes of such portions are parallel to the external field, than if at right angles. The electric intensity is proportional to the

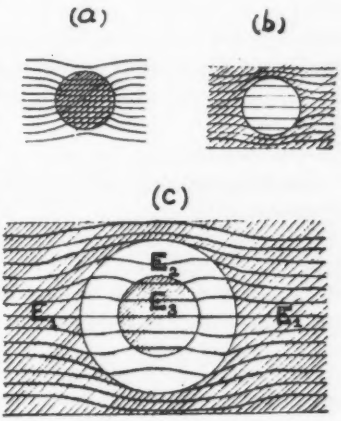

FIG. 11. *Distribution of lines of force in a sphere, (a) of dielectric constant greater than that of its surroundings; (b), of dielectric constant less than that of its surroundings; (c), of high dielectric constant in a sphere of low dielectric constant which is itself surrounded by the medium of higher dielectric constant.*

density of the lines of force divided by the dielectric constant ($E = \frac{4\pi N}{K}$).

Fig. 11 shows the distribution of lines of force in the case of a sphere

(a) of dielectric constant greater than that of its surroundings;

(b) of dielectric constant less than that of its surroundings;

(c) of high dielectric constant in a sphere of low dielectric constant, which is itself surrounded by the medium of higher dielectric constant. This is the case realized in our experiment with the vacuum jacketed sphere. The shielding effect of the jacket is seen; the field E_2 is very much less than it would be if the jacket space were not there, *i.e.*, E_2 is much less than E_1. Assuming that the inner sphere occupies a small volume of the larger one we could apply the formula for a sphere twice to deduce E_2 approximately.

$$E_2 = E_1 \frac{3K}{K' + 2K}$$

$$E_3 = E_2 \cdot \frac{3K'}{K + 2K'} = E_1 \cdot \frac{9KK'}{5KK' + 2K'^2 + 2K^2}$$

$$= \frac{9KK'}{9K.K' + 2(K' - K)^2}$$

$$i.e., E_3 = E_1 \frac{9 \cdot \frac{K'}{K}}{9\frac{K'}{K} + 2\left(\frac{K'}{K} - 1\right)^2} \quad \left(\text{For } \frac{K'}{K} = 80 \quad E_3 = E_1 \times \frac{1}{18}\right)$$

We see that, whether K' is greater or less than K_1, E_2 is always less than E_1. That is, whenever a portion of the medium is isolated from the rest by a surrounding layer of a different dielectric constant, whether greater or less, the heating in the interior is less than if the layer were absent. This may have some application to the heating of cells in the body, or of areas enclosed by bone, etc.

Current and Heating Produced

Knowing the intensity of field in the medium, we can calculate the currents produced by it.

Consider an element bounded by two plane areas A at right angles to the field and of thickness l. Let the potential difference between the two areas be V, the resistance of the element to a steady current flowing between them be R, and the capacity of the element be C. Then the equation for the element is

$$\frac{dV}{dt} - R\frac{dI}{dt} - \frac{I}{C} = 0.$$

Let the intensity of field in the medium be $E' = E'_0 \sin \omega t$

$$i.e., V = E'l = E_0 l \sin \omega t = V_0 \sin \omega t \text{ or } V_0 e^{i\omega t}$$

The solution of the differential equation is

$$I = Ae^{i\omega t} \text{ where } A = \frac{i\omega V_0}{\frac{1}{C} + i\omega R}$$

The component of I in phase with V is the real part of this,

$$i.e., I_r = \frac{\omega^2 V_0 R}{\frac{1}{C^2} + \omega^2 R^2}$$

and the power loss, or heat produced per sec. is

$$P = \tfrac{1}{2} V_o I_r = \tfrac{1}{2} \frac{V_o^2 \omega^2 R}{\frac{1}{C^2} + \omega^2 R^2} \qquad (1)$$

Introducing now x the specific conductivity of the medium and K, its dielectric constant

$$R = \frac{l}{xA} \text{ and } C = \frac{KA}{4\pi l}$$

$$\therefore \frac{1}{RC} = \frac{4\pi x}{K} \qquad (2)$$

This relation is used by Pierce in an unpublished theorem.
We can write (2) as

$$P = \tfrac{1}{2} \frac{V_o^2 \frac{1}{R}}{\frac{1}{\omega^2 R^2 C^2} + 1} \text{ and substituting for } \frac{1}{RC} \text{ and } R$$

$$P = \tfrac{1}{2} \frac{V_o^2 \frac{xA}{l}}{1 + \left(\frac{4\pi x}{K\omega}\right)^2}$$

But $V_o = E'_o l$ and writing $\frac{4\pi x}{K\omega} = a$

We get $P = \frac{\tfrac{1}{2} E_o'^2 x (Al)}{1 + a^2}$

i.e. heat produced per sec. $= \frac{\tfrac{1}{2} E_o'^2 x}{1 + a^2} \times$ (Volume of element).

Apparently, in the case of these high frequency currents we can assume that for any shaped volume element of the medium the relation (2) holds, and so can integrate for the whole specimen.

$$\text{Heat produced in specimen per sec.} = \frac{\tfrac{1}{2} E_o'^2}{1 + a^2} \times \text{(Volume of specimen)} \qquad (3)$$

where E'_o is given by multiplying the external field E_o by $f(K, \epsilon, \theta)$ as explained in the previous section. The complete expression for the heating is then

$$P = \frac{\tfrac{1}{2} E_o^2 f(K, \epsilon, \theta)\ x}{1 + a^2} \times \text{(volume)}$$

or for the rise in temperature we have

$$\frac{dT}{dt} = \frac{\tfrac{1}{2} E_o^2 f(K, \epsilon, \theta)\ x}{1 + a^2} \times \frac{1}{\rho s} \qquad (4)$$

where ρ = density and s = specific heat.

Existence of a Maximum

If, as in our experiments, we change only the liquid used, keeping the other conditions the same, we have

$$P = C \frac{x}{(1 + a^2)}$$

$$\therefore \frac{dP}{dx} = C \frac{(1 + a^2) - 2a \frac{da}{dx}}{(1 + a^2)^2} .$$

If the dielectric constant remains the same, $\frac{da}{dx} = \frac{4\pi}{K\omega}$

and $x \frac{da}{dx} = a$

$$\therefore \frac{dP}{dx} = C \frac{(1-a^2)}{(1+a^2)^2}$$

We get a maximum when $\frac{dP}{dx} = 0$, *i.e.* when $a^2 = 1$

i.e., $\frac{4\pi x}{K\omega} = 1$

$$\text{or } x \text{ max.} = \frac{K}{4\pi} \times \omega \qquad (5)$$

giving the law of dependence of the maximum upon frequency. Pierce deals with the case realized in the experiments of Richards and Loomis (13) where the liquid fills a cell occupying a large space of the condenser formed by the "heater plates", and obtains a more complicated formula involving the capacities of the oscillator as well as that of the cell. The maximum power loss in this case occurs at

$$\text{max.} = \frac{K\omega}{4\pi} \frac{1+\beta}{\beta}$$

where β is the ratio of the capacity of the cell to the capacity between the face of the cell and the plate of the oscillator. The transition from this to the field problem is made by letting β become very large, when our formula (5) is reached. The cases met with in practice, as in electro-therapy, would be intermediate, though the field problem seems to offer the best line of attack.

We had $\frac{dP}{dx} = C. \frac{1-a^2}{(1+a^2)^2}$;

differentiating we find $\frac{\partial}{\partial a}\left(\frac{dP}{dx}\right) = C \frac{2a(a^2-3)}{(1+a^2)^3}$.

Now below the point of inflection of the curves, where $a^2 = 3$, (a^2-3) is negative, *i.e.*, $\frac{\partial}{\partial a}\left(\frac{\partial P}{\partial x}\right)$ is negative. Then the slope of the curves near the maxima increases as a is decreased, *i.e.*, as the frequency is increased, and the selective heating effects are more marked at the higher frequencies.

Though there is a maximum with respect to conductivity, there is no maximum with respect to frequency; the power loss for a given field intensity increasing as the frequency is increased. When this is taken into consideration, the conclusion reached by Christie and Loomis (3) that the shorter waves have less lethal effect may be invalidated. The NaCl thermometer used by them to estimate the intensity of the field would give the same reading for smaller values of the field at higher frequencies than for the lower frequencies.

Verification of the Formulae

Fig. 10 shows that the formula 5 for the maxima is verified experimentally. This, incidentally, indicates that the dielectric constant does not change appreciably between these frequencies, or with the concentration. (This seems to be the conclusion of the latest researches (16) — though there is disagreement.) In the region of wave-lengths less than two or three metres,

however, we might expect to find anomalous dispersion, and the use of equation 5 to find the dielectric constant might be a possible method of investigation. Using the value given by the slope of the graph in Fig. 10 we get for the value of the dielectric constant

$$K = \frac{4\pi x\ max}{\omega} = \frac{2x}{n} \quad (n = \text{frequency})$$

$x_{max.} = 10 \times 10^{-4}\omega^{-1} = 10\times10^{-4}\times9\times10^{11}$ e.s.u. at $n = 22{,}000$ kilocycles giving $K=81.7$ at 22.5° C.

Drake, Pierce and Dow (4) have found that for these frequencies $K=79.6$ at 21.5° C.

Formula 4 for the heating cannot be compared with the results in absolute magnitudes, as we have no absolute measurements of the field intensity, and the heating of the containing vessel is a complication. But, by using the theoretical values of a, the values of the function $\frac{x}{1+a^2}$ can be calculated for the different concentrations and frequencies, and the curves so obtained fitted on to the experimental ones by multiplying by an arbitrary factor. That the agreement is good is shown by the points marked by crosses in two of the curves of Fig. 9.

Calculations were made to see if the heating predicted by formula 4 were of the right order of magnitude in a given case. The best estimate of the potential difference between the heater plates is obtained by using the formula for the current between them, which was registered by the radio-frequency ammeter:

$$\overline{I}_o = C\omega\overline{V}_o. \quad (\overline{I}_o \text{ and } \overline{V}_o \text{ are the R.M.S. values})$$

where C, the capacity, is calculated approximately from their size and distance apart. In the experiment, $\overline{I}_o$ was 2.85 amps and this gives $\overline{V}_o=19$ e.s.u. or 5,700 volts, *i.e.* $V_o = 19\sqrt{2}$ e.s.u. Then $E_o = .8\times\sqrt{2}$ e.s.u. per cm.

For a sphere $F\ (K.\epsilon.\theta.) = \frac{1}{27}$. Substituting in the formula for a liquid of known conductivity x, the calculated rate of production of heat $= 2.75\times10^7$ ergs per sec. The observed value in the experiment with the spherical vessel was 1.02×10^7 ergs per sec. The difference may be attributed to the shielding effect of the glass of the vessel.

The application of the formula 4 to a heterogeneous system may be made to some extent. The distribution of the fields may be predicted as has been discussed. In the cases where the dielectric constant does not alter very greatly, though the conductivity may, the shape and position of the various parts of the body does not affect the field greatly and the problem is simpler. Where the dielectric constant is constant the greatest heating will be produced where the conductivity is such that equation 5 is satisfied. With a different wave-length the heating of a part that has a different conductivity will be favored. Where the dielectric constant also changes the problem is a complex one. It is possible, however, that if we knew the electric properties of the component parts of the body, we would be able to favor the heating of one

portion rather than another by the proper choice of wave-lengths, although, of course, the effect of such preferential heating is minimized by heat exchange between the parts. A possibility of this kind would have great application to medical science.

Fürth (6) has determined the dielectric constants of a large number of substances of biological interest. He gives the value 85.5 ± 0.5 for human blood, and finds the same value for blood serum (from which the corpuscles have been removed). The conductivity of the cells, however, is very much less than that of the plasma in which they are suspended. Bugarszky and Tangl (1) give for the conductivity of blood serum $110 \times 10^{-4}\omega^{-1}$, and for the proteins in the dispersion in which they exist in the blood, the value $10 \times 10^{-4}\omega^{-1}$. From equation 5 we can calculate the wave-lengths that would favor the heating of the electrolyte of the plasma or of the protein respectively. They are for the electrolyte about 1.3 metres, and for the protein about 14 metres. The wave-length that would heat both alike is the geometric mean of these, *i.e.*, 4.3 metres. We should expect then that at wave-lengths greater than four metres the heating of the protein would be favored rather than that of the rest of the plasma, while for shorter wave-lengths the reverse would be the case. The intimate heat exchange of course lessens any selective effect, but it might be possible to carry the heating of the protein to a greater degree with safety if the proper wave-lengths were chosen, than if an unsuitable one were used. (The above numerical values are to be accepted only as furnishing an illustration.) To investigate the actual heating of the various constituents of blood three specimens were prepared. A was whole horse blood, defibrinated to prevent clotting, B was serum produced from it by centrifuging off the corpuscles, and C was the serum after 12 hr. dialysis to remove the electrolytes. (The volume increased here by 20%.) The results of experiments at three different wave-lengths are given in the Table II.

TABLE II

EXPERIMENTAL RESULTS

Solution	Heating produced at different wave-lengths.		
	43 metres	15 metres	9 metres
A	1.21	1.39	1.43
B	1.00	1.00	1.00
C	3.81	3.53	3.21

The figures indicate that in the blood, most heat originates in the proteins, less in the corpuscles and least in the electrolyte fluid of the plasma. It is interesting to see that as the frequency is increased, the relative heating of the corpuscles increases, whilst that of the protein decreases. The results though rough, suffice to show the possibilities of control of the heating by choice of wave-length.

Summary

1. The heating by short electromagnetic waves, of wave-lengths 10 metres to 200 metres, of solutions of simple electrolytes of varying concentrations has been determined.

2. It is shown that the heating depends not on the composition but on the specific conductivity of the liquid, and rises to a maximum for a certain conductivity, whatever the size and shape of the specimen heated. This maximum is the more marked the higher the frequency.

3. The conductivity at which the maximum effect occurs is shown to be proportional to the frequency.

4. Skin effect is shown by experiment and theory to be negligible for the low conductivities involved and the heating effects are produced throughout the depth of the specimen heated.

5. A theory is given explaining how the field inside the specimen depends on the shape and orientation in the external field and on the dielectric constant of the specimen. Calculation is made of the currents and heating produced and is shown to be in accord with the experimental results.

6. The law of dependence of the maximum upon frequency is deduced and when applied to the results gives 81.7 as the dielectric constant of water.

7. Application of the theory to a heterogeneous body is discussed. The distribution of the field in the interior is determined largely by the dielectric constants, and the heating then upon the conductivities. The possibility of directed selective heating is suggested, and illustrated by experiments on blood.

Acknowledgment

We are indebted to Dr. Whitney of the General Electric Company for arranging the gift of the machine with which much of the work was done, to Mr. Arnold Pitt for advice in construction of the valve oscillators, and to Professor Wasteneys of the Department of Biochemistry of the University of Toronto for his interest and criticism and for the blood serum supplied by that Department.

References

1. BUGARSZKY, S. and TANGL, F. Arch. ges. Physiol. 72: 531. 1898.
2. CARPENTER, C. M. and PAGE, A. B. Science, 71: 450-452, 1930.
3. CHRISTIE, R. V. and LOOMIS, A. L. J. Exp. Med. 49: 303-321, 1929.
4. DRAKE, F. H., PIERCE, G. W. and DOW, M. T. Phys. Rev. 35: 613-622, 1930.
5. FLEMING, J. A. Proc. Phys. Soc. London, 23: 103, 1911.
6. FÜRTH, V.R. Ann. Physik, 70: 63-80, 1923.
7. GOSSET, A., CUTMANN, A., LAKHOWSKY, G. and MAGRON, J. Compt. rend. soc. biol. 91: 626-628, 1924.
8. HOSMER, H. R. Science, 68: 325-327. 1928.

9. KAHLER, H., CHALKLEY, H. W. and VOEGTLIN, C. U. S. Pub. Health Rep. 44: 339-347, 1929.
10. MAXWELL, J. C. A Treatise on Electricity and Magnetism, 1904, Vol. 2. Chap. 13.
11. PARISEAU, L. E. Can. Med. Assn. J. 20: 146-152, 1929.
12. RAYLEIGH, LORD. Phil. Mag. 5: 21, 381, 1886.
13. RICHARDS, W. T. and LOOMIS, A. L. Proc. Nat. Acad. Science, Wash. 15: 587-593, 1929.
14. SCHERESCHEWSKY, J. W. U.S. Pub. Health Rep. 41: 1939-1963, 1926; 43: 927-945, 1928.
15. WOOD, R. W. and LOOMIS, A. L. Phil. Mag. 4: 417-436, 1927.
16. WYMAN, J. Phys. Rev. 35: 623-634, 1930.

ACTION OF HIGH SPEED ELECTRONS ON METHANE, OXYGEN AND CARBON MONOXIDE[1]

By J. C. McLennan[2], F.R.S., and J. V. S. Glass[3], B.A.

Abstract

This paper deals with the action of cathode rays on gases and gas mixtures. Methane, methane-oxygen mixtures, carbon monoxide and carbon monoxide-oxygen mixtures were examined. Methane gave small percentages of hydrogen and ethane. Methane and oxygen mixtures gave as gaseous products, carbon monoxide, carbon dioxide and hydrogen, the only other products being water and formic acid. The relative proportions of the products do not vary widely under a wide variation of conditions.

The reaction was found to be of the first order with respect to pressure. The reaction rate increases linearly with the voltage up to a certain value, after which it becomes nearly independent of the voltage.

The action of cathode rays on carbon monoxide produces carbon dioxide and a solid brown suboxide which is extremely soluble in water, and its composition corresponds to a formula $(C_3O)_n$. If the carbon monoxide is moist, no visible amount of solid or liquid is found and there is less carbon dioxide.

Carbon monoxide-oxygen mixtures under the action of cathode rays form carbon dioxide. Presence of water vapor has a retarding effect on the reaction. For mixtures of the same composition the reaction rate is proportional to the total pressure. For dry mixtures the product increases with the carbon monoxide present; when moist it is much less, and independent of the carbon monoxide.

There has been much research, especially recently, on the action of various types of electrical discharge on methane and on admixtures of it with another gas. Ionization is usually the chief cause in bringing about condensation, oxidation, etc., but its specific effect is difficult to gauge precisely, since thermal and photochemical processes play a great part in such experiments. High speed electrons offer a method for studying the chemical effect of ionization, in which those complicating subsidiary processes are absent, and yet at the same time it is more flexible than the method developed by Lind and his collaborators involving ionization by α-rays from radon.

Lind and Bardwell (10) found that α-rays caused extensive decomposition of methane into hydrogen, ethane, and a condensed ethylenic compound. The same authors investigated the production of ozone from oxygen by means of α-rays and also found that the action of α-rays on methane-oxygen mixtures was to cause a complete oxidation to carbon dioxide and water. Krüger (8) used electrons from a Tesla apparatus to examine the formation of ozone from oxygen. He found yields of less than 0.01%. Marshall (12), Busse and Daniels (3) have extended this investigation with a Coolidge tube.

Apparatus

High speed electrons were generated in a cathode ray tube operated by a transformer system similar to that described by Coolidge (4). A diagrammatic sketch of the arrangement is given in Fig. 1. The mains of the 110-volt,

[1] *Manuscript received May 30, 1930.*
Contribution from the Physical Laboratory of the University of Toronto, Toronto, Canada, with financial assistance from the National Research Council of Canada.

[2] *Professor of Physics and Director of the Physical Laboratory, University of Toronto.*
[3] *Research student, University of Toronto.*

50-cycle current were connected in series with a variable resistance A, an ammeter B and the primary of a 2:1 transformer C. The secondary of this transformer supplied current to the primary of a 1:1 insulation transformer D having a secondary insulated for 125 K.V. The primary of a 200 K.V. Snook transformer E was fed by the secondary of transformer D. The case of the high tension transformer was insulated from ground and connected to the primary and to the middle of the secondary. One terminal of the secondary was connected to the cathode of the tube and the other was joined to earth through a milliammeter F. This method of operation was a convenience, since the window of the cathode ray tube and any connecting apparatus could be grounded.

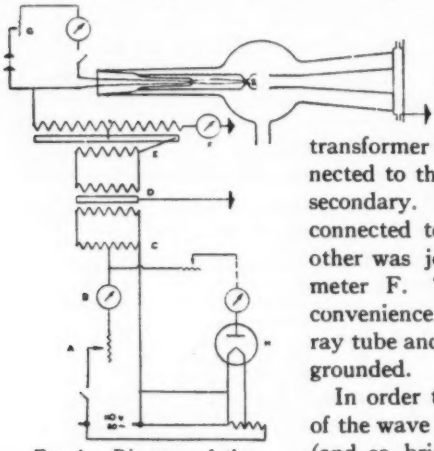

FIG. 1. *Diagram of the apparatus used.*

In order to decrease any voltage of that half of the wave not utilized by the cathode ray tube (and so bring the 'inverse' voltage below the 'useful') a Tunger valve H was connected in parallel across the primary of the transformer C. The voltage applied to the tube was measured by means of a standard Victor X-ray spark gap.

The batteries and adjustable rheostats of the filament circuit were placed in an insulated zinc box, having edges rounded to reduce corona. The window of the cathode ray tube consisted of 'resistal' (nichrome steel) foil, and was cooled by a water jacket.

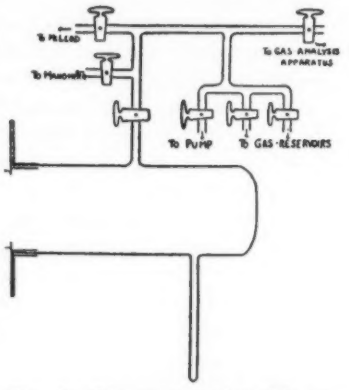

FIG. 2. *Diagrammatic view of the reaction chamber and connections.*

The reaction chamber (Fig. 2) of 900 cc. capacity, was waxed into an annular groove of the brass end piece of the tube. It had connections to a manometer, a McLeod gauge, a Hyvac oil pump, the gas reservoir and to a gas analysis apparatus. The reaction chamber was maintained at a constant temperature by a copper spiral wound round it lagged on the outside, carrying a stream of water from a thermostat held at 20°. The water jacket around the window was likewise maintained at the same temperature. The gas analysis apparatus is shown in Fig. 3. It consisted of a reservoir for drawing gas from the reaction chamber, a measuring burette, an explosion burette, absorption pipettes and a copper oxide furnace for estimating hydrogen. The capillaries were filled with mercury to avoid dead space.

Preparation of Gases

Oxygen was prepared in the usual way by heating potassium permanganate in an evacuated apparatus of pyrex glass. The gas was dried over phosphorus pentoxide and liquefied in a liquid air trap, then fractionated into the reservoir.

Methane was found to be most conveniently prepared by heating a mixture of anhydrous sodium acetate and barium hydroxide. The gas was carefully purified by passage through two bubblers each of fuming sulphuric acid, dilute nitric-chromic acid, and 25% potassium hydroxide. The gas was dried over calcium chloride and phosphorous pentoxide, and liquefied in a liquid air trap; from this the middle fraction was taken. Both gases distilled at constant vapor pressure in liquid air. Each preparation was checked by analysis before using.

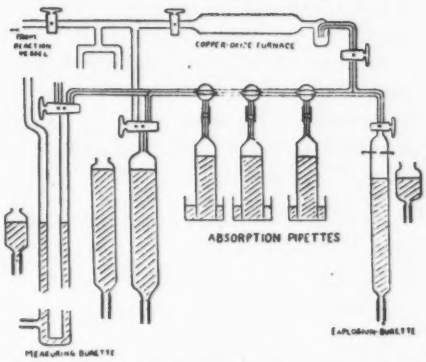

FIG. 3. *Diagrammatic view of the apparatus used for gas analysis.*

Exposure to Rays

Methane Alone

Experiments at different pressures were performed. After four hours' exposure in an experiment at 20 cm. pressure, (136 K.V. tube current 0.13 milliamps), change in pressure was insignificant. Some action, however, occurred. The gas was found to contain 16.0% hydrogen, 14.3% ethane, the rest being unaltered methane. (All hydrocarbons richer than methane were reckoned as ethane.) No deposition of tarry or oily matter took place. In a few experiments with moist methane small percentages of carbon dioxide and carbon monoxide were formed, but the main decomposition into hydrogen and ethane proceeded to the same extent.

Oxygen Alone

Work had already been reported on this. Nevertheless for comparative purposes several experiments were performed. Ozone was formed but in no case was the yield more than 0.02%. (Estimated by iodine.)

Methane and Oxygen

Above a voltage of 85,000, exposure caused a progressive decrease of pressure that continued until one of the gases was used up. Measurements, however, were for the most part made in the initial stages of the reaction.

Condensation of a liquid occurred—largely water. For this reason, in order to keep the water vapor pressure constant throughout the reaction, the gases were always saturated with water vapor (at 20° C.) at the start.

Products

The gaseous products were carbon dioxide, carbon monoxide and hydrogen. In addition, the liquid condensing was found to consist of a solution of formic acid. No other product was detected—no tarry or oily deposits. Some analysis of the products under various conditions of experiment are given in Table I. The tube current was in all cases 0.13 milliamps.

TABLE I

EFFECT OF RAYS ON METHANE AND OXYGEN

Kilovoltage	Pressure in cm.	Ratio methane: oxygen	Time of exposure, (min.)	Product as % of total methane			
				CO_2	CO	H_2	Formic acid
136	20	3:1	215	12.1	4.1	16.3	4.3
136	15	2:1	255	18.3	6.4	18.0	10.0
136	10	1:1	255	29.0	10.0	24.4	10.0
124	20	1:1	450	28.2	10.3	22.8	13.7
113	20	1:1	484	23.2	7.3	20.4	10.0
160	40	1:1	480	35.0	12.0	20.0	12.5
160	20	1:1	150	15.9	7.8	18.0	2.0
89	20	1:1	680	4.0	3.6	15.6	4.2

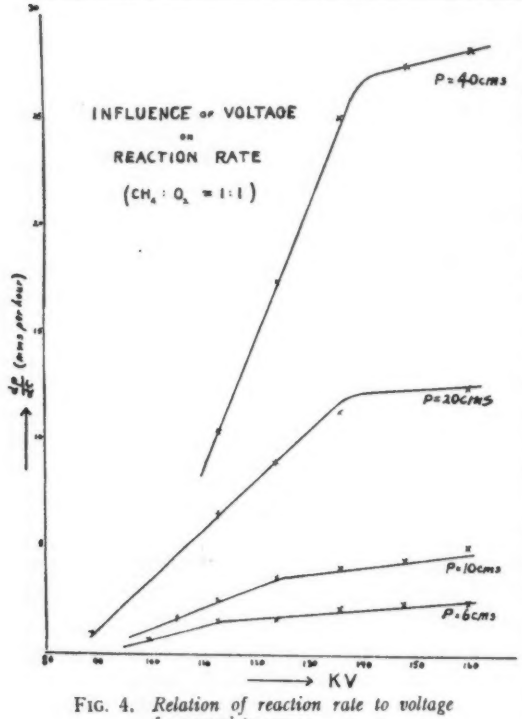

FIG. 4. *Relation of reaction rate to voltage for several pressures.*

The figure for formic acid was determined by assuming that formic acid was the only product in the condensate containing carbon.

The difference in products obtained in these experiments from those obtained by Lind and Bardwell (10) is striking. These cathode rays ionize some 100 times less effectively than α-rays, and so the products obtained in these experiments appear to be the intermediate stages of the more intense oxidation of methane by α-rays—which is complete into carbon dioxide and water. The formation of formic acid may be a subsidiary reaction

between the gaseous products since the amount is relatively small in the initial stages. This view is supported by the experiments of Brodie (2) who observed the formation of formic acid on passing an electric discharge through a mixture of hydrogen and carbon dioxide.

The ratio, carbon dioxide:carbon monoxide alters very little even in prolonged experiments. This cannot be the result of an equilibrium merely between the two gases, since other experiments show that carbon dioxide is not apparently decomposed by the cathode rays, although carbon monoxide and oxygen combine to form carbon dioxide on exposure to the rays. The removal of carbon dioxide by the formic acid reaction may be the reason for this observed balance.

Kinetics of the Reaction

Except in the beginning of the reaction the ratio of the products varies little with widely varying conditions. This is especially true with equivalent mixtures. Hence the pressure decrease may be taken as a rough index of the amount of reaction.

The effect of total pressure and of voltage on the reaction rate can best be studied with reference to Fig. 4. in which the reaction rate (rate of pressure decrease) is plotted against voltage for several pressures. The data from which Fig. 4 is constructed are given in Table II.

TABLE II

INFLUENCE OF VOLTAGE ON REACTION RATE

Pressure of methane-oxygen	Rate of pressure decrease (mm. per hour)						
	89	100	113	124	136	148	160 K V
40 cm.	—	7.4	11.0	17.4	24.3	27.3	28.0
20 cm.	1.0	—	6.5	9.0	12.9	—	12.5
10 cm.	—	1.2	2.5	3.6	4.1	4.4	5.1
6 cm.	—	0.7	—	1.7	2.2	2.4	2.5

NOTE: For mixtures $CH_4:O_2 = 1:1$. Tube Current 0.13 ma.

From the graph and from these data it is seen that

(1) The reaction is approximately of the first order with respect to pressure. (Fig. 5).

(2) There is a linear relation between voltage and reaction rate up to a critical value.

(3) Above this critical value, the reaction rate is nearly independent of the voltage.

Discussion of Kinetics

There is little doubt from the form of these relationships that the rate of reaction is directly connected with the rate of ionization. It is difficult, however, to express the results quantitatively since (a) the electron beam is not

homogeneous, and (b) the proportion of electrons hitting the wall is not known. A. Eisl (5) has recently demonstrated very clearly in experiments with high speed cathode rays, the strictly linear relationship between the total ionization of air and the energy of the electrons. The linear relation between the reaction rate and the voltage found in these experiments is in good agreement with his results.

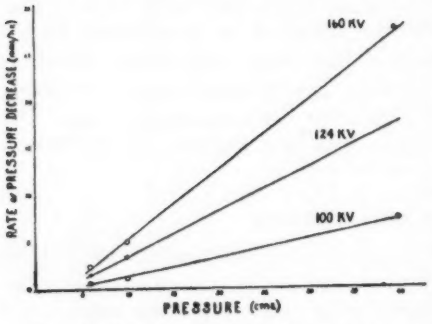

FIG. 5. *Relation of pressure decrease to pressure.*

The break in this linear relation above a certain voltage is due to the electrons being fast enough to reach the walls. The range of the electron is proportional to the square of its energy (Whiddington's Law), and is inversely proportional to the pressure. Thus the saturation pressure, (*i.e.*, when the range is constant) is proportional to the square of the voltage. The parabolic relationship between pressure and critical voltage is easily seen in Fig. 4. Below this critical voltage the electrons are stopped by the gas and total ionization should be independent of pressure. The rate of reaction, however, varies with the pressure. This, of course, is natural, since the greater the pressure the more frequent the collisions between the ionized and neutral molecules that result in chemical action.

This implies in addition that any succeeding rearrangements are rapid compared with the initial process.

The Action of High Speed Electrons on Carbon Monoxide and Carbon Monoxide-Oxygen Mixtures

Previous Work

B. C. Brodie (2) observed that pure dry carbon monoxide, subjected to the silent electric discharge showed a steady decrease in volume. Carbon dioxide was formed; in addition, a red-brown solid was deposited on the walls of the vessel. This solid was readily soluble in water; the solution was colored and strongly acid. The solid was a mixture of oxides of carbon, according to Brodie, that formed a homologous series of which he isolated two C_4O_3,C_5O_4.

Berthelot (1) repeated Brodie's work and gave for its formation the equation

$$5\ CO \longrightarrow CO_2 + C_4O_3\ .$$

He noted also that the solution of the solid gave precipitates with silver nitrate, lead acetate, and baryta. When the solid is heated to 300-400° C. in an atmosphere of nitrogen, it decomposes into carbon dioxide, carbon monoxide and a new brown oxide (C_8O_3) thus

$$3\ C_4O_3 \longrightarrow 2\ CO + 2\ CO_2 + C_8O_3\ .$$

This oxide on stronger heating gives carbon that still contains oxygen.

Lind and Bardwell (11) give an account of the action of α-rays on carbon monoxide. A brown suboxide was again formed. Carbon was deposited. The suboxide however differed completely from Brodie's and Berthelot's substance in being inert to water. The authors give for the reaction an equation

$$6\ CO \longrightarrow 2\ CO_2 + C_3O_2 + C$$

The variation in formula given for these suboxides of carbon is very striking and serves to emphasize Brodie's contention that carbon functions in these suboxides as in hydrocarbon chains. The ready condensation suffered by these bodies suggests that oxygen can enter the carbon lattices much in the same way as it enters the corresponding silicon lattice.

Preparation of Carbon Monoxide

Carbon monoxide was prepared by dropping concentrated sulphuric acid on to sodium formate. The apparatus was evacuated and washed out several times with the gas.

The carbon monoxide was dried over phosphorus pentoxide and passed through a liquid air trap into the reservoir. The experimental arrangement was the same as before.

When the dry gas was exposed to the rays, a steady reduction of pressure took place. On the walls of the reaction vessel appeared a light-brown deposit and carbon dioxide was formed on the gas. Two experiments gave the results indicated in Table III (A and B).

TABLE III

EFFECT OF RAYS ON CARBON MONOXIDE

Experiment	% CO reacted	% CO_2 produced	% Contraction of original pressure
A	20	7	12.0
B	21.0	8.4	12.6
C	8.8	6.1	1.7

NOTE: KV = 136. *Tube current, 0.13 ma. Pressure, 20 cm. Time, 4 hr.*

That is, the ratio CO reacted: CO_2 produced : contraction = 5:2:3 corresponding to an equation

$$5\ CO \longrightarrow 2\ CO_2 + (C_3O)\ \text{solid}.$$

The brown coating on the walls had no measurable vapor pressure. Where water vapor was admitted to the reaction vessel the solid was immediately assimilated leaving in its place a transparent skin of brown liquid.

When carbon monoxide was exposed to the rays in presence of water vapor no visible deposit was produced. The contraction in pressure and amount of carbon dioxide formed were much less. (See Expt. C, Table III).

The presence of hydrogen in the gas pointed to the occurrence of such a reaction as

$$CO + H_2O \longrightarrow CO_2 + H_2\ .$$

The mechanism of the carbon monoxide reaction will be discussed in the next section.

Carbon Monoxide and Oxygen

When a dry mixture of carbon monoxide and oxygen was exposed to the cathode rays, reduction in pressure occurred. The rate of pressure decrease fell off with time to a constant rate. Carbon dioxide was produced in the gas phase.

The pressure of water vapor had a remarkable influence upon the reaction. The pressure decrease was much smaller and constant. The amount of carbon dioxide formed was much less.

In neither case however did any reaction but that of carbon dioxide formation occur.

TABLE IV

EFFECT OF CATHODE RAYS ON A DRY MIXTURE OF CARBON MONOXIDE AND OXYGEN

Mixture		Pressure decrease (mm.)			
		1st hr.	2nd hr.	3rd hr.	4th hr.
20 cm. CO, 20 cm. O_2	Dry	21.4	9.9	7.8	5.2
20 cm. CO, 20 cm. O_2	Moist	4.5	4.4	4.3	4.0
10 cm. CO, 30 cm. O_2	Dry	13.4	6.8	4.9	5.0
10 cm. CO, 30 cm. O_2	Moist	3.5	5.0	4.2	4.0

NOTE: *KV = 136; tube current, 0.13 ma.*

The retarding effect of water vapor was independent of its concentration

TABLE V

EFFECT OF CONCENTRATION OF WATER VAPOR

Water vapor pressure, in mm.	% CO as CO_2
nil	34.6
4.1	12.9
16.1	12.7

NOTE: KV = 136; *tube current, 0.13 ma. Time, 4 hr. Mixture, 15 cm.CO, 5cm.* O_2.

Table VI shows the effect of varying composition and pressure of the mixture, and of the presence of water vapor on the percentage of carbon monoxide oxidized to carbon dioxide.

The moist mixtures were saturated with water vapor at 20° C.

TABLE VI

EFFECT OF COMPOSITION AND PRESSURE OF MIXTURE AND OF WATER VAPOR ON OXIDATION OF CARBON MONOXIDE

Pressure	Dry		Moist	
	% CO_2 of CO present	% CO_2 of whole mixture	% CO_2 of CO present	% CO_2 of whole mixture
10 cm. CO, 30 cm. O_2	50.6	12.7	30.4	7.6
20 cm. CO, 20 cm. O_2	44.0	22.0	18.4	9.2
30 cm. CO, 10 cm. O_2	30.6	23.0	10.3	7.7
5 cm. CO, 15 cm. O_2	47.5	11.9	34.2	8.6
10 cm. CO, 10 cm. O_2	28.4	14.2	16.6	8.3
15 cm. CO, 5 cm. O_2	34.6	26.0	12.7	9.5

It is seen that

1. The rate of reaction varies as the total pressure, the composition of the mixture being the same.

2. In the case of the 'moist' reaction, the amount of carbon dioxide formed is independent of the composition of the mixture.

3. In the case of the 'dry' mixtures the amount of carbon dioxide formed increases with the proportion of carbon monoxide in the mixture.

This retarding effect of water vapor on the combination of carbon monoxide and oxygen when exposed to cathode rays is the more surprising since H. B. Dixon (4*a*) showed that the thermal reaction was greatly accelerated by water vapor (13).

The elementary processes which can occur in ionization by electron collision in a carbon monoxide-oxygen mixture include (7):

$$CO \longrightarrow C^+ + O$$
$$CO \longrightarrow C + O^+$$
$$CO \longrightarrow CO^+$$
$$O_2 \longrightarrow O_2^+$$
$$O_2 \longrightarrow O + O^+$$

Let us assume the following processes for the mechanism of the oxidation:

1. $\epsilon + CO \longrightarrow C + O^+$
2. $C + O_2 \longrightarrow CO_2$
3. $\epsilon + O_2 \longrightarrow O + O^+$
4. $CO + O^+ \longrightarrow CO_2$
5. $C + H_2O \longrightarrow CO + H_2$
6. $\epsilon + H_2 + O_2 \longrightarrow H_2O_2 = H_2O + \frac{1}{2}O_2$

Let the velocity constants of these reactions be $k_1, k_2, k_3, k_4, k_5, k_6$ respectively. Let ϵ be the available energy of the cathode rays.

The rate of production of carbon atoms is

$$\frac{dp_c}{dt} = \epsilon k_1 p_{co} - k_2 p_c p_{o_2} - k_5 p_c p_{H_2O} = 0$$

The rate of production of ionized oxygen atoms is

$$\frac{dp_{o^+}}{dt} = \epsilon k_3 p_{o_2} + \epsilon k_1 p_{co} - k_4 p_{o^+} p_{co} = 0$$

The rate of formation of carbon dioxide is

$$\frac{dp_{co_2}}{dt} = k_2 p_c p_{o_2} + k_4 p_{o^+} p_{co} = \frac{\epsilon k_1 k_2 p_{o_2} p_{co}}{k_2 p_{o_2} + k_5 p_{H_2O}} + \epsilon k_3 p_{o_2} + \epsilon k_1 p_{co}$$

Now k_3 and k_1 will be very nearly equal. We shall assume k_5 to be large in comparison with the other constants. For a dry mixture then, the rate of formation of carbon dioxide is

$$\frac{dp_{co_2}}{dt} = \epsilon k_3 p_{o_2} + 2\epsilon k_1 p_{co} = \text{approx } \epsilon k_1 (p_{o_2} + 2p_{co})$$

For a moist mixture $\frac{\epsilon k_1 k_2 p_{o_2}}{k_2 p_{o_2} + k_5 p_{H_2O}}$ is small and hence

$$\frac{dp_{co_2}}{dt} = \epsilon k_1 p_{o_2} + \epsilon k_3 p_{co} = \text{approx } \epsilon k_1 (p_{o_2} + p_{co})$$

These expressions describe the results obtained with fair approximation.

The reaction $C + H_2O \longrightarrow CO + H_2$ may be a surface reaction, the water molecule being adsorbed on the wall. This reaction will explain the non-formation of polymerized carbon suboxide when moist carbon monoxide is exposed to the cathode rays: for this condensation probably occurs thus,

$$C + CO \longrightarrow (C_2O) \ldots \text{etc.}$$

Removal of carbon atoms in other ways would prevent this.

Summary

1. Methane is only very slowly attacked by cathode rays, giving small percentages of hydrogen and ethane.

2. Methane and oxygen combine when exposed to cathode rays, and give as gaseous products, carbon monoxide, carbon dioxide, and hydrogen. Water and formic acid are the only other products. The production of formic acid may be a subsidiary reaction between hydrogen and carbon dioxide. The relative proportions of these products do not differ widely under a wide variation in conditions of pressure, composition of the gas mixture and energy of the rays.

3. With the pressure decrease as an index of the amount of reaction, the effect of voltage and pressure on the reaction rate has been investigated. The reaction is found to be of the first order with respect to pressure. The reaction

rate increases linearly with the voltage passing the window up to a certain value, after which it becomes nearly independent of the voltage. This break in the linear relation is due to the saturation of the gas by the electrons.

4. The action of cathode rays on carbon monoxide produces carbon dioxide and a solid brown suboxide, discovered by Brodie in 1873. The oxide is extremely soluble in water and its formation corresponds to a formula $(C_3O)_n$. This differs from the formula given by Brodie and Berthelot. If the carbon monoxide is moist, less carbon dioxide is produced and no visible amount of solid or liquid is deposited.

5. The action of cathode rays on carbon monoxide-oxygen mixtures cause carbon dioxide formation. Presence of water vapor has a remarkable retarding effect on the reaction. For mixtures of the same composition the reaction rate is proportional to the total pressure. For dry mixtures the amount of carbon dioxide formed increases with the proportion of carbon monoxide in the mixture; for moist mixtures the amount of carbon dioxide formed is much less and is independent of the proportion of carbon monoxide. The retarding effect of water vapor appears to be independent of its concentration.

A brief theory of the reaction is given.

References

1. Berthelot, M. Bull. soc. chim. 26: 101-104. 1876.
2. Brodie, B. C. Ann. 169: 270-271. 1873.
3. Busse, W. F. and Daniels, F. J. Am. Chem. Soc. 50: 3271-3286. 1928.
4. Coolidge, W. D. J. Franklin Inst. 202: 693-721. 1926.

4a. Dixon, H. B. Chem. News. 46:151. 1883.

5. Eisl, A. Ann. Physik. 3: 277-313. 1929.
6. Farkas, L., Goldfinger, P. and Haber, F. Naturwissenschaften. 18: 266. 1930.
7. Kallmann, H. and Rosen, B. Z. Physik. 61: 61-68. 1930.
8. Krüger, F. Physik. Z. 13: 1040-1043. 1912.
9. Lind, S. C. Chemical Effects of Alpha Particles and Electrons. p. 97. 1921.
10. Lind, S. C. and Bardwell, D. C. J. Am. Chem. Soc. 48: 2335-2352. 1926.
11. Lind, S. C. and Bardwell, D. C. J. Am. Chem. Soc. 51: 2751-2758. 1929.
12. Marshall, A. L. J. Am. Chem. Soc. 50: 3178-3204. 1928.
13. Topley, B. Nature. 125: 560-561. 1930.

THE PHYSICAL CHARACTERS OF PENUMBRAL SHADOWS AND THEIR SIGNIFICANCE IN ROENTGENOGRAPHY[1]

By Paul M. Andrus[2]

Abstract

A new observation regarding the visual characters of penumbral shadows is recorded. It is pointed out that penumbral shadows appear to be laid down as a series of bands arranged serially as to density. This occurrence results in far-reaching effects in radiography as well as in other sciences concerned with the observation of images.

The object of this paper is to indicate a peculiar formation which may be observed in marginal shadows or penumbrae. This formation which is characterized by the occurrence of bands arranged serially as to density, was found greatly to influence many factors in practical roentgenography. An analysis of these factors will appear in later publications. Accordingly the essential data is presented herewith which has been gathered regarding this observation, a phenomenon which is apparently not generally familiar to physicists of this continent.

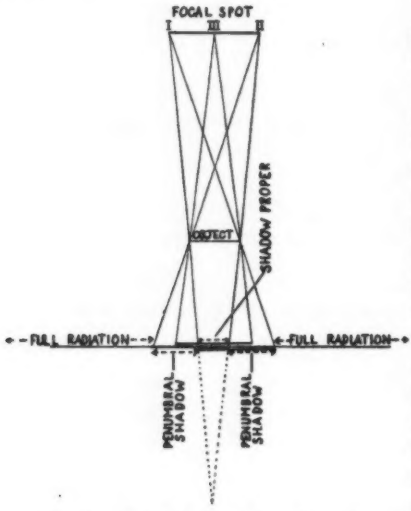

Fig. 1. *Multiple silhouettes of a radio opaque object.*

Of fundamental importance in radiography is the fact that the source of radiations in an X-ray tube is a "spot" and not a point. Focal "spots" range from about one-ninth to one-third inch in diameter in tubes commonly used in radiography. Just as multiple incandescent bulbs will project multiple shadows of a light opaque object, so the surface of the focal spot comprises multiple sources of X-ray beams, and will project multiple silhouettes of a radio-opaque object. In Fig. 1 the shadows projected from the parts I, II and III, of the focal spot, are indicated on the film by heavy lines. Only in the central bracketed area marked "shadow proper" do these silhouettes overlap and give a true or ray-free shadow, or umbra. The marginal areas marked "penumbral shadow" are exposed to partial radiation from the focal spot.

[1] *Manuscript received July 19, 1930.*

Contribution from the Department of Roentgenography, Queen Alexandra Sanatorium, London, Ontario, with financial assistance from the National Research Council.

[2] *Radiologist and Pathologist, Queen Alexandra Sanatorium.*

The width of these penumbral shadows is dependent on the size of the source of the rays (the focal spot), and the relative distances of the object from the film and the tube, as well as on the angular relations of the plane of the focal spot to the film. The penumbral shadow can be absent only if the source of the rays is a point, or if the object is in contact with the film.

The further importance of the size of the focal spot (aside from tube capacity) arises when the diameter of the object radiographed is less than that of the focal spot. In Fig. 1 it will be seen that if the object were much smaller than the size depicted, or the object-film distance much greater, the penumbral shadows on either side would meet or overlap, and the shadow proper be obliterated.

In the diagram also it will be seen that no rays passing directly from the focal spot can reach the film within the area marked "shadow proper". Beyond the penumbral shadow on either side, rays from all parts of the focal spot reach the film. Within the penumbral shadows, rays from only a limited part of the focal spot can reach the film, increasing in amount from the shadow side outward.

Thus if the quantitative distribution of rays is reasonably uniform, one would tentatively expect the density within a penumbral shadow to increase gradually from no exposure on the shadow side to complete exposure on the opposite side.

That such is apparently not the case, is shown in this communication.

Physical Characters of Penumbral Shadows

The physical characters of penumbral shadows may be readily reviewed by exposing to X-radiations a piece of metal placed midway between the source of radiation and the film. If such a negative of medium density and free from fog, is viewed by transmitted light, it will be seen that the penumbral shadows are apparently laid down as a series of bands of varying density. This distribution is not characteristic for X-radiations, but may be seen equally well at the edge of a shadow cast by any type of actinic radiation.

On the outer side of the penumbral shadow, *i.e.*, furthest from the shadow proper, will be seen a band of actually greater density than the surrounding opacities. This is remarkable in view of the fact that the surrounding areas are presumably exposed to all the available

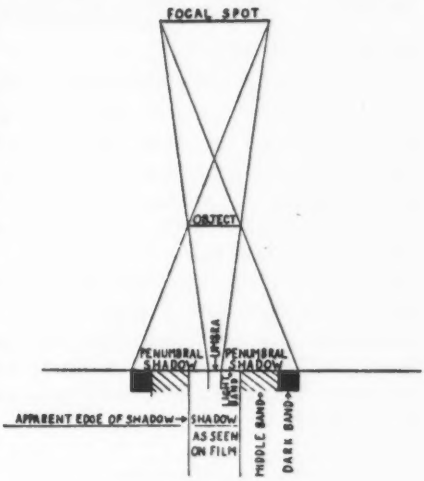

FIG. 2. *Penumbral density bands.*

rays. Inside this band again, a careful examination will reveal another narrow band of actually less density than the basic fog of the shadow itself, which is a remarkable fact. This band, as will be shown, is of fundamental importance in the physics of radiography. Such a film shadow is reproduced in Fig. 3, Plate I and a diagrammatic representation given in Fig. 2. The edges of the bands are marked by scratches at one position. The details of the apparent structure of penumbral shadows are as follows:—

Width of the Density Bands

Inasmuch as the intrapenumbral density bands are only relatively sharply demarcated, highly precise measurements are not possible. The average of about 4,000 measurements, made with a measuring microscope, of films exposed under varying conditions of radiographic technique, and marked by hand, showed the clear band to comprise 22.75% of the total penumbra. The dark band was in a similar range averaging 23.95%, and the middle band 53.3%. These figures are variable up to 5% in either direction depending probably upon tube and electrical factors as discussed later in the paper. The relative widths of the bands, however, remain constant when the total width of the penumbra is changed by altering the tube-object or object-film distances.

Other Rays

As before mentioned, the phenomenon is not characteristic for X-radiations. It has been observed in the penumbral shadows cast by white light, by monochromatic and polarized light, and also by ultra-violet radiations. It can readily be seen in the penumbral shadow from any light source, and is equally apparent whether viewed directly, or as the image developed on photosensitive material.

Margins of the Bands

The junction of the clear* band with the shadow proper or umbra, is sharp, although visibility is low from lack of contrast. The clear band is well demarcated from the middle band, but the junction can be termed sharp only when the total penumbra is relatively narrow. The other band margins are progressively less sharp from the umbra outwards. In viewing a radiograph, the junction of the clear band with the middle band is interpreted as the edge of the shadow. The clear band is interpreted as a part of the shadow due to its lack of density, and the other bands are interpreted as being outside the shadow on account of their increased density (Fig. 2). It follows that the junction of the clear band with the middle band determines the *degree* of sharpness. Since the sharpness of this edge appears to vary as the total width of the penumbral shadow, the latter may be used as a measurable index to sharpness.

* *"Clear" in the developed photosensitive negative; the same band is "dark" when the shadow is directly viewed, or in a copied positive.*

Positive reproduction of the penumbral shadow cast by an object placed in a beam of X-rays, and showing a "dark" outer band.

Effect of Density on the Bands

The outer dark band is most clearly seen in films of low density, and the inner clear band improves in visibility with greater density; in both cases the reason is that contrast is increased.

The middle and outer bands increase in density with exposure until the saturation point of the emulsion is reached, when they cease to be visible. The inner clear band however, does not become more dense with increased exposure except by fogging, which is common to the rest of the film. There may, however, be some encroachment of density from the middle band and this is apt to appear as a milkiness in the outer half or more of the clear band. But this does not exceed the density of the shadow proper for exposures under 50% of saturation of the emulsion. Beyond such an exposure it may assume greater density, and thus lessen the effective width of the clear band.

Density of Object

The phenomenon is not affected by the characters of the causative object. It is identical when the heavy metals or the soft tissues of the body are rayed, except that with the latter, visibility may be impaired by fog.

Tube and Electrical Factors

An occasional tube will show an unusual relative width of one or another of the intrapenumbral density bands, or project an additional narrow band. This is reasonably explained by irregularity of cathode ray distribution resulting in breaks in the continuity of the focal area, with resulting bends in the density curve. Certain electrical and thermal factors may also alter the total width of the penumbra under otherwise fixed conditions. These we attribute to actual change in the size of the focal area on the anode of the tube. They will be dealt with in a later study dealing with focal spot measurements.

Proof

It is necessary however, to demonstrate that all of the density bands actually belong to the penumbral shadow. This was done by casting shadows from exactly measured sources of radiation (both X-radiations and light) under exact distance conditions, and correlating the penumbral measurements with those they should geometrically attain. When all density bands described were included, the penumbral measurement agreed with the mathematical calculation to 0.004 in. If any of the bands were excluded from the penumbral measurement, errors of 20% or more would be incurred. This has also been confirmed by the use of the Moll recording microphotometer as described below.

Application to Radiography

These relate to two essentials of radiography, namely sharpness and radiability. It is shown in the third section and Fig. 2, that the apparent edge of a shadow as seen on the film, is actually the junction of the clear with the middle penumbral band, *i.e.*, that the sharpness of this junction, and

therefore the sharpness of the visible shadow, varies as the total width of the penumbral shadow. The sharpness of shadow is therefore a function of penumbral width. Sharpness is, of course, also dependent on penumbral visibility, which in turn is a matter of contrast, and may be adversely affected by fog from any source.

Radiability, or success in registering a distinct shadow of fine detail, is also greatly influenced by the banded formation of the penumbrae. This relation is twofold, affecting first, contrast, and secondly, width of shadow. Since the apparent density of the inner clear penumbral bands is less than the basic fog of the umbra itself, it follows that the contrast between the density of the apparent shadow and the surrounding opacities is increased, and sharpness and shadow enhanced.

Fig. 2 also shows that the apparent width of a shadow is always greater than the true width, since the clear bands on each side appear as part of the umbra. As each clear band occupies about one-quarter the width of a penumbra, the resulting addition to the shadow is thus approximately one-half the width of one penumbral shadow. Delicate shadows are thus made more visible by an artificial increase of width.

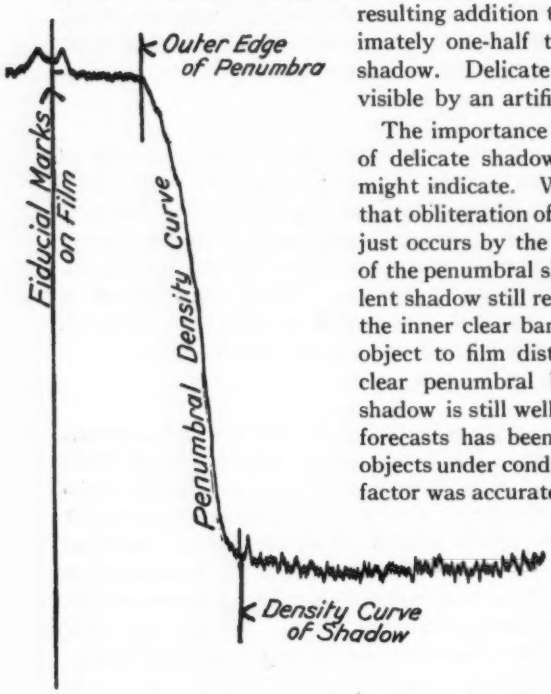

FIG. 4. *Moll microphotograph showing the actual density changes through a penumbral shadow.*

The importance of this addition to the width of delicate shadows, is even greater than this might indicate. When the film position is such that obliteration of the shadow proper, or umbra, just occurs by the meeting of the inner margins of the penumbral shadows on each side, an excellent shadow still remains, which is produced by the inner clear band of each penumbra. If the object to film distance is increased so that the clear penumbral bands overlap, an apparent shadow is still well seen. The accuracy of these forecasts has been confirmed by radiographing objects under conditions where every dimehsional factor was accurately controlled, and the relative positions of the penumbral shadows thus closely known.

These physical phenomena are extremely useful in taking roentgenographs If shadows were not unwittingly saved by this happy provision of nature, radiographs made under present day routine would be detailless masses, inasmuch as all detail which it is attempted to radiograph is very much smaller in size than the dimensions of the focal spots commonly used.

Explanation of the Phenomenon

The explanation of the phenomenon becomes apparent if a tracing is made of the actual density changes through a penumbral shadow, by means of a recording microphotometer. Such an instrument (Moll) projects a narrow and intense beam of light, through which the field under study is moved. The beam of light after traversing the film, falls upon a small vacuum thermopile, and a galvanometer registers the changes of voltage that are induced in the thermopile by the changing intensity of the beam. The movements of the galvanometer mirror cause deflections of a second beam of light which is projected upon it, and this reflected beam of light registers upon a moving roll of bromide paper a graph of the density changes in the field under study. Such a graph is shown in Fig. 3. The sensitivity of the instrument is indicated by the multiple small irregularities in the tracing, these irregularities indicating the changes in density due to the distribution of the silver particles of the emulsion. By means of fiducial density marks placed upon the film the dispersion is known, and the actual density changes in the field under study may be observed and measured from the graph.

The curve thus traced through a penumbral shadow approaches a straight line, the actual curve varying with the shape of the source of the radiations as well as its homogeneity. Such tracings do *not* show the existence of banded density changes as described in this article. It follows that the phenomenon is an optical illusion, and that the apparent density bands are not present in fact. It is none the less a very real illusion, and this explanation in no way lessens the importance of the observation as it relates to practical radiography and to other sciences concerned with images.

Historical

The observation of the apparent banded density changes in penumbral shadows as described in this article, was made independently by the author, who knows of no direct reference to the subject. The observation in its basic sense, *i.e.*, that intensities may not be interpreted in their correct proportions by the human optical system, is however not new, and was described in Austria as early as 1865. An extensive theoretical and mathematical review of this subject is given by Kühl (1). He describes the experiments of the original observer (Mach), and includes a large bibliography. Some of the essentials of Kühl's material are reviewed here.

This author points out in substance, that when the edge of an object is directly viewed with sufficient illumination, a narrow band of considerable brilliancy is seen immediately adjacent to the edge of the object on the side having the greater illumination, *i.e.*, whether this be the object or the background. Immediately adjacent to the other side of the edge, is a dark band. The author records that in this dark band, "a more profound darkness* is perceived than that due to mere absence of light".

* *The conditions of illumination under which Kühl bands are seen, of course preclude diffraction as the direct cause. If the edge of a black fountain pen is viewed with good illumination and a white background, using a magnification of say ten diameters, the clear band appears quite brilliant. It may be seen quite well without magnification, although it is then less conspicuous.*

Kühl quotes experiments to show that these bands are not represented by corresponding changes in the actual intensity of illumination, and concludes that they represent an optical illusion. He shows that the essential factor which induces the optical interpretation of such bands, is a more or less abrupt bend in the curve of illumination, and that the curve of the illusion follows the second differential of the illumination curve. If the bend in the illumination curve is positive, *i.e.*, if the intensity increases, a dark band is perceived, and if negative, it is a clear band. The sharper the bend, the more conspicuous the bands become. Such density changes, occurring as they do at the edge of an image no matter how sharp (by reason of the diffraction pattern) induce the optical interpretation of the two density bands observed by Kühl at the edge of a directly viewed image.

The mechanism of the illusion he ascribes to the inability of the receiving and transmitting organs of the optical system to evaluate correctly within close limits, the relative values of proximate intensities, and especially when such intensities are substantially dissimilar. A correct estimate of the relative values of adjacent intensities is thus not passed on to the perception centres—a defect as it were in the perfection of the conducting mechanism. Such defect however, results in an artificial improvement in apparent contrast: the "contrast-function" of the optical mechanism.

Kühl submits that this illusion "must have important effects upon all kinds of precision measurements", by reason of the uncertainty as to position of the geometrical image in the marginal densities. He maintains that this is particularly the case when two images become proximate, resulting in still further uncertainty as to the position of the geometrical image. He is particularly concerned with errors in astronomical measurements, and he gives mathematical corrections for such errors.

Discussion

Reverting to the density or contrast bands in penumbral shadows as described in this article, it is apparent that these bands have a common basis with those described by Kühl, namely an illusory optical interpretation of density changes, induced by bends in the illumination curve. Such bends being pronounced at each end of the density curve of a penumbral shadow, (Fig. 4) the contrast bands are thus interpreted at these points.

The chief differences between the contrast bands in penumbral shadows and those seen at the edge of a directly viewed object, are first, the great variation in width to which penumbral bands are subject, and secondly, the presence of the middle band in penumbral shadows, this not being observable in the Kühl phenomenon.

There is however, nothing in either the experimental or mathematical data examined, to explain why the width of the penumbral density bands is a function of the total penumbral width. If the foregoing explanations are complete, a narrow band should be seen at each edge of a penumbral shadow, and the width of such bands should be constant irrespective of the total width

of the penumbra. Again, while Kühl states that the second differential of the illumination curve is the curve of the optical illusion, the second differential of the density curve of penumbral shadows definitely is not the curve of the illusion described in the present article.

Although it is outside the scope of this communication to consider the physical and mathematical details of the phenomenon, it is important that the Kühl phenomenon does not furnish a complete explanation of the contrast bands of penumbral shadows.

This communication then constitutes a preliminary review for the purpose of recording the observation, and pointing out particularly the relations of the phenomenon to practical radiography. The theoretical and practical aspects of the subject open a large field to the physicist and the roentgenologist alike. It is rather astonishing that the phenomenon is so little recognized in view of its universal occurrence, and its necessarily fundamental relations to all physical measurements and observations in which direct images, or their reproductions on photosensitive material, are involved.

Acknowledgment

The author is greatly indebted to Mr. Lorne A. Matheson of the Department of Physics of the University of Michigan, for locating the reference to Kühl's article, and for preparing preliminary tracings with the microphotometer.

Reference

1. KÜHL, A. Physik. Z. 29: 1-34. 1929.

DISTRIBUTION OF STRESS IN PARALLEL WELDING FILLETS[1]

By H. M. MacKay[2] and A. M. Bain[3]

Abstract

A mathematical theory is developed for the distribution of stress in welded joints with parallel fillets, in the case where each of the members connected by the weld is of uniform cross section. The theory is verified by strain measurements on two specimens of the type of joint considered.

Introduction

In the application of welding processes to structural work, many cases arise where the welding fillets are parallel to the axis of loading. In such cases the load is transmitted from one member or unit to the other by shearing forces in the fillets and along the surfaces of contact between the fillets and the members connected. In this paper attention is directed to the variation in the magnitude of these forces along the length of the fillet, when the members connected are of uniform rectangular cross section.

In the case of riveted joints, it has long been known that when there are more than two rivets in the line of loading, or more than two rows of rivets cut by the axis of loading, the load, in general, cannot be divided equally between them. Several years ago Batho (1) developed a theory for the distribution of load in riveted joints, which he verified experimentally in the case of certain types of joint. The considerations applying to riveted joints apply with equal force to welded joints with parallel fillets. In fact, the variation in the distribution of stress may possibly be of more practical importance in the latter case than in the former. In riveted joints it is fully recognized that when certain rivets are stressed beyond the elastic limit, a redistribution of load takes place, owing to plastic deformation of the rivets or the adjoining metal, which tends to equalize the stress throughout the group. At the same time, the overstressed rivets retain in a large measure their power of resistance. The assumption of uniform distribution of load which is made in practice, coupled as it is with conservative unit stresses, therefore gives satisfactory results. It is not yet known to what extent similar compensating conditions may be expected in the case of welded joints.

Theory Proposed

The theory of distribution of stress in the class of joints under consideration may be developed as follows.

[1] *Manuscript received August 6, 1930.*

Contribution from the Civil Engineering Laboratories of McGill University. The paper is based on a thesis submitted by the junior author in partial fulfilment of the requirements for the degree of M.Sc., May, 1929.

[2] *Dean of the Faculty of Applied Science, McGill University, Member of the National Research Council.*

[3] *Graduate student in Civil Engineering, McGill University.*

Fig. 1 represents a simple lap joint in which two plates X and Y, each of uniform cross sectional area, are spliced by means of fillets FF, indicated by hatched lines along the edges of the plate X.

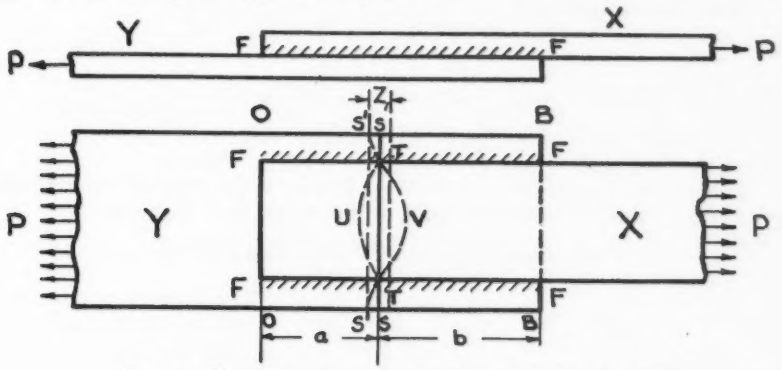

FIG. 1. *Simple lap joint showing two plates, each of uniform cross sectional area, spliced by means of fillets.*

A_1 is the sectional area of the plate X.

A_2 is the sectional area of the plate Y.

P is the total load (*e.g.*, tension) in the joint.

p is the average unit stress in a section across X at a distance x from the origin.

p' is the corresponding stress in Y.

L is the length of the splice.

The bending stresses to which the joint indicated would be subjected need not be considered, since in structural practice the design is usually such as to eliminate such stresses, or to reduce them to negligible proportions.

p must vary in some manner between the values 0 at OO and P/A at BB. In like manner p' must vary between the values P/A at OO and 0 at BB. Further, the values of p and p' at any section are connected by the relation $pA_1+p'A_2=P$.

A little consideration will show that, generally, any originally plane section TT of the plate X, will, when the load is applied, be distorted into some such shape as TVT; and that the originally plane section $STTS$ of the plate Y will assume some such shape as $S'TUTS'$. Sections of X and Y originally lying in the same plane $STTS$, will therefore be displaced relatively to one another by some amount Z_1, where Z_1 is the sum of the average displacements of the sections TT and $STTS$ to the right and left, respectively, of their original positions.

If p and p' were constant and equal, all else remaining unchanged, the same relative displacement would take place at all sections. At some section indeed, p and p' are equal. Suppose that p and p' are equal at $STTS$, which may, for the moment, be taken as the origin of co-ordinates. To the left of

this section values of p are less than those of p'. If any section be considered distant x from $STTS$, and to the left, the average displacement of particles of X and Y respectively, originally lying in the same transverse plane, will after load is applied be

$$Z_1 + \frac{1}{E}\int p'dx - \frac{1}{E}\int pdx .$$

At OO the corresponding displacement will be

$$Z_1 + \frac{1}{E}\int_o^a p'dx - \frac{1}{E}\int_o^a pdx$$

which may be written $Z_1+Z_2=\Delta_1$. Similarly, the average relative displacement of particles originally lying in the same plane BB will be

$$Z_1 + \frac{1}{E}\int_o^b pdx - \frac{1}{E}\int_o^b p'dx = Z_1+Z_3=\Delta_2 .$$

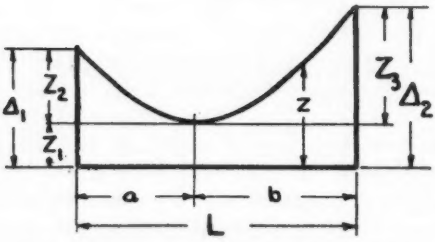

FIG. 2. *Graphic representation of the average relative displacements of all sections of the two plates due to the load.*

The average relative displacements, due to the load, of all sections of the two plates originally co-planar, may be indicated graphically by some such curve as that shown in Fig. 2.

Inasmuch as the section where $p=p'$ is generally unknown, it will be convenient to shift the origin to one end of the splice as at OO. The relative displacement of any section distant x from OO, will therefore be

$$z=\Delta_1 + \frac{1}{E}\int pdx - \frac{1}{E}\int p'dx \qquad (1)$$

Load is transmitted from the plate Y to the plate X through the fillets. Let ρ be the load transmitted by the fillets per unit of length, the two fillets being regarded as one unit of length L. The relation between ρ and z is unknown.

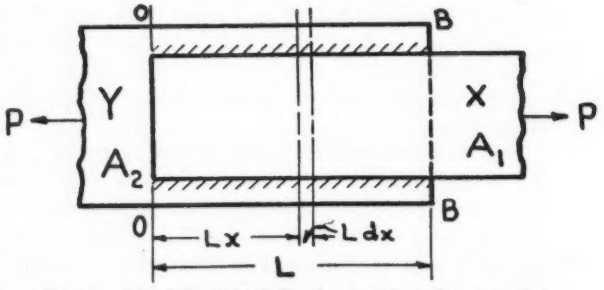

FIG. 3. *Simple lap joint indicating a section taken at random.*

It will be assumed, however, subject to experimental verification that ρ is proportional to z, or, that $\rho=K'z$ where K' is an empirical constant.

For convenience in numerical computation it will be better to express the distance of any section from the origin as a fraction x of the length L, as in Fig. 3.

Then from equation (1)

$$\rho = K'z = K'\Delta_1 + \frac{K'L}{E}\left[\int p\,dx - \int p'\,dx\right] \tag{2}$$

But $p' = \frac{P - pA_1}{A_2}$

and writing $K = \frac{K'}{E}$

$$\rho = EK\Delta_1 + KL\left[\frac{A_1+A_2}{A_2}\int p\,dx - \frac{P}{A_2}\int dx\right] \tag{3}$$

Now

$$\rho L\,dx = A_1\,dp, \text{ or, } \rho = \frac{A_1}{L}\frac{dp}{dx} \tag{4}$$

Hence

$$\frac{dp}{dx} = \frac{EKL\Delta_1}{A_1} + \frac{KL^2(A_1+A_2)}{A_1A_2}\int p\,dx - \frac{KL^2P}{A_1A_2}\int dx \tag{5}$$

and

$$\frac{d^2p}{dx^2} = \frac{KL^2(A_1+A_2)}{A_1A_2}\,p - \frac{KL^2P}{A_1A_2} \tag{6}$$

This may be written

$$\frac{d^2p}{dx^2} = \alpha^2 p - \beta \tag{7}$$

where $\alpha^2 = \frac{KL^2(A_1+A_2)}{A_1A_2}$ and $\beta = \frac{KL^2P}{A_1A_2}$.

The solution of equation (7) is

$$p = C_1e^{\alpha x} - C_2e^{-\alpha x} + \frac{\beta}{\alpha^2} \tag{8}$$

where e is the base of the Napierian system of logarithms, and C_1 and C_2 are constants of integration.

Obviously $\frac{\beta}{\alpha^2} = \frac{P}{A_1+A_2}$ and, noting that $p=o$ when $x=o$, and $p = \frac{P}{A_1}$ when $x=1$, it follows easily that

$$C_1 = \frac{P(A_2+A_1e^{-\alpha})}{2A_1(A_1+A_2)\sinh\alpha} \text{ and } C_2 = \frac{P(A_2+A_1e^{\alpha})}{2A_1(A_1+A_2)\sinh\alpha}.$$

Hence

$$p = \frac{P}{A_1+A_2}\left(1 + \frac{A_2+A_1e^{-\alpha}}{2A_1\sinh\alpha}\,e^{\alpha x} - \frac{A_2+A_1e^{\alpha}}{2A_1\sinh\alpha}\,e^{-\alpha x}\right) \tag{9}$$

which may be written

$$p = \frac{P}{A_1+A_2}\left(1 + B_1e^{\alpha x} - B_2e^{-\alpha x}\right) \tag{10}$$

now

$$\rho = \frac{A_1}{L}\,\frac{dp}{dx} = \frac{P\alpha A_1}{L(A_1+A_2)}\left(B_1e^{\alpha x} + B_2e^{-\alpha x}\right) \tag{11}$$

If $A_1 = A_2 = A$, equation (9) becomes

$$p = \frac{P}{2A}\left(1 + \frac{1+e^{-\alpha}}{2\sinh\alpha}\,e^{\alpha x} - \frac{1+e^{\alpha}}{2\sinh\alpha}\,e^{-\alpha x}\right) \tag{12}$$

or,
$$p = \frac{P}{2A}\left[1 + \frac{2\cosh\frac{a}{2}\sinh a\left(x - \frac{1}{2}\right)}{\sinh a}\right] \tag{13}$$

and
$$\rho = \frac{Pa}{A}\frac{\cosh\frac{a}{2}\cosh a\left(x - \frac{1}{2}\right)}{\sinh a} \tag{14}$$

The force transferred by the fillet at any point is thus fully determined.

Experimental Verification

In order to test the validity of the theory developed above, two specimens designated as T_1 and T_2 were designed and fabricated.

T_1 consisted of two lengths of 6 in. × 5/8 in. plate, 2 ft. 6 in. long, placed end to end and spliced by two cover-plates whose nominal dimensions were 5 in. × 3/8 in. × 1 ft. 8 in. Each cover-plate was arc-welded to the main plates by parallel longitudinal fillets, as indicated in Fig. 4., which shows the details of the joint. It was intended that the cross sectional area of the two splice plates taken together should be equal to that of each of the main plates, *viz.*, 3.75 sq. in. Commercial stock was used, however, and it was found that while the main-plates were true to gauge, the cover-plates were about 4.5% too thick, their joint sectional area being 3.92 sq. in. The workmanship in this specimen was satisfactory.

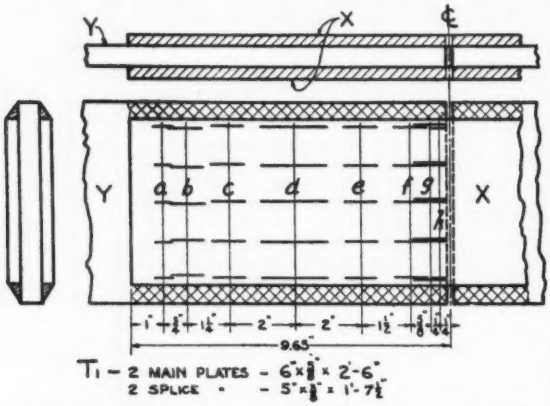

FIG. 4. *Details of joint, specimen T_1, showing position of extensometers and gauge lengths.*

In T_2 the main-plates were the same as in T_1, but the cover-plates were 4 × 3/8 × 14 in., giving a cross sectional area of 3.00 sq. in., or 20% less than the main-plates. The workmanship was defective. The most serious defect was that one of the cover-plates was bent in a longitudinal plane so that the inner face was concave, leaving, at the joint, an opening of 3/32 in. between it and the main-plate. This seriously affected the stress measurements.

The experimental work consisted in measuring the stress at different sections along the length of the cover-plates. The difference between the average stresses in any two adjacent sections multiplied by the sectional area of the plate is, of course, equal to the force transmitted to the cover-plates by the fillets in the distance between the sections. Hence an experimental value of ρ, the force so transmitted per unit of length, is readily obtained.

Strain measurements were necessarily confined to the cover or splice-plates since the main-plates, throughout the length of the splice, were inaccessible except at the extreme edges. Indeed only the outer faces of the cover-plates were accessible. In the case of riveted joints of a similar general type, it had been indicated by MacKay (2) in 1912, and confirmed by Batho (1, p. 575) in 1916, that strain measurements on the outer face gave a satisfactory indication of the stress throughout the thickness of the plate. In riveted joints, however, the component parts are firmly held together by the rivets at short intervals, while in welded joints of the type here considered they are so held at the edges only. It was found, however, that measurements on the outer faces at the centre of the splice, where the workmanship was not visibly poor, accounted for the total applied load, within reasonable limits of experimental error. It was therefore assumed that measurements on the outer faces indicated the true stresses at other sections.

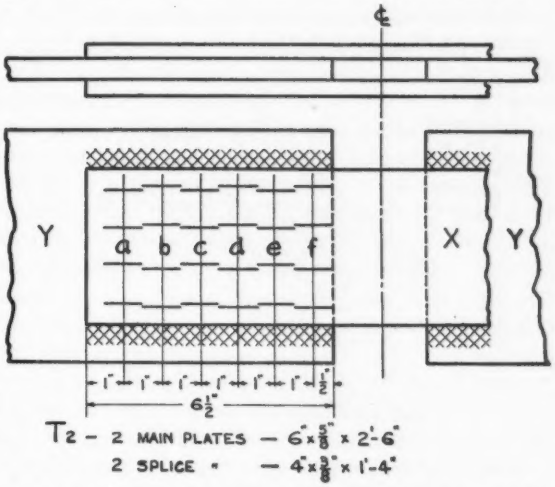

FIG. 5. *Details of joint, specimen T_2, showing positions of extensometers and gauge lengths.*

Mirror extensometers of the Martens type were used. Positions of the extensometers for specimens T_1 and T_2 are shown in Fig. 4 and 5 respectively. Where, as in this case, stress varies rapidly along the length of the specimen, and not according to a linear law, it is necessary to use very short gauge lengths to obtain correct results. Thus, in specimen T_1, one-half inch gauge lengths were employed at sections a and h; two-inch lengths at section d; and one-inch lengths at all other sections in both specimens.

The use of such short gauge lengths is sometimes deprecated. Swain (3), whose opinions properly carry much weight, states that he would place no reliance on measurements based on gauge lengths of one inch. Such doubts are not shared by the authors, nor by other workers in the same laboratories who have had wide experience with Martens extensometers. Possibly much of the doubt arises from failure to appreciate that commercial rolled sections (such as plates) are never flat, but are full of undulations, often invisible, but of quite sufficient magnitude to affect delicate extensometers. Under tension these undulations straighten out to some extent, causing the whole extensometer, including the mirror, to rotate. This introduces large errors which

may usually be eliminated by repeating the readings with the mirror reversed. It should, of course, be remembered that, working with steel, an error of .00001 in. corresponds to 600 lb. per sq. in. for a half-inch gauge, and to only 30 lb. per sq. in. for a ten-inch gauge, and that discretion should be used in adopting the gauge length to the problem in hand.

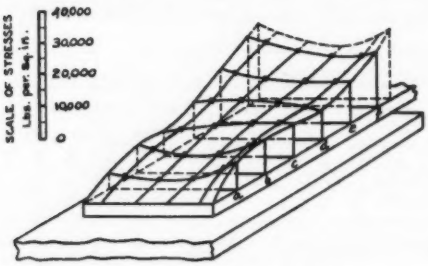

FIG. 6. *Showing distribution of stress at various sections of specimen T_1, as measured by extensometers.*

The specimens were tested in a 100-ton Wicksteed hydraulic machine. In the case of each the extensometers were set to zero at a load of 1,000 lb. Final readings were taken at a total load of 100,000 lb. for specimen T_1, and 75,000 lb. for T_2. The range of loads for which strain measurements were made was, therefore, 99,000 lb. and 74,000 lb. for T_1 and T_2 respectively. Readings were also taken at intermediate loads to check the operation of the extensometers, but are not recorded herein. The loads chosen were such as to keep the stresses at all points of the specimens within the elastic limit of the material. All extensometers were again read when the load was reduced to the initial 1,000 lb.; and whenever the final readings varied more than .00002 in. from zero the work was repeated.

In all reductions of extensometer readings E (Young's modulus) was assumed to be 30×10^6 lb. per sq. in. Also in each specimen the two cover-plates were regarded as a single unit. The stresses at the various sections measured are shown graphically in Fig. 6 and 7, in which the measured stresses at the various ranges across the width of the cover-plates are plotted, the points so plotted being joined by smooth curves. The average stress at each section may be conveniently obtained by a planimeter.

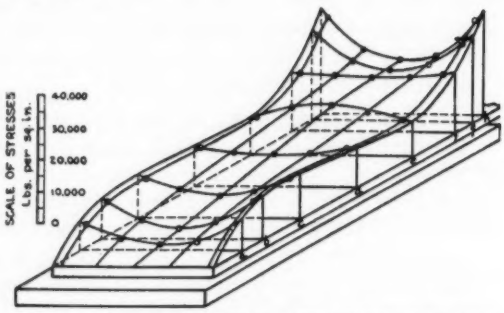

FIG. 7. *Showing distribution of stress at various sections of specimen T_2, as measured by extensometers.*

Calculation of values of p and ρ

It was intended that three-eighths-inch fillets should be used. In both specimens, however, the actual size provided was 3/8 in. × 1/2 in., giving a cross sectional area of .375 sq. in. for the four fillets taken together. As

this amounted to roughly 5% of the total area of main and splice plates, it was too large to be neglected. Two methods of dealing with this matter suggested themselves. First, the fillets might be assumed to be under a tensile stress constant from end to end and equal to the total applied load divided by the total cross sectional area of the specimen including the fillets themselves. The load carried by the fillets on this assumption might then be deducted from the applied load, and the remainder considered as the load on the plates; or, second, the cross sectional area of the fillets might be divided proportionally between the cover-plates and main-plates, thus considering the junction of the plates to be along a longitudinal plane cutting all cross sections of the fillets. Investigation having shown that both methods gave practically the same results, the latter of the two was chosen. It was considered sufficiently accurate, however, to divide the fillets equally between the main and cover-plates.

It has already been pointed out that the assumed constant $K=K'/E$ is empirical. It must be found by trial. Suspecting that K' would lie between E (Young's modulus) and G (the coefficient of rigidity), values in the neighborhood of the latter constant were tried. It was soon found that a value of $K'=12.5\times10^6$, or a corresponding value of $K=0.4$ would fit the observations as well as any other in the case of the two specimens under consideration.

The calculations for specimen T_1 may be given as follows:

Dividing the fillets equally between the cover-plate A_1 and the main-plate A_2,

$A_1=3.92+0.19=4.11$ sq. in.

$A_2=3.75+0.19=3.94$ sq. in.

$L=9.65$ in.

$K=0.4$

$$\alpha^2=\frac{0.4\times9.65^2\,(4.11+3.94)}{4.11\times3.94}=18.52$$

$\therefore \alpha=4.3;\ e^{\alpha}=73.7;\ e^{-\alpha}=0.0136$

Referring to equations (9) and (10)

$P/(A_1+A_2)=99{,}000\div8.05=12{,}300$ lb. per sq. in.

$$\frac{A_2+A_1e^{-\alpha}}{2A_1\sinh\alpha}=\frac{3.94+4.11\times0.0136}{8.22\times36.84}=0{,}0132=B_1$$

$$\frac{A_2+A_1e^{\alpha}}{2A_1\sinh\alpha}=\frac{3.94+4.11\times73.7}{8.22\times36.84}=1.0132=B_2$$

Hence $$p=12{,}300\ (1+0.0132e^{\alpha x}-1.0132e^{-\alpha x})$$

And referring to equation (11)

$$\frac{Pa\,A_1}{L\,(A_1+A_2)}=\frac{99.000\times4.3\times4.11}{9.65\times8.05}=22{,}600$$

Hence, $$\rho=22{,}600\ (0.0132e^{\alpha x}+1.0132e^{-\alpha x})$$

Similar values may be worked out for specimen T_2, and the following table constructed. The equation above gives values of ρ for four fillets. These values are divided by four to give the results in Table I.

TABLE I

THEORETICAL VALUES OF p AND ρ

x	Specimen T_1		Specimen T_2	
	p (lb./sq. in.)	ρ (lb./lin. in.)	p (lb./sq. in.)	ρ (lb./lin. in.)
0	0	5800	0	4400
.05	2460	4700	1690	3840
.1	4450	3830	3140	3380
.2	7400	2590	5600	2680
.3	9450	1790	7550	2240
.4	11000	1440	9300	2000
.5	12300	1300	10900	1970
.6	13500	1420	12500	2120
.7	15000	1790	14400	2480
.8	16900	2530	16600	3060
.9	19700	3680	19400	3950
.95	21600	4500	21200	4530
1.00	24000	5550	23150	5230

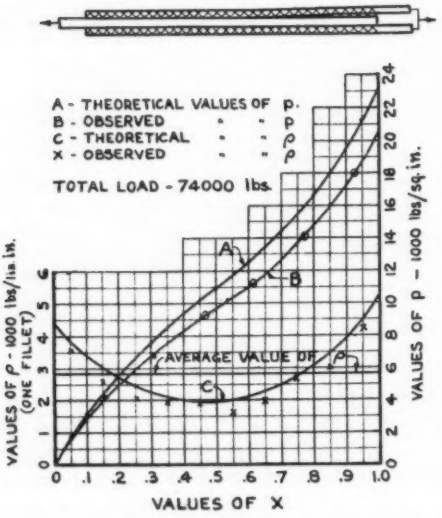

FIG. 8. *Showing theoretical and observed values of p and ρ for specimen T_1.*

The theoretical values of p and ρ given above are plotted for specimens T_1 and T_2 in Fig. 8 and 9 respectively in comparison with the observed values. The observed values of ρ are obtained by dividing the difference in the total observed stresses at any two sections by the distance between these sections. The result gives the average force per unit of length transmitted by all four fillets in the region considered. The observations provide no satisfactory means of determining any difference which may occur in the action of the different fillets. They are therefore assumed to participate equally in the transmission of force. The plotted values of ρ are for one fillet.

In the specimens, more particularly T_1, the sections at which stresses were observed are spaced too irregularly to be used satisfactorily for the purpose just explained. The expedient was therefore employed of drawing as smooth

a curve as possible through the points representing the observed values of p (Curves B in Fig. 8 and 9.). Values of p were then read from the curve at any desired points. Actually readings were made for points whose abscissae were 0.05L, 0.15L . . . . 0.95L. If p_n and p_{n+1} are the values of p so determined at any two adjacent points, $\rho = \frac{p_{n+1} - p_n}{0.1\,L \times 4}$, is the average force transmitted by one fillet per unit of length in the space between the points.

In the case of specimen T_1 (Fig. 8), little comment is required as to the agreement between the theoretical and observed values of p and ρ. In T_2 (Fig. 9) observed values of p were consistently lower than the theoretical ones. This may be attributed to the curvature of one of the cover-plates mentioned previously. Strains were necessarily measured on the convex side only of this plate, and as it straightened under load a result of the kind observed was inevitable. Observed values of ρ were, of course, affected accordingly. In spite of this, the observations even in this case seem to the authors to confirm strongly the validity of the proposed theory.

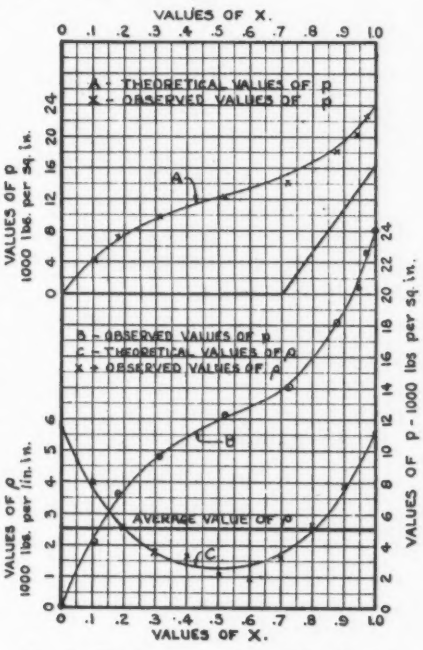

FIG. 9. *Showing theoretical and observed values of p and ρ for specimen T_2.*

Fig. 10 and 11 are intended to give a picture of the stress distribution in the cover-plates. They were constructed by erecting the stress diagrams at the various sections observed (Fig. 6 and 7) in their proper positions along the length of the plate, as the cross frames of a structure which is then shown in isometric projection.

The ratio of the maximum to the average value of ρ is 2.26 for specimen T_1 and 1.87 for speciment T_2. While the effect of these ratios on the strength of the joint is not yet known, it is worth while to consider the values likely to occur in practice. The longer the joint, the greater is the ratio of maximum to the mean shearing stress, in the fillet. The joints herein described were purposely made longer than necessary, in order to magnify the variation of shearing stress and to facilitate measurement of stress. The unit shearing stresses in the fillets were consequently low.

Suppose two members of equal sectional area, A, to be spliced by parallel fillets.

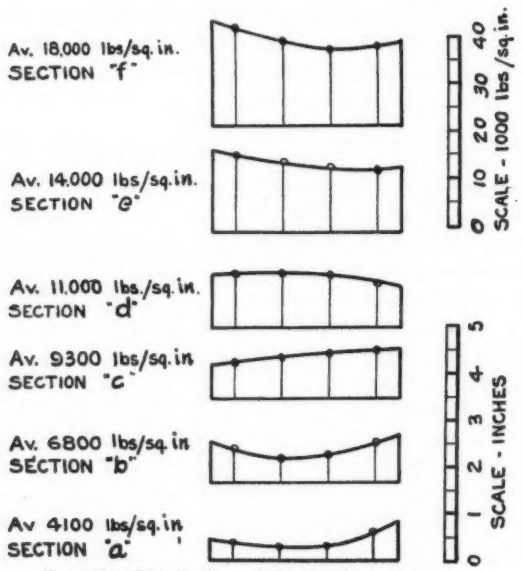

FIG. 10. *Distribution of longitudinal stress in splice plate of* T_1.

Let f = unit stress in tension.

v = average unit shearing stress in the fillets.

n = number of parallel fillets.

Then, using the previous symbols for other quantities

$$P = Af = nvL \tag{15}$$

From equation (14)

$$\rho = \frac{a\,P}{A} \cdot \frac{\cosh\frac{a}{2}\,\cosh a\left(x-\frac{1}{2}\right)}{\sinh a}$$

This is a maximum when $x = O$ or 1. In either case $\rho \max = \frac{Pa}{nA}\,\frac{\cosh^2\frac{a}{2}}{\sinh a}$ for each fillet.

$$\text{But } \rho \text{ average} = \frac{P}{nL} = \frac{Pv}{Af} \text{ and } \frac{\rho\ max}{\rho\ ave} = \frac{f}{nv}\,\frac{a\cosh^2\frac{a}{2}}{\sinh a} \tag{16}$$

where $\alpha^2 = \frac{2KL^2}{A} = \frac{2KfL}{nv}$

Assuming that $K = 0.4$, $f = 16000$ lb. per sq. in., $n = 4$ and $v = 4000$ lb. per lin. in.,

$$\alpha^2 = 0.8\ L \text{ and } \alpha = 0.9\sqrt{L}, \text{ approx.} = 0.9\sqrt{A}\ .$$

Assuming a number of different values of A, from 1 sq. in. to 25 sq. in., the ratios of ρ max. to ρ ave. may be determined as in Table II.

TABLE II

CALCULATED RATIO OF MAXIMUM TO AVERAGE LOAD

A sq. in.	1	4	9	16	25
a	0.9	1.8	2.7	3.6	4.5
$\cosh^3 \frac{a}{2}$	1.22	2.04	4.22	9.65	23.0
$\sinh a$	1.026	2.94	7.41	18.28	45.0
$\frac{\rho \text{ max}}{\rho \text{ ave}}$	1.07	1.25	1.54	1.9	2.3

It is doubtful whether much higher ratios need be incurred even should welding be applied to joints in large sections; since it will usually be easy to increase the number of fillets and thus reduce the length.

It remains to test the validity of the theory proposed by the authors in the case of members consisting of structural shapes such as angles, H-beams, and channels. Possibly different values of the empirical constant K may be required in such cases. It is hoped to make this question the subject of a future contribution. It is still more important to ascertain the effect of the distribution of stress in the fillet upon the strength of the joint. Specimens of fair size will, in the authors' judgment, be required for that purpose, and correspondingly heavy testing equipment.

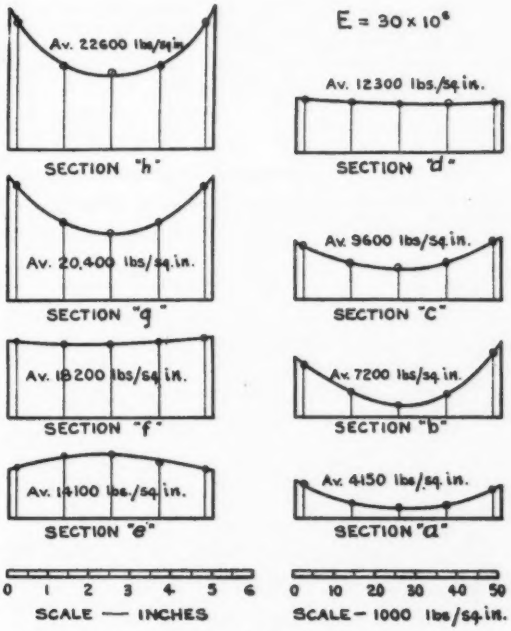

FIG. 11. *Distribution of longitudinal stress in splice plate of* T_2.

References

1. BATHO, C. J. Franklin Inst. 182: 553-604. 1916.
2. MACKAY, H. M. Report of Board of Engineers, Quebec Bridge, Vol. I, p. 235.
3. SWAIN, G. F. Structural Engineering, New York, 1924, p. 561.

THE DESIGN OF CORNERS IN FLUID CHANNELS[1]

By G. J. Klein[2], K. F. Tupper[2] and J. J. Green[2]

Abstract

The information contained in this report is the result of a detailed investigation of the characteristics of a variety of modified corners in a wind tunnel. The modification of the corner was effected by the insertion of banks or cascades of vanes along the diagonal, the intention being to secure minimum losses due to turbulence, coupled with uniformity in the issuing air stream. Apart from the specific application of this research to the design of wind tunnel corners, it has a real value in assisting the solution of the problem of corner losses in water, steam and air systems.

The report includes data on vane shape, spacing and incidence, on the variation of the accompanying air flow, and on the resulting influence on corner resistance. A variety of methods have been employed to analyse the conditions existing in the air stream at the vanes and, from the information so obtained, it is possible to select the vane section and method of use which will lead to the most desirable features in the flow at the corner.

Introduction

The object of this research was to investigate the design and most efficient way of using a cascade of vanes for turning an air stream through 90°. The problem arose in connection with the building of the National Research

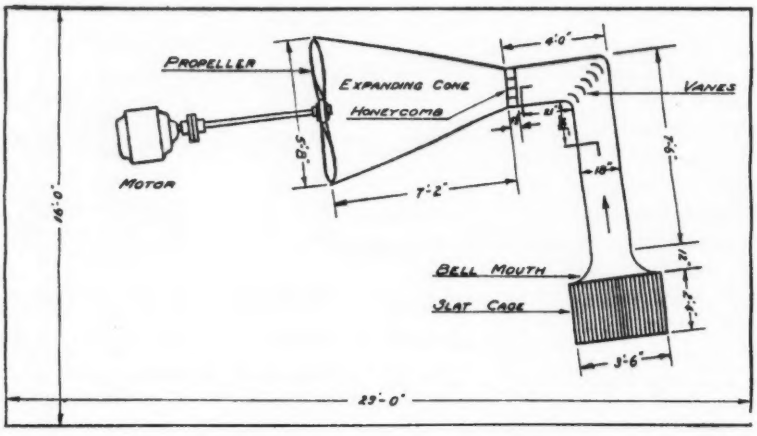

FIG. 1. *Plan showing general arrangement of wind tunnel.*

Laboratories' nine-foot wind tunnel at Ottawa. In this tunnel there are two closed return passages, which necessitate the incorporation of eight right-angled corners.

[1] *Manuscript received August 18, 1930.*
Contribution from the National Research Laboratories, Ottawa.

[2] *Junior Research Physicist, National Research Laboratories, Ottawa.*

To redirect the air smoothly and to minimize the losses due to turbulence, it had been decided to use sets of vanes located along the diagonals of the corners similar to those developed at Göttingen (2). The information as regards variety of vane shape and spacing was rather meagre, and the suggestion that vane shape was not critical, seemed to indicate the possible existence of "burbling". In one of the Aeronautical Research Committee reports (1) it was further indicated that, with the incidences at which vanes would be employed, "burbling" was a very likely condition. As there was no existing information on this point, it was decided to make a full analysis of the flow conditions round a variety of vanes, to investigate their relative merits.

The most desirable properties were minimum turbulence and uniform velocity distribution on the exit side of the corner. It was likely that these would result in highest efficiency, which would be indicated by minimum pressure drop across the vanes. Finally, it was necessary that the air should be turned through an exact right angle.

Apparatus

With the intention of making a fairly comprehensive analysis of flow conditions at corners, a small wind tunnel was built incorporating a right-angled bend to reproduce the conditions existing in the full size tunnel. This model channel was 18 in. × 36 in. in cross section, the dimensions being in the same 1:2 ratio as in the large tunnel. The description will be better understood by reference to Fig. 1, which shows a plan of the general arrangement, and to the photographic reproduction, Fig. 2. The entrance consisted of the usual bell mouth, which was enclosed by a wooden slat cage, one-inch slats with a one-inch spacing, a type of construction which yields reasonably good entry conditions. Velocity traverses measured across the tunnel and behind the entrance showed substantially constant velocity distribution to within three inches of the wall. The tunnel was made to swing open at the corner to facilitate the insertion and removal of cascades of vanes, which were mounted in frames for that purpose. Intermediate between the straight section of the tunnel and the expanding cone leading to the propeller, a honeycomb was placed, having 4.5 in. square cells 4.5 in. deep to remove the swirl which was induced upstream from the

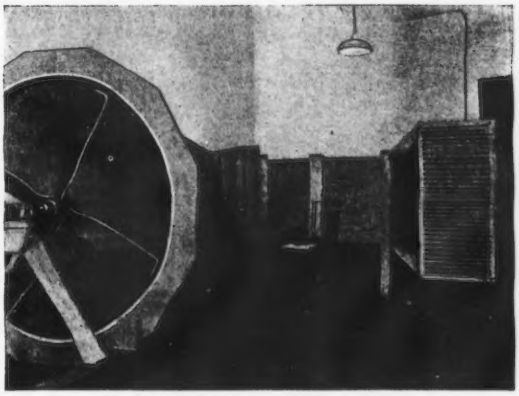

FIG. 2. *Photograph of wind tunnel.*

propeller. The expanding cone was much shorter than was desirable, in fact the complete layout was barely large enough to be satisfactory, the cramping being due entirely to the smallness of the space available in the room set aside for this wind tunnel. The wooden propeller had four blades, was 5.5 ft. in diameter, and was driven by a squirrel cage induction motor, at one speed only, *i.e*, 900 r.p.m. The tunnel itself was constructed of wood and was readily fitted with plate glass windows for observational purposes and with metal holders for pitot tubes.

Velocities ranging from 30 to 80 ft. per sec. could be attained, depending on the resistance of the corner, which varied with the type of vane and spacing employed.

Types of Vanes Tested

Four 16 gauge sheet metal vanes of 6-in. chord, one 26 gauge sheet metal vane of 1⅛-in. chord and two thick sections of 6-in. chord represent the total number of vanes examined. The sections are shown in Fig. 3, and Table I gives the dimensions of the two thick sections.

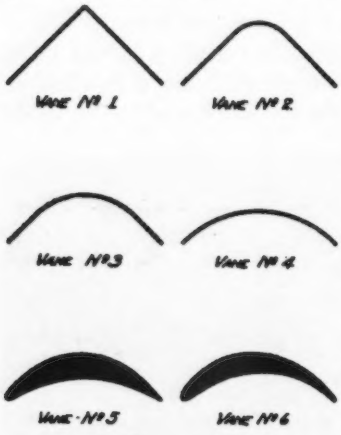

FIG. 3. *Diagram of the vane sections employed.*

The square vane No. 1 was tested to see how closely the flow and resistance resembled that of the corner without vanes, since the effect of this particular section is merely to divide the passage into a number of square cornered passages.

Vane No. 4 is a simple quarter circular arc, and vanes No. 2 and No. 3 are transition sections between No. 1 and No. 4, comprising circular arcs of radii $^1/_3$ and $^2/_3$ respectively that of No. 4 vane, the remaining portions of the sections being flats, tangential to the circular parts of the vanes.

Vane No. 5 is a thick section resembling to some extent the shape of the vanes employed in the Göttingen tunnel.

Vane No. 6 is a modification of a foreshortened R.A.F. 30-section arranged along a circular arc, the thickest portion occurring approximately 1/3 chord from the leading edge, whereas vane No. 5 is thickest at about the mid-chord position.

The vanes were all of the same length or span and were fitted between two end boards: photograph Fig. 4 shows a group of vanes set up ready for use. The complete vane assembly then fitted into a recess in the corner of the tunnel as shown in photograph Fig. 5, where the tunnel has been swung open to disclose a bank of vanes in position.

The 1⅛-in. chord vanes were chosen in order that some test could be made to indicate the nature of scale effect. The six-inch chord was chosen initially as being a likely value for the vanes in the full size tunnel.

TABLE I

DIMENSIONS OF THICK SECTION VANES

Distance from leading edge along chord as % of chord	Vane No. 5		Vane No. 6	
	Top surface, distance from chord as % of chord	Bottom surface, distance from chord as % of chord	Top surface, distance from chord as % of chord	Bottom surface, distance from chord as % of chord
0	2.03	2.03	2.36	2.36
2.5	6.66	0.07	8.44	0.11
5.0	9.68	1.14	12.50	1.24
10.0	14.45	3.70	17.60	4.28
20.0	21.65	8.14	24.70	10.25
30.0	26.70	11.43	28.70	14.90
40.0	29.30	13.45	30.60	17.60
50.0	29.93	14.12	30.60	18.70
60.0	28.79	13.78	29.10	18.40
70.0	25.90	12.37	25.90	16.40
80.0	20.44	9.41	20.30	12.40
90.0	12.71	5.14	11.80	6.42
95.0	7.40	2.62	5.14	2.93
100.0	0.27	0.27	0.79	0.79

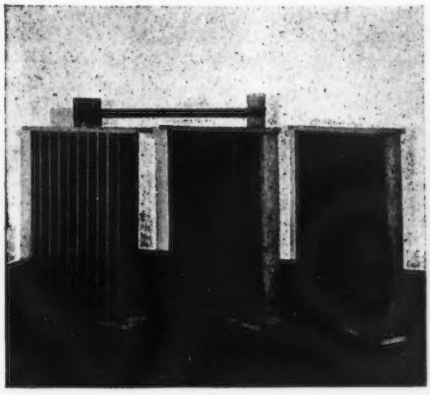

FIG. 4. *Photograph of typical banks of vanes. Note the pressure plotting vane lying horizontally across the two banks on the left.*

FIG. 5. *Photograph showing a bank of vanes mounted in the tunnel. Note how the tunnel can be opened at the corner.*

Preliminary Tests with Paint

The location of the stream lines behind the banks of vanes was initially nvestigated by a method of visualizing the air flow which was developed for erodynamic use at McCook Field.

A thin sheet of steel was cut to fit the tunnel and was placed in a horizontal ane at the centre line, just behind the vanes, and extending downstream for me 27 in. This sheet was first painted with a white enamel and then coated

with a mixture of lampblack and kerosene. When the wind was turned on, the excess lampblack was blown away and the remainder was left streaked across the plate, giving a clear indication of the flow pattern in the immediate neighborhood of the surface of the plate.

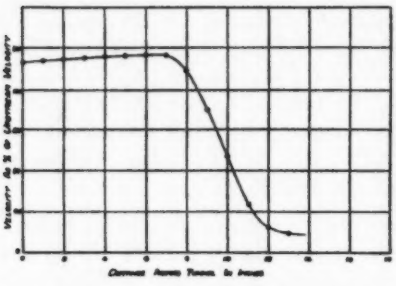

FIG. 6a. *Velocity traverse corresponding to flow picture in Fig. 6.*

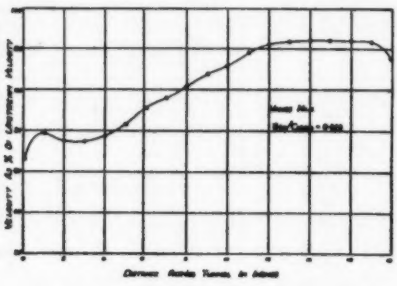

FIG. 7a. *Velocity traverse corresponding to flow picture in Fig. 7.*

Fig. 6 shows the flow around an open square corner when no vanes are present. The flow picture indicates the existence of a very large eddy on the inside wall of the downstream channel. This compares very favorably with the velocity traverse which is plotted in Fig. 6a.

Fig. 7 is the flow picture taken behind a set of No. 1 square sheet metal vanes. The air has obviously been turned through more than 90° with the result that a higher velocity exists on one side of the tunnel than on the other. This is in very marked agreement with the velocity traverse, or pitot tube traverse, which has been plotted in Fig. 7a for comparison.

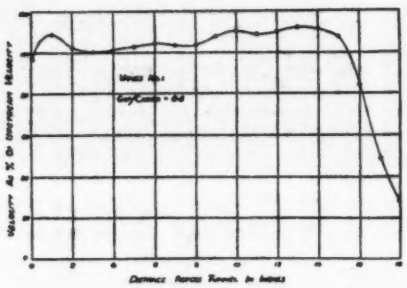

FIG. 8a. *Velocity traverse corresponding to flow picture in Fig. 8.*

By extending the metal sheet into the space between the vanes, an attempt was made to obtain visual indication of the air flow in this region. The resulting diagrams were for some time quite mystifying; the flow was far from what was to be expected and it was quite obvious that the presence of the metal sheet was distorting the normal flow. Fig. 8 and 9 show typical paint records obtained in this manner and the flow along the plate appears to run across the passage from the outer wall to the inner. Similar conditions were observed by Wirt (3), when taking his numerous flow casts of pipe corners. This phenomenon is easily accounted for when examining the modifications which the metal plate imposes on the conditions existing at the bend. Owing to the rotation of the air at the corner, the centrifugal force gives rise to a pressure gradient across the space between each pair of vanes,

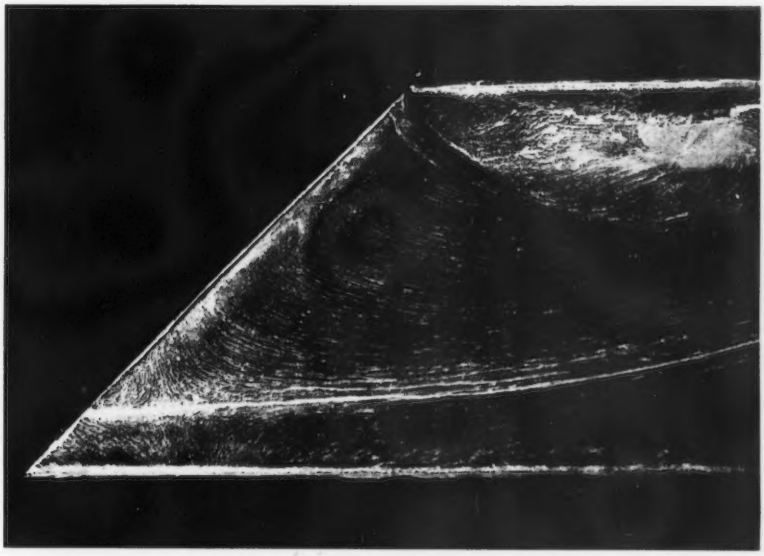

FIG. 6. *Characteristics of the square corner with no vanes. Note how the existence of the eddy is indicated both in the paint test record and in the velocity distribution.*

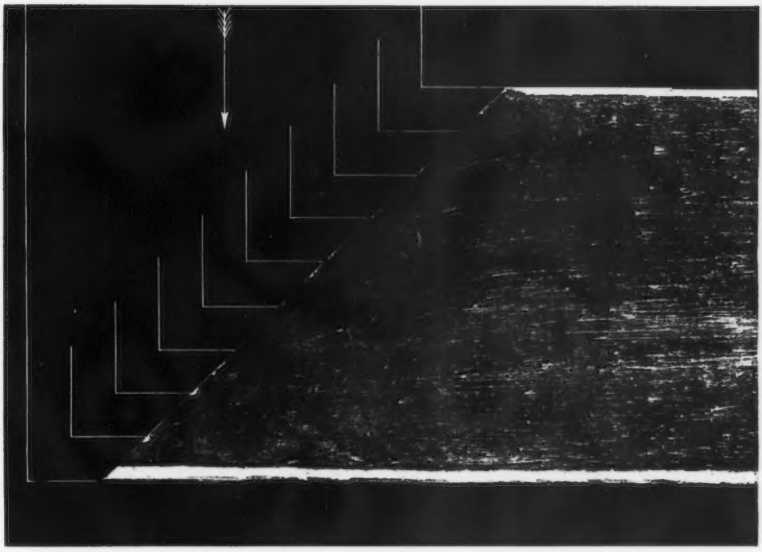

FIG. 7. *Characteristics of the corner modified by a bank of eight No. 1 vanes. Note that the air has turned through more than 90° and therefore a greater velocity exists in the inside wall of the downstream passage than on the outside.*

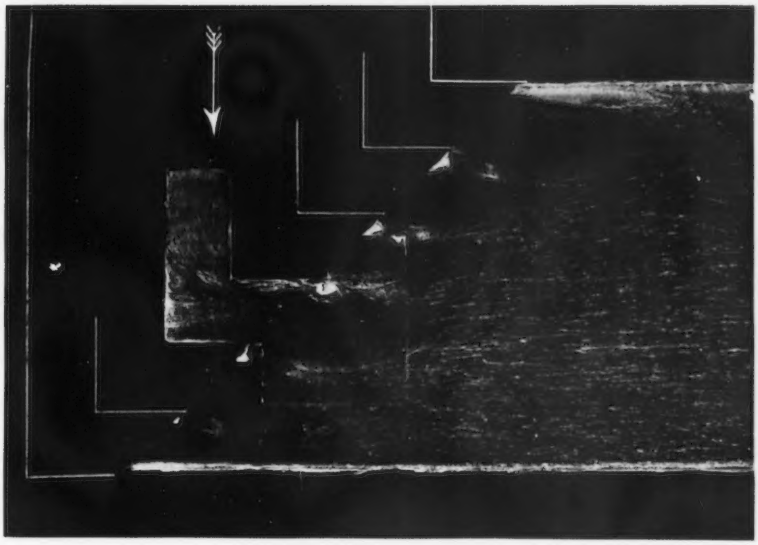

FIG. 8. *Typical paint record and velocity distribution for a bank of No. 1 vanes. Note the intervane swirl caused by the centre line spacers.*

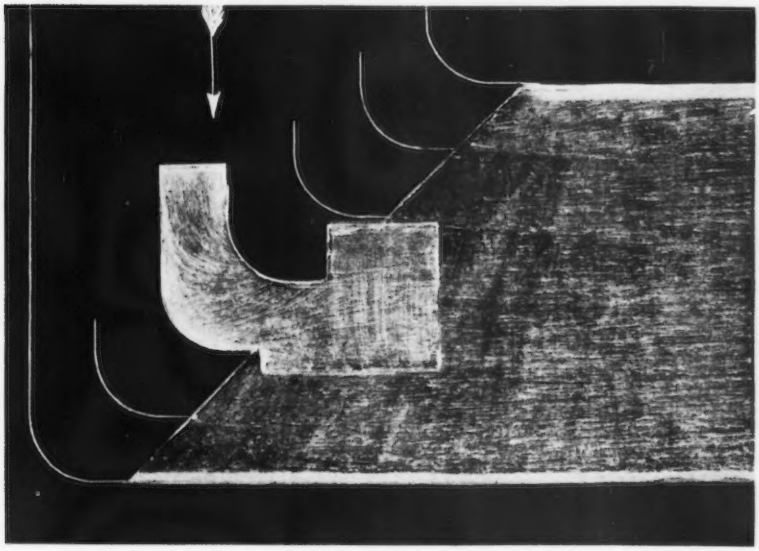

FIG. 9. *The intervane swirl for a group of No. 3 vanes.*

the outside of the turn being the region of high pressure. At the surface of the metal plate, the air stream is considerably retarded by skin friction, and the centrifugal forces in consequence, being still further reduced, it follows that the pressure gradient across the intervane space is much smaller than at a position more removed from the metal plate. The effect of this is to introduce pressure gradients along the vertical surfaces of the vanes, the directions of these gradients being as shown in Fig. 10. Their direct effect is then to

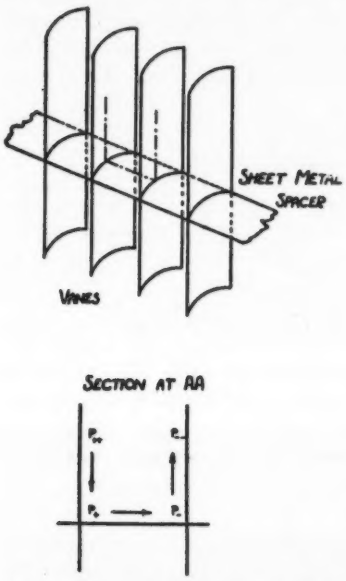

FIG. 10. *Diagram to explain the intervane swirl induced by spacers. The pressure gradients, derived from centrifugal action at the turn, are indicated in their relative magnitudes by the + and − signs.*

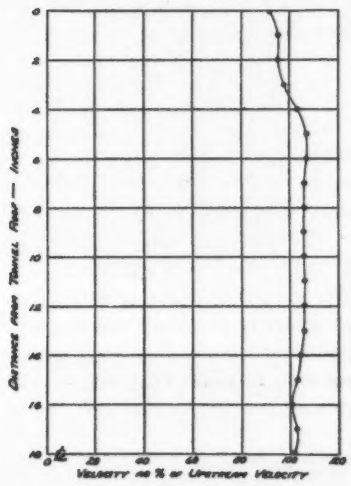

FIG. 12. *Vertical velocity distribution behind a bank of No. 3 vanes with centre line spacers.*

Note the interference at the centre line due to the existence of the spacers.

introduce a "swirl", the resultant motion of the air in the passage being helical and recording itself as in Fig. 8 and 9. It will be obvious from this explanation that similar flow conditions, as here described, will be obtained to a greater or less degree in any pipe or duct in which sharp bends are located.

In view of the fact that a proposal had been made to use plate spacers or stringers to act as stiffeners between long vanes, it was thought that an investigation of their effect on the air stream would be valuable. A set of vanes was assembled, with sheet spacers between them and the large paint test sheet placed downstream, on the same plane. Fig. 11 and 11A show the result. Each swirl arising between the vanes continues downstream for some considerable distance. The result of omitting the spacers is shown in Fig. 13.

A vertical velocity traverse was made 22 in. behind the vanes, measured along the tunnel centre line, and this revealed a sudden drop in velocity immediately behind the spacers, resulting from the interference they create (Fig. 12). Fig. 13 shows the paint record obtained behind a set of reasonably good vanes.

It is desirable, at this stage, to indicate that the method of flow analysis which employs painted metal sheets has only a very limited application, and a too rigid interpretation of records obtained with them may lead to false conceptions regarding the flow. Due to the low velocities in the boundary layer, there must always be a distortion of curvilinear flow. In any case, the paint streaks show the flow actually along a boundary only and do not exhibit the flow conditions in the free stream.

Velocity and Pressure Measurements

For the purpose of running series of tests on banks of vanes, two pitot tubes were fitted in the tunnel, one located in the upstream channel and the other behind the vanes, in the downstream passage. The position of these pitot tubes with reference to the vanes is given in Fig. 1.

The upstream pitot tube, which was permanently located on the centre line of the tunnel, was employed to give the upstream velocity at the centre line; this was taken as a reference velocity, all downstream velocities being expressed as percentages of this value. In the routine tests on vanes, horizontal velocity traverses behind them were made with the downstream pitot tube, the measurements being taken at one-inch intervals across the 18-inch section. The static pressure difference across the corner was also measured, by connecting the

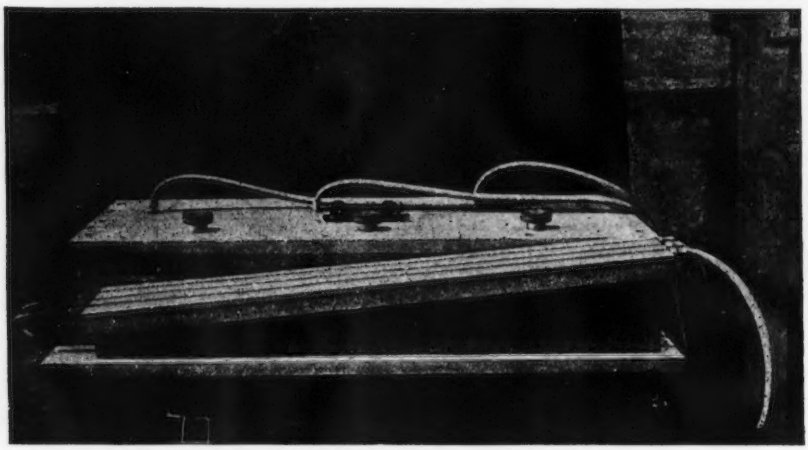

FIG. 14. *Photograph of the slant tube manometer. Three tubes are incorporated in this instrument.*
Note the spirit level and also the adjustment for the three reservoirs on the top of the instrument.

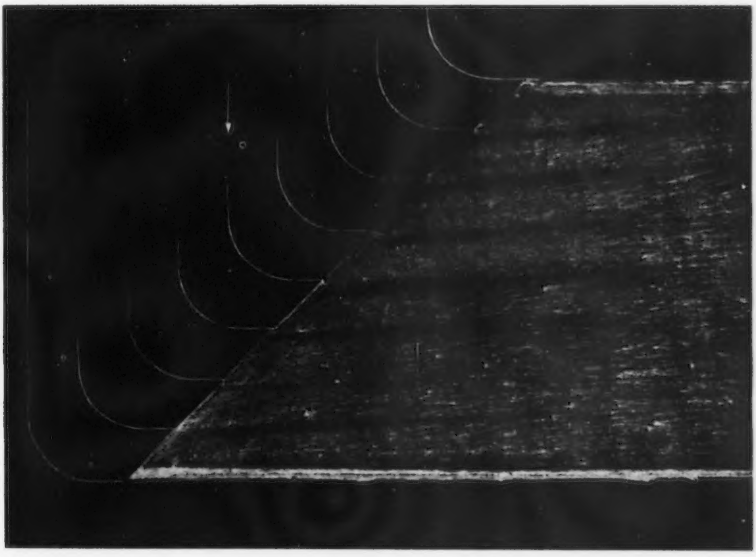

FIG. 11. *Paint test record showing how the intervane swirls persist downstream. Fig. 13 shows the effect of omitting the spacers.*

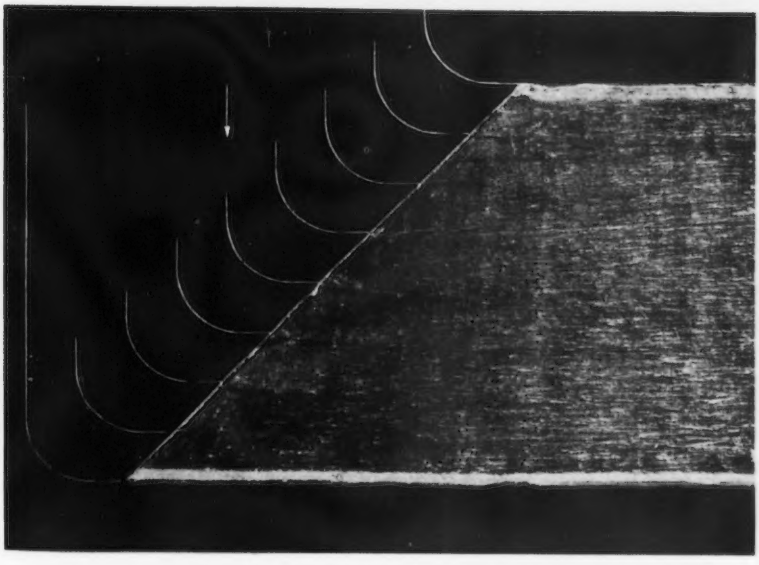

FIG. 13. *Paint test record for a set of No. 3 vanes at a gap/chord spacing of 0.375. Note that the character of the flow in the downstream channel appears to be quite good with this arrangement of vanes.*

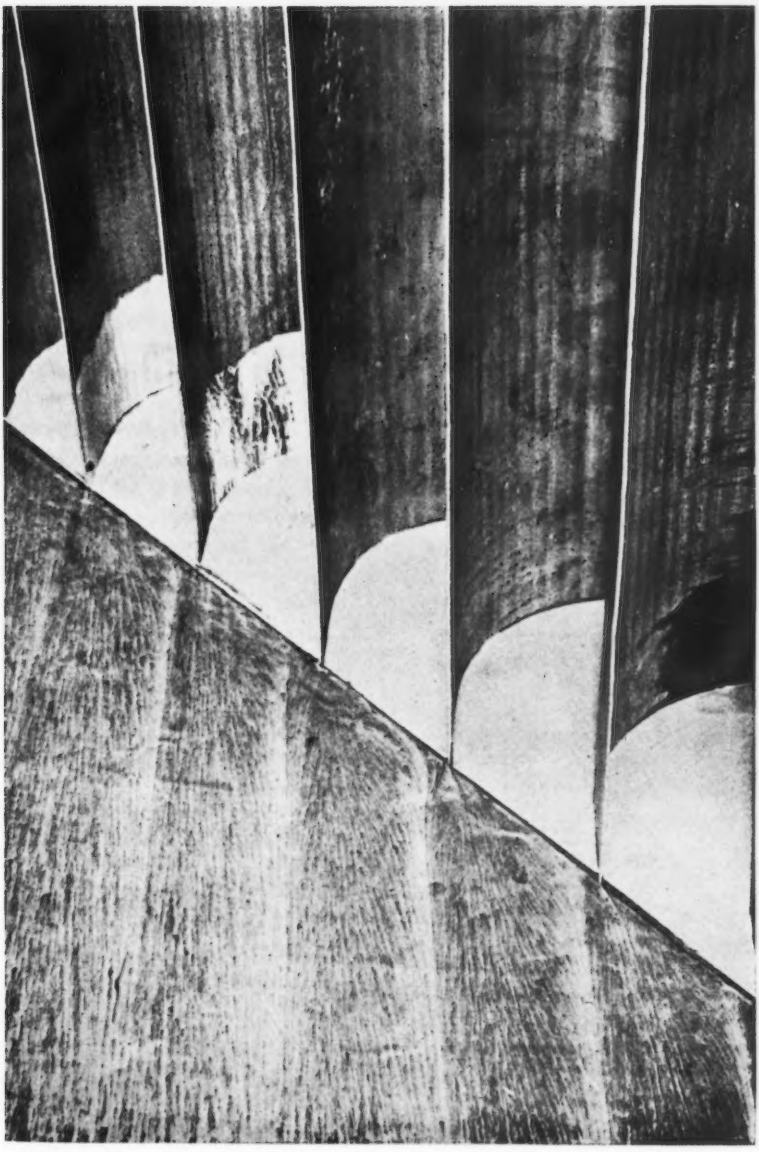

FIG. 11-A. *Photograph showing the paint test sheet in place, and intervane spacers.*

static holes of the two pitot tubes to opposite sides of a third manometer. This pressure drop has been expressed in percentages of the upstream impact pressure, and its mean value was taken to be a measure of the resistance of the corner.

The manometers used (Fig. 14) were of the slant tube type. Each of the three tubes, which were all located on the same base board, was connected to a movable reservoir of large cross section so that the drop in level in the reservoir was negligible. The three tubes being on the same base were accurately parallel, so that comparative readings were independent of the absolute slope of the base. The slope could be maintained constant by means of a spirit level, mounted on a horizontal portion of the manometer base and graduated in minutes of arc. The indicating fluid employed was colored alcohol.

Fig. 15 shows a group of typical velocity traverses. The gap/chord ratio was 0.5 as measured in Fig. 16, and the curves included are for vanes No. 1, 3, 4 and 5; Fig. 6a shows one for the corner without vanes. It will be seen that even the crudest vane has a remarkable effect in smoothing out the velocity distribution across the downstream passage. It is also apparent that vanes No. 4 and No. 5 are superior to the others, in that they produce a more uniform velocity distribution on the exit side of the tunnel. As the research proceeded, it became obvious that the vane shape was not really a very critical factor,

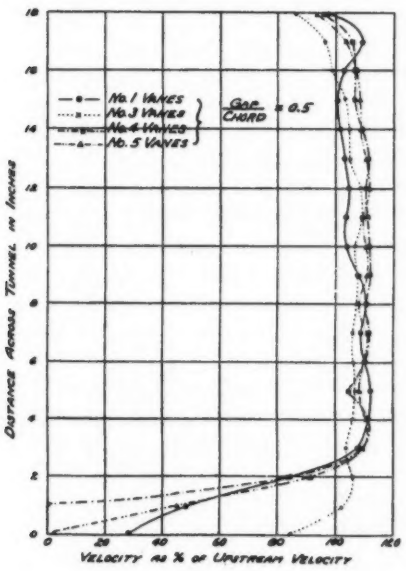

FIG. 15. *Velocity distribution behind vanes of various shape.*

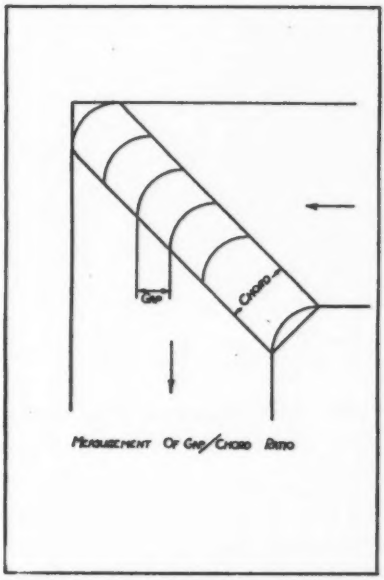

FIG. 16. *Diagram illustrating the method of evaluating gap/chord.*

in that any reasonably shaped vane, such as No. 3, 4, 5 or 6, would give good characteristics to the corner, as outlined in the introduction. Their individual improvements on a corner without vanes is so enormous that the slight differences among themselves become small in comparison. The research was continued with the intention of discovering the properties of each vane shape, under varying conditions of spacing. As would be expected, there was, for each vane, a spacing or range of spacings, over which the efficiency was highest. The search was then for the vane shape and spacing that would be most efficient in use.

A large number of tests were made with all the vanes at various spacings. In Fig. 17, the velocity distributions are plotted for four different spacings of the vane No. 4 and indicate the quality of the results obtained in the majority of cases. It was exceedingly difficult to compare, in any quantitative way, the curves for each vane; yet it appears to be a general rule, that the most uniform velocity distribution is obtained with the closest vane spacing.

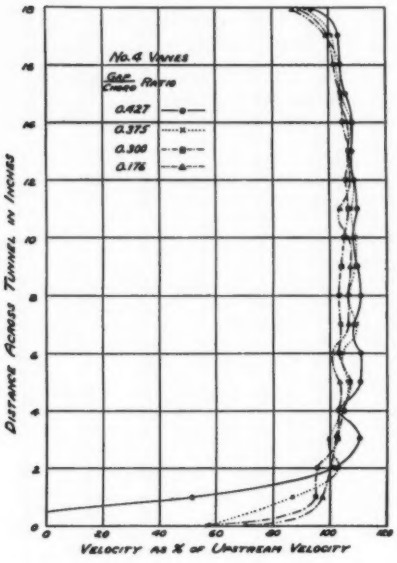

FIG. 17. *Velocity distribution behind vanes at various spacings.*

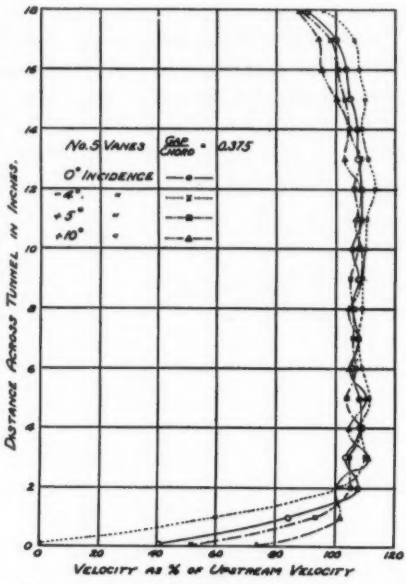

FIG. 18. *Velocity distribution behind vanes at various incidences.*

The effect on the velocity distribution, of changing the incidence over a fairly wide range, was examined for the thick section vane No. 5. The results such as they are, are given in Fig. 18; the gap/chord ratio was 0.375 and incidences of $-4.0°$, $0°$, $+5°$ and $+10°$ were used. The datum of incidence was chosen as the position at which the vanes would be normally set, that is with the chord perpendicular to the plane of the corner. Incidences were

measured by the angular departure of the chord from this position. The uniformity of the distribution is approximately the same for all these incidences; but it is obvious, from the relative positions of the curves, that the change of incidence has produced a corresponding change in the direction of the emerging air stream. It appears from the curves that no particular advantage is gained by using any incidence other than 0°.

The single test on scale effect was performed with 50 small vanes of No. 4 section, chord 1⅛ in., spaced at a gap/chord ratio of 0.33 (Fig. 19). This bank of vanes was then an accurate scale model of a corner of the full size tunnel, equipped with No. 4 vanes, of six-inch chord, at a gap/chord spacing of 0.33. This figure for the spacing is one that subsequent measurements of resistance have shown to be the ideal for No. 4 vane. The model contained two metal rods as stringers, and once again the bad effect of such spacers on velocity distribution has been recorded. Fig. 20 shows the semi-vertical velocity traverse and indicates rather strongly the shadow of the wire stringer. The distribution is otherwise quite regular and smooth, and the horizontal traverse gave results comparable with those obtained from the larger scale, six-inch chord No. 4 vanes at the same spacing.

FIG. 19. *Photograph showing 50 small vanes set up in the tunnel. Note the horizontal stringers.*

Corner Resistance

It was mentioned, in the description of the velocity and pressure measurements, that the mean value of the static pressure drop across the corner, as a percentage of the upstream impact pressure, has been taken as an indication of corner resistance.

From all the readings taken on the various types of vanes, the curves shown in Fig. 21 have been secured; they show the variation of corner resistance with vane spacing. The gap/chord ratio varies from 0.176 to 0.75 and the pressure drop was found to range from 20% to 110% of the impact pressure.

The curves are similar in one respect, namely, they all fall to a minimum somewhere in the gap/chord range 0.3 to 0.5, and rise more steeply on the side of increasing spacing. A second observation from the curves is that low

resistance is obtained with any reasonably good stream-line shape, of large fineness ratio, at its most favorable gap/chord value. The spacing is obviously a critical factor. At large spacings, the turbulence in the stream passing through the vanes creates a large corner resistance. As the spacing decreases, this turbulence is more and more reduced, until finally the corner resistance is at its minimum value, and any closer spacing results in a slight rise of resistance due possibly to the increased skin friction or to some interference effect not accounted for.

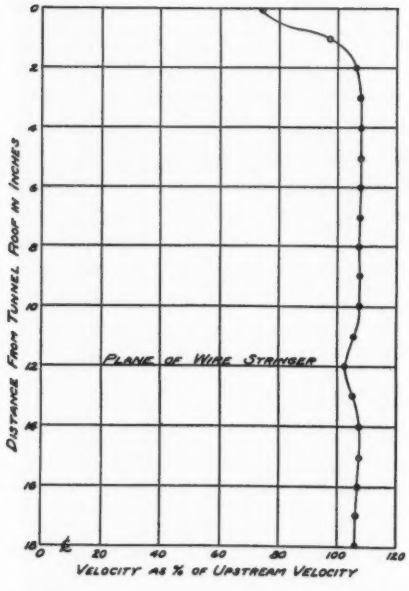

FIG. 20. *Semi-vertical velocity distribution behind 50 small No. 4 vanes showing the shadow of the wire stringer.*

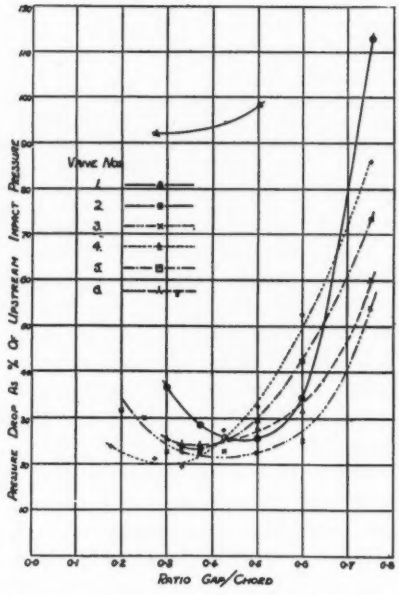

FIG. 21. *Corner resistance curves for all vane shapes.*
Note that vane No. 4 gives the minimum resistance at a gap/chord ratio of 0.3

The curves indicate that vane No. 4 has the least resistance of all at a spacing of 0.33, although calculation shows that quite large variations of vane resistance would have very little noticeable effect on the top speed of the wind tunnel. Vane No. 1 is obviously useless.

The effect of incidence on resistance was examined in the case of vane No. 5. Over a moderately large range of incidences, the resistance does not vary appreciably, and the variation as shown in Fig. 22 is of a nature more or less to be expected.

Scale Effect

The small scale model of the No. 4 vanes which was tested gave a corner resistance of 26.8%. This value is in excess of that for the larger scale six-inch chord vanes which was 20%. This information, although rather meagre, would

indicate that, on still further increasing the chord from 6 in. to say 12 in. there would probably be a further decrease in corner resistance. It was found that the vane passage on the inside of the corner was always stalled no matter what vane section was being employed, so that increasing this gap probably increases the resistance of the corner. These two effects are in opposition so that the fact that the net resistance was decreased by an increase in chord would indicate that increasing the scale decreases corner resistance.

Pressure Distribution on the Surface of a Vane

When testing the thick section vanes No. 5, it was surmised that a measurement of the pressure distribution on one of them near the tunnel centre line would give a valuable clue as to the presence or absence of "burbling".

Accordingly, one of the vanes was fitted up as a pressure measuring vane, see Fig. 23. A number of holes, of 0.02 in. diameter, were drilled at approximately half-inch intervals all the way round the profile, at the centre section.

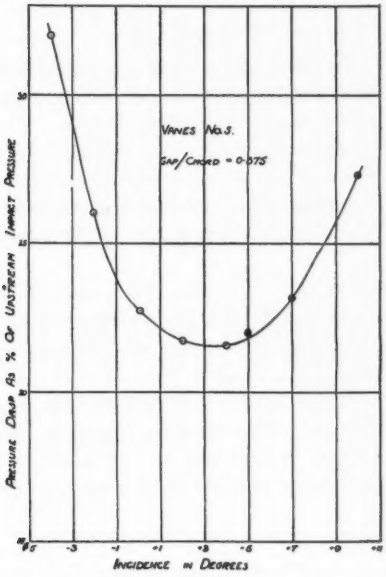

FIG. 22. *Variation of corner resistance with incidence.*

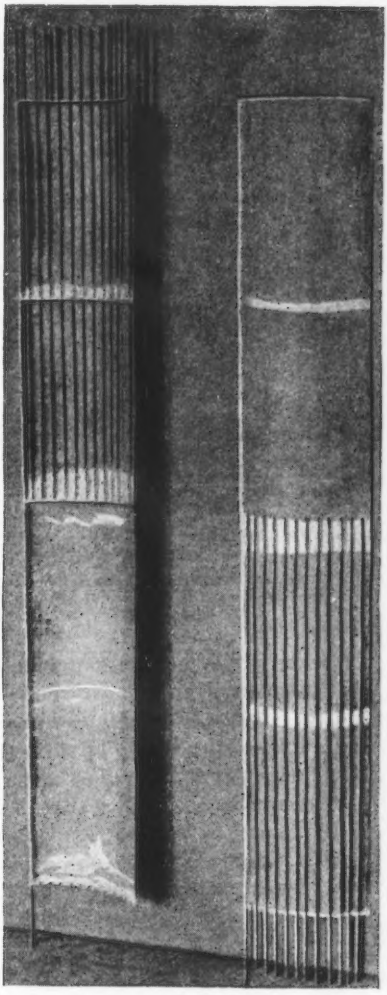

FIG. 23. *Photograph showing construction details of the pressure plotting vane.*

Brass tubes were soldered on the inside of the vane, behind each hole, and were led away through the ends of the vane. These tubes were then connected to slant manometers, by means of rubber tubing, and the pressures at the various holes were read off directly. In this way pressure distributions were made at one value of the vane spacing and at three different values of incidence, the pressure measuring vane being set up just as any other vane, in the middle of a bank of otherwise similar ones.

Vane incidences of 0°, 3° and 6°, with a gap/chord ratio of 0.5, were tried.

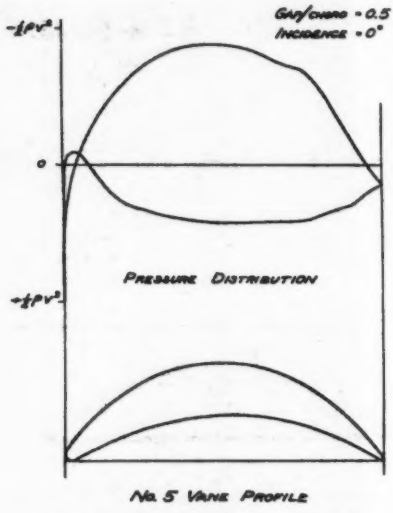

FIG. 24. *Diagram showing a typical pressure distribution curve. Note that there are no indications of any serious changes in the type of flow round the vane profile.*

Had there been any considerable back pressure gradient discovered, "burbling" might have been suspected; instead of this the pressure distribution for this spacing was so good that an investigation at closer spacing was deemed unnecessary. Fig. 24 shows a typical pressure distribution curve obtained in this manner.

In indicating the presence of laminar flow round this vane, the results of this test are in agreement with those obtained by the use of smoke for indicating air flow characteristics and showing up any existing "burble".

Smoke Tests

In place of the usual titanium tetrachloride, tin tetrachloride was employed in some initial experiments. This necessitated saturating the air of the room with ammonia first to destroy the acid fumes emitted by the tetrachloride; it was found also that this had the effect of increasing the denseness of the smoke given off.

The liquid was poured on to one of the vanes and a slow wind turned on. This enabled the flow to be studied visually, by observing the smoke given off, and an instant decision to be made as to whether the motion was laminar or turbulent near the trailing edge of the vanes.

In the case of thick section vanes No. 5, 6 and vane No. 4 (circular arc) the flow at the trailing edge was decidedly laminar. The results of tests on the other vane sections indicate that where flats exist there is a tendency to "burble" at the point where the curvature suddenly changes by a large amount.

Conclusion

The results of this investigation have a wide field of application. In the design of pipes and ducts for steam, water or air systems, the inclusion of any

device which will minimize the resistance of corners or bends should have profitable results in reducing power expenditure. The research indicates that, as a commercial proposition, the design of vanes for corners need not be too elaborate, since the reduction of the losses is enormous with even the most elementary type of vane.

In cases where the strength of the material of the vanes or the loading on them is an important factor, it might be considered more advisable to employ a thick section with a rounded leading edge, such as vanes No. 5 and 6.

Acknowledgment

In concluding, the authors wish to acknowledge their indebtedness to J. H. Parkin, Assistant Director, Division of Physics, in charge of aeronautic research for his guidance and continued assistance throughout the work.

References

1. HARRIS, R. G. AND FAIRTHORNE, R. A. Wind tunnel experiments with infinite cascades of aerofoils. Reports and Memoranda Aeronautical Research Comm. No. 1206. 1928-9.
2. WIESELSBERGER, C., BETZ, A. AND PRANDTL, L. Ergebnisse der aerodynamischen Versuchsanstalt zu Göttingen. Vol. I. 1925.
3. WIRT, L. New data for the design of elbows in duct systems. Gen. Elec. Rev. 30: 286-296. 1927.